Action of monochloramine on biofilms of Pseudomonas aeruginosa and Klebsiella pneumoniae
by Rohini Srinivasan

A thesis submitted in partial fulfillment of the requirements for the degree of Master of Science in Chemical Engineering
Montana State University

Abstract:
The disinfection efficacy of monochloramine on mono- and binary population biofilms of P. aeruginosa and K. pneumoniae was investigated. Biofilms grown in continuous flow annular reactors on stainless steel surfaces were treated with a pulse/step delivery of 4 mg/I monochloramine for 2 hours. Biofilm samples were disaggregated and assayed for colony forming units by plating on R2A agar and for total cell numbers by acridine orange direct counts. The decrease in plate count numbers indicated the overall decay, the decrease in total cell number indicated the overall removal. The overall decay rate depended strongly on the initial biofilm areal cell density. The decay rate followed a parabolic trend with respect to initial biofilm areal cell density. Decay was fastest at around 1012 cfu/m2 and lower at all other cell densities. Disinfection predominated over detachment in almost all experiments. No evidence of species interactions was found. Decay rates of the individual species were comparable in mono- and binary population biofilms. The addition of abiotic particles (kaolin and calcium carbonate) reduced the efficacy of monochloramine.

Different measures of biofilm activity were compared to assess the efficacy of monochloramine on binary population biofilms of P. aeruginosa and K. pneumoniae. Active microbial numbers measured by colony forming units on R2A or MT7 agar media declined by approximately 3 orders of magnitude. Integrated measures of biofilm respiratory activity, including the oxygen flux determined from microelectrode measured oxygen concentration profiles and the overall glucose consumption rate calculated by material balance declined by only 10 to 15%. The total number of bacteria remaining in the biofilm, as measured by acridine orange direct counts declined by 29% in the same interval. These data suggest that respiratory activity and plate count data yield widely differing estimates of biocide efficacy.

ACTION OF MONOCHLORAMINE ON BIOFILMS OF *Pseudomonas aeruginosa* AND *Klebsiella pneumoniae*

by

Rohini Srinivasan

A thesis submitted in partial fulfillment
of the requirements for the degree

of

Master of Science

in

Chemical Engineering

MONTANA STATE UNIVERSITY
Bozeman, Montana

May 1994

APPROVAL

of a thesis submitted by

Rohini Srinivasan

This thesis has been read by each member of the thesis committee and has been found to be satisfactory regarding content, English usage, format, citations, bibliographic style and consistency and is ready for submission to the College of Graduate Studies.

4/27/94
Date

Philip A. Stewart
Chairperson, Graduate Committee

Approved for Major Department

4/27/94
Date

John T. Sears
Head, Major Department

Approved for the College of Graduate Studies

5/5/94
Date

R C Bross
Graduate Dean

STATEMENT OF PERMISSION TO USE

In presenting this thesis in partial fulfillment of the requirements for a master's degree at MONTANA STATE UNIVERSITY, I agree that the Library shall make it available to borrowers under rules of the Library.

If I have indicated my intention to copyright this thesis by including a copyright notice page, copying is allowable only for scholarly purposes, consistent with "fair use" as prescribed in the U.S. Copyright Law. Requests for permission for extended quotation from or reproduction of this thesis in whole or in parts may be granted only by the copyright holder.

Signature Rohini S.

Date 4/27/94

ACKNOWLEDGEMENTS

I am grateful to my mentor and advisor Dr. Philip S. Stewart for his guidance and insight into formulation of my research career. I also thank him profusely for allowing me to interact with other groups and people to perform some "fun" experiments. I would like to extend my sincere thanks to Thomas Griebe, for being an excellent teacher and for having helped me immensely in developing a passion for biofilms. I would like to thank Dr. Warren Jones and Anne Camper for their encouragement and advice throughout my graduate work. I am thankful to David Chen and Dr. McFeters for their help and support. I am grateful to Dr. John Sears for his support and encouragement. I like to thank Dirk for imparting extremely useful knowledge about microelectrodes. I am grateful to Dr. Gill Geesey and his group for their input into the thesis. I would like to extend my gratitude to Marty Hamilton for his help on statistics.

I would like to extend my gratitude to the Center as a whole, which has become my "home" in the US. I am thankful to my friends Ricardo, Jysotna, Shannon, Dave, Philip, Jason, Sam, Raj, Chris, Ace, Kristi, Alma, Susan, Jamie, Peg, Cheryl, Peter, Rick, and Xiaoming for their friendship and technical help. I am thankful to Mary Williams for her patience and affection.

Last but not the least I am extremely grateful to my family for their undaunted support during the most turbulent years of my life. This thesis is dedicated to my parents, Rashu and Giri.

TABLE OF CONTENTS

Page

Page

LIST OF TABLES

Table | Page

LIST OF FIGURES

Figure Page

ABSTRACT

The disinfection efficacy of monochloramine on mono- and binary population biofilms of *P. aeruginosa* and *K. pneumoniae* was investigated. Biofilms grown in continuous flow annular reactors on stainless steel surfaces were treated with a pulse/step delivery of 4 mg/l monochloramine for 2 hours. Biofilm samples were disaggregated and assayed for colony forming units by plating on R2A agar and for total cell numbers by acridine orange direct counts. The decrease in plate count numbers indicated the overall decay, the decrease in total cell number indicated the overall removal. The overall decay rate depended strongly on the initial biofilm areal cell density. The decay rate followed a parabolic trend with respect to initial biofilm areal cell density. Decay was fastest at around 10^{12} cfu/m^2 and lower at all other cell densities. Disinfection predominated over detachment in almost all experiments. No evidence of species interactions was found. Decay rates of the individual species were comparable in mono- and binary population biofilms. The addition of abiotic particles (kaolin and calcium carbonate) reduced the efficacy of monochloramine.

Different measures of biofilm activity were compared to assess the efficacy of monochloramine on binary population biofilms of *P. aeruginosa* and *K. pneumoniae*. Active microbial numbers measured by colony forming units on R2A or MT7 agar media declined by approximately 3 orders of magnitude. Integrated measures of biofilm respiratory activity, including the oxygen flux determined from microelectrode measured oxygen concentration profiles and the overall glucose consumption rate calculated by material balance declined by only 10 to 15%. The total number of bacteria remaining in the biofilm, as measured by acridine orange direct counts declined by 29% in the same interval. These data suggest that respiratory activity and plate count data yield widely differing estimates of biocide efficacy.

INTRODUCTION

Statement of the problem

A biofilm is a surface accumulation of microbial cells and organic polymers of microbial origin that may also contain inorganic particles or precipitates. Biofilm formation can be both beneficial and detrimental in industrial systems (Characklis et al (1990), Sandohlm et al (1992)). One of the harmful effects of biofilm formation in industrial systems is reduction in mass, momentum and heat transfer capacity, which leads to increased production and maintenance costs. This phenomenon is commonly termed biofouling.

Many methods are used to alleviate biofouling. Mechanical cleaning of pipelines, antifouling coatings and chemical agents commonly known as biocides are the most common treatment procedures. Sometimes a combination of these procedures is used. Chemical additives have the advantage of inactivating microbial cells in addition to removing the biofilm. The effectiveness of chemical control is limited by the fact that bacteria in biofilms are often much more resistant than planktonic organisms to the wide range of biocides that are commonly used. Oxidizing biocides such as chlorine and monochloramine are typically used in industrial systems, because of their strong reactive capacities.

Antimicrobial agents added to a system to control biofouling are affected by various biofilm parameters. The diversity of the biofilm with respect to species composition, biotic and abiotic particle content and total

biomass significantly impacts disinfection efficacy. Most of the academic research done so far has been in relation to either mono population (Wende (1991), Chen et al (1993)) or undefined mixed population biofilms (LeChavellier et al (1990)). Monopopulation biofilms may be useful for addressing fundamental mechanisms, but they lack real world relevance and overlook possible species interactions. Undetermined mixed population biofilms are difficult to characterize in the detail required to address fundamental issues. This thesis project moves a step forward by investigating disinfectant efficacy in defined binary population biofilms.

There are various methods available to measure biocide efficacy, each with limitations and advantages. Plate count measurements have traditionally been used to determine kill efficiency. As part of this thesis, alternative measures of biofilm activity during disinfection were evaluated and compared.

Goal and Objective

The long term goal of the research project of which this thesis constitutes a part is to understand the mechanisms that reduce the efficacy of anti-microbial agents used to disinfect and remove biofilms. An overall experimental objective of the thesis is to extend research methods for analyzing biocide action against monopopulation biofilms to defined binary population biofilms. Specific objectives of the thesis research include

i) Comparison of biocide action on mono and binary population biofilms.

ii) Comparison of culturability and respiratory activity during disinfection.

iii) Identification of biofilm parameters affecting disinfectant efficacy.

LITERATURE REVIEW

Biofouling

Almost every surface in contact with non-sterile water can harbor a biofilm. The biofilms can influence various industrial processes either in a beneficial or deleterious way. Biofouling is the undesirable formation of microorganisms on surfaces in association with inorganic and organic materials. The harmful effects of biofouling include decreased water quality due to contamination, corrosion or deterioration of the substratum, decreased product quality, loss in plant performance, increased cleaning expenses and down time, and security and health problems for both personnel and the environment (Flemming H.C (1991)).

Table 1 summarizes the various methods adopted to control biofouling in industry.

Table 1 Common control methods (Characklis and Marshall (1990))

Fundamental process	Control method
Water phase transport	Filtration
Water-substratum interaction	Biodispersants
Transformation in the deposit	Biocides, biocidal coatings
Detachment	Biocides, mechanical methods

Antimicrobial agents are the most common control method used, because they kill cells in addition to removing biomass. Table 2 shows some commonly used biocides, with their advantages and limitations.

Table 2 Common biocides used in industrial systems (Sandholm et al (1992))

Biocide	Advantages	Disadvantages
Chlorine	Destroys biofilm matrix, residual effect	Toxic by products, corrosive, lower penetration
Hypochlorite	Cheap, effective, promotes detachment	Poor stability, corrosive, toxic byproducts
ClO_2	Effective at low concentrations.	Toxic byproducts, safety problems.
Chloramine	Good penetration, higher residual effect, less toxic byproducts	Resistance observed, less active against planktonic bacteria
Bromine	Effective against a broad microbial spectrum	Toxic byproducts
Ozone	Weakens biofilm matrix decomposes to oxygen, no residues	Corrosive, shorter life span, reacts with organic to form epoxides
H_2O_2	Supports detachment and removal, non toxic	Corrosive, higher concentrations needed
Peracetic acid	Penetrates biofilm, kills spores, no toxic byproducts	Corrosive, unstable
Formaldehyde	Easy application, stability, broad antimicrobial spectrum	Toxic, legal restrictions, carcinogenic, fixes biofilm
Glutaraldehyde	Cheap, noncorrosive, effective in low concentrations, cheap	Does not penetrate biofilms, degrades to formic acid
Isothiazolones	Effective in low concentrations, broad antibiotic spectrum	Compatibility problems, inactivation by primary amines, expensive
Quaternary ammonium compounds (QUACs)	Effective in low concentrations, supports detachment, non toxic, prevents biofilm growth	Inactivation at low pH

Oxidizing biocides

This class of biocides is more effective because of their high reactivity. Halogens such as chlorine, bromine and related compounds are widely used in industry. Chlorine is a very effective biocide that inactivates pathogenic bacteria, viruses and other microorganisms which are a bane in the water industry. One of the major problems of chlorination is the formation of trihalomethanes (THM), which are toxic environmental pollutants (Water Chlorination (1984)). Combined chlorine, the main product of reaction of chlorine with amines, plays an important role in both water and waste water disinfection.

Monochloramine

Hypochlorous acid (HOCl) reacts rapidly with ammonia to form monochloramine (NH_2Cl), dichloramine ($NHCl_2$), or nitrogen trichloride (NCl_3). Usually monochloramine is the only chloramine present when pH values are greater than 8.0 and when the molar ratios of hypochlorous acid to ammonia are less than or equal to 1.0. Monochloramine is a colorless, water soluble liquid, with a freezing point of -66°C. It is an oxidizing agent (Water Chlorination (1984)).

The biofouling problem has historically been controlled using free chlorine, though monochloramine may be more effective for disinfection of biofilm cells (Griebe et al (1993)). Free chlorine is clearly more effective against planktonic cells. The lower disinfection efficacy of chlorine applied to

biofilms may be due to the significant demand of the biofilm cells for the highly reactive free halogen. Monochloramine was not reactive to system components used while free chlorine (Griebe et al (1993)) exhibited a relatively high system demand. LeChevallier et al (1988) also observed the same effect when investigating *K. pneumoniae* biofilms. The authors discuss the possibility that the increased efficacy of monochloramine may be explained by better penetration of bacterial biofilms. Jacangelo et al (Water Chlorination (1984)) reported that monochloramine reacted rather specifically with nucleic acids, tryptophane, and sulfur containing amino acids. They observed that monochloramine did not react with EPS. Free chlorine is known to react with a wide variety of compounds. Investigations by other groups also reveal that NH_2Cl is very effective against waste stream bacteria (Water Chlorination (1984)). Monochloramine appears to be in competition with free chlorine as a biofilm disinfectant. It also has the advantage of forming fewer hazardous by- products.

Conversion of NH_2Cl to N-chloroorganic compounds, an extremely slow reaction, is undesirable within a treatment facility because the latter compounds have weak bactericidal properties. Because monochloramine contains reduced nitrogen, it can be a nutrient source for nitrifying bacteria. Both reactions can reduce the efficacy of monochloramine as a disinfectant.

Microorganisms

K. pneumoniae and *P. aeruginosa* were used as test organisms used to study the efficacy of monochloramine against biofilms. Some relevant characteristics of these two species are shown in Table 3. Pseudomonads are a major group of aerobic, motile gram negative rods with polar flagellae, that grow at temperatures up to 43°C. *P. aeruginosa* infections are also common in patients receiving treatment for severe burns. It is an opportunistic pathogen that causes urinary infections and is the primary infectious agent in patients with cystic fibrosis. Pseudomonads are also widely found in cooling water, industrial food processing, and drinking water systems.

Klebsiella pneumoniae, oragnism in the coliform group is found in the intestines of warm blooded animals. Coliforms are used to evaluate bacterial contamination of water, as their presence indicates possible fecal contamination of water.

Microbial interactions

Biofilm microbial communities are very diverse (LeChavellier et al (1990), Characklis and Marshall (1990)). Heterotrophic bacteria are widely present since they utilize dissolved carbon as their major energy source. Each biofilm present in industry has a different consortium which reflects source of water, nutrients, temperature and other factors (Sandholm et al (1992)). The processes that occur in a biofilm are complex and to determine the effect of

all these species on each other is almost an impossible task (Characklis and Marshall (1990)).

Table 3: Characteristics of *P. aeruginosa* and *K. pneumoniae* (Siebel et al (1991)

	K. pneumoniae	*P. aeruginosa*
Shape	rod shaped	rod shaped
Breadth (μm)	0.3 - 1.5	0.5 - 0.8
Length (μm)	0.6 - 6.0	1.5 - 4.0
EPS composition	glucose, fucose, glucuronic and pyruvic acid	mannuronic and guluronic acid
Motility	nonmotile	polar flagellum
Respiration	facultative anaerobic	obligate aerobe
Gram stain	negative	negative
Optimal temperature	35 - 37°C	35 - 37°C
Optimal pH	7.2	6.8
μ_{max} (hr^{-1})	2.0	0.4

Microbial interactions have been investigated in chemostats (Bailey and Ollis (1986)), which under certain conditions allow microorganisms to coexist. One such study (Bailey and Ollis (1986)) revealed an unstable system, where the species distribution varied according to pH and other environmental changes. Siebel et al (1991) have compared the growth and other related processes between mono and binary population biofilms of *P. aeruginosa* and *K. pneumoniae*. Although the two organisms compete for the same substrate and have different growth rates, they coexist in a biofilm. They also concluded that there seems to be no apparent interaction between the two species.

Most of the available literature cites the effect of antimicrobial agents on single species (Anwar et al (1992), Chen et al (1993), Wende (1991)) or undefined multi- species biofilm (LeChavellier et al (1990)). These studies do not reflect the effect of possible species interactions and composition. They do confirm the relative resistance of biofilms to disinfection in an array of systems.

Measures of biofilm activity

The efficacy of antimicrobial agents has traditionally been evaluated by colony formation on agar plates. This approach has severe limitations, since bacterial growth on a particular media is influenced by medium composition (Roszak et al (1987)), injury (McFeters (1990)) and dormancy (Kaperlyants et al (1993)). The recovery or regrowth (Chen et al (1993), Wende (1991)) phenomenon commonly seen in biofilm could be attributed to the overestimation of biocide efficacy by the plate count method. The direct viable count measurement (Yu et al (1993)) is a good technique to assess cell viability, but different organisms exhibit different responses to nalidixic acid and therefore the technique is unreliable for a mixed population biofilm . Some other methods used to measure biocide efficacy include bioluminescence (Walker et al (1992)), an impedimetric method (Dhaliwal et al (1992)), in situ microscopic method (Yu et al (1993)), and physiological probes (Rodrigruez et al (1992)). Respiratory indicators such as glucose and oxygen uptake rates could be used to measure biocide efficacy. However,

very little effort has been made to compare various assays of physiological activity to evaluate the performance of antimicrobial agents.

Factors affecting biocide efficacy

Various factors affect bactericidal action against microorganisms. The attached state of the organism may provide a physical and chemical barrier to biocide penetration (J.W Costerton et al (1987), Tashiro et al (1991)). Environmental parameters such as temperature and pH of the system (Cameron et al (1989)), the substratum on which the organism grows (Chen et al (1993), LeChavellier et al (1988)), and the presence of particles in a biofilm can have a significant effect (Whitman et al (1993)). The age of biofilms (Anwar et al (1992)) and the growth status of the bacteria are also thought to be important. All these studies indicate that the mechanism of biocide action cannot be depicted in simple terms. Rather they suggest a complex process and multiple factors affecting disinfection efficacy.

EXPERIMENTAL SYSTEM & METHODS

Rotating Annular Reactor

An annular reactor consisting of two concentric cylinders, a rotating inner cylinder and a stationary outer cylinder, was used in all experiments. The reactor was fabricated from polycarbonate. Twelve removable slides formed an integral part of the inside wall of the outer cylinder and permitted sampling of biofilms growing on them. The inner cylinder has four draft tubes drilled at an angle along the axis so that the centripetal acceleration caused by rotation forces liquid up through the angled tubes and promotes vertical mixing. The reactor approximates a completely mixed stirred tank reactor, so the effluent liquid samples represent the reactor bulk liquid composition. The reactor has a high surface area to volume ratio. The inner surface area upon which biofilm can grow is approximately 0.19 m^2, and the liquid volume is approximately 6.5×10^{-4} m^3.

The outer cylinder experiences a uniform shear stress since the annular gap is constant over the height of the reactor. Because shear stress is uniform and the reactor is well mixed, it is assumed that the biofilm from any of the twelve slides is a representative sample. The shear stress is dependent on the rotational speed of the inner cylinder, but is independent of the fluid flow rate. The rotational speed was 150 rpm in all experiments, corresponding to a uniform shear stress of approximately 1.4 N/m^2 (Chen et al (1993)). The residence time was 17 mins at a flow rate of 32 mL/min.

Nutrient Media and Start up

Stainless steel slides (316L) were immersed in a solution containing acetone and cleaned later with ethanol before aligning them in the reactor. The reactor and all the system components were autoclaved at 121°C for 25 mins. The composition of the nutrient media is tabulated in Table 4. The composition shown is the final concentration that enters the reactor, after dilution. The medium was continuously formulated by mixing nutrients (1 mL/min), buffer (1 mL/min) and dilution water (30 mL/min) solutions. Nutrient and buffer solutions were autoclaved before connecting them to the system through silicone tubing (Masterflex 6411-14 and 6411-16). Glucose was added to the nutrient solution after filter sterilization through 0.2 μm Gelman Sciences filter (Chen et al (1993)). Dilution water was similarly passed through two Gelman Sciences filters (0.2 μm). The reactor was continuously fed using peristaltic pumps (Masterflex 7553-30, Cole-Parmer). During disinfection studies the buffer solution was replaced by biocide that was prepared in a phosphate buffer solution. The temperature of the system was maintained at 25 $\pm$ 0.5°C. The system was set up as shown in Figure 1. Flow was started and the reactor was ready for inoculation.

To inoculate, the reactor was filled with medium, then flow was stopped. To obtain a binary population biofilm, one mL each of frozen stock cultures of *P. aeruginosa* and *K. pneumoniae* (10^8 cells/mL) were dosed into

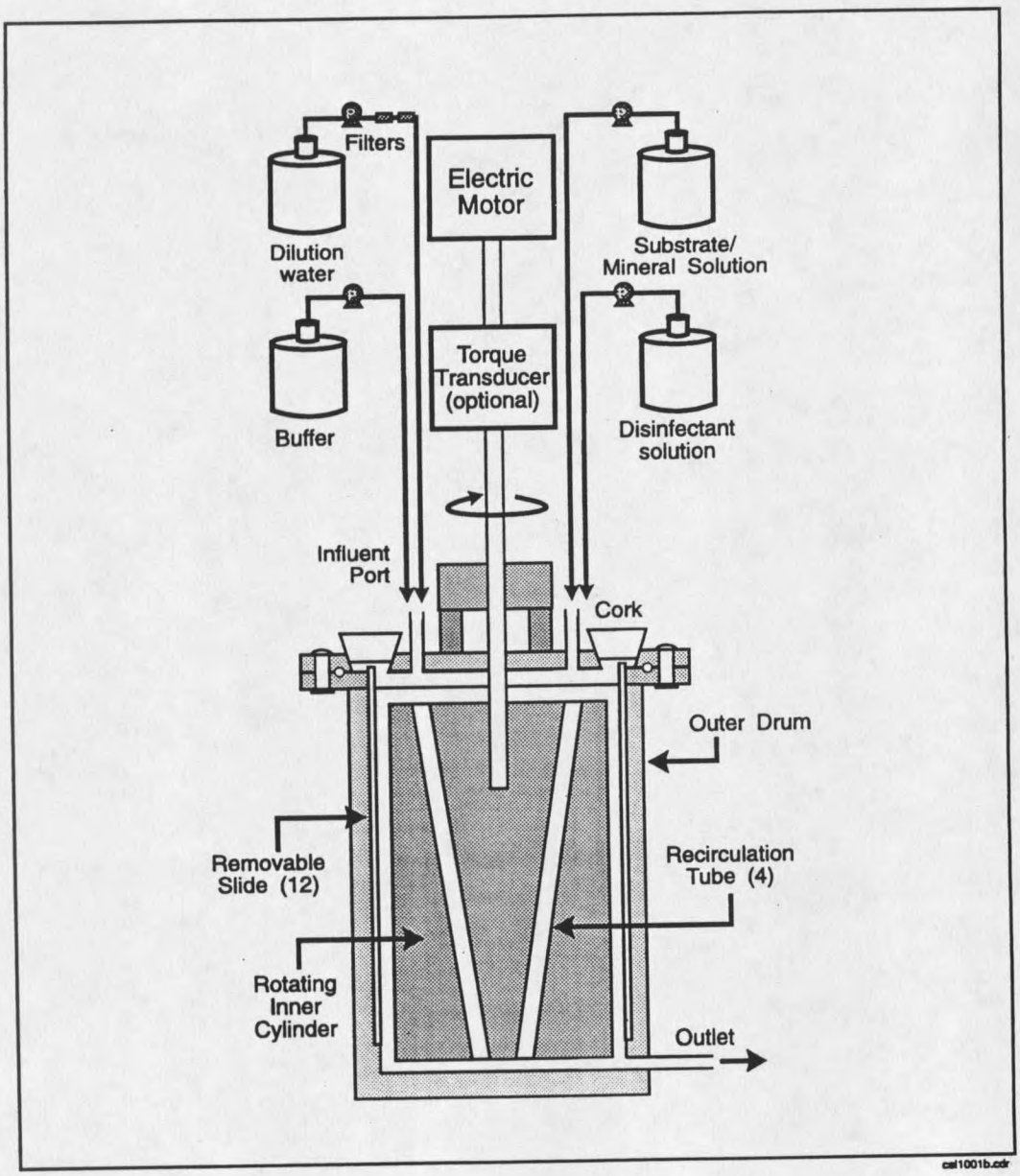

Figure 1 Schematic representation of the annular reactor system.

the reactor. For the development of pure culture biofilms of *K. pneumoniae* or *P. aeruginosa,* the inoculum consisted of the respective single culture. The cells were allowed to grow and attach in batch mode for about 24 hrs. The inner drum was rotating throughout this incubation period. The influent flows to the reactor were then started. The high dilution rate in the reactor quickly washed out unattached cells. Two reactors were started simultaneously.

Sampling of the Reactor

The reactor effluent was sampled daily to check for contamination and to monitor growth. The reactor was allowed to run for about 6 to 14 days before the addition of the biocide. Biofilm and bulk fluid were sampled during the disinfection process.

Biocide addition and sampling

Monochloramine at 4 mg/L was dosed into the reactor by a combined pulse and step procedure. In experiments in which the biofilm was sampled, monochloramine was supplied continuously for a period of two hours. In experiments in which the bulk fluid was sampled, monochloramine was supplied for a period of one hour. A portion of the sample obtained during bulk fluid sampling was used to determine monochloramine concentration using a test kit (Hach).

Biofilm sampling

Biofilm slides from the reactor were removed periodically to analyze the

Table 4 Composition of the nutrient media

Substance	Concentration
Glucose ($C_6H_{12}O_6$)	20 mg/L
Potassium Nitrate (KNO_3)	13.6 mg/L
Magnesium Sulphate ($MgSO_4.7H_2O$)	1.0 mg/L
Ammonium Molybdate ($(NH_4)6Mo_7O_{24}.4H_2O$)	1.4 mg/L
Zinc Sulphate ($ZnSO_4.7H_2O$)	142 μg/L
Manganese sulphate ($MnSO_4.7H_2O$)	11.4 μg/L
Copper Sulphate ($CuSO_4.5H_2O$)	2.8 μg/L
Sodium Borate ($Na_2B_4O_7.10H_2O$)	1.4 μg/L
Ferrous Sulphate ($FeSO_4.7H_2O$)	159 μg/L
Nitrilo acetic acid ($(HOCOCH_2)_3N$)	200 μg/L
Calcium Carbonate ($CaCO_3$)	1.0 μg/L
Cobalt Nitrate ($CO(NO_3)_2.H_2O$)	2.3 μg/L
Potassium Phosphate (K_2HPO_4)	205 mg/L
Sodium Phosphate ($NaHPO_4$)	426 mg/L

biofilms during treatment. They were scraped using a cell scraper into 150 mL of phosphate buffer solution which also contained 0.01% sodium thiosulfate as a neutralizer. The solution was then homogenized for 3 mins using a tissue homogenizer (Tekmar). Aliquots were taken to obtain plate counts on R2A agar, total cells by acridine orange direct count (AODC), and total organic carbon (TOC).

Bulk fluid sampling

The effluent of the reactor was monitored during biocide treatment. Around 60 mL of the effluent was collected in a sterilized beaker containing 0.01% sodium thiosulfate. 20 mL of the sample was centrifuged to obtain glucose and soluble organic carbon concentrations. The remaining 40 mL of sample was homogenized, and aliquots were taken to obtain plate counts, total cell counts, and TOC.

Abiotic particle study

Kaolin and calcium carbonate were added to biofilms in two experiments to assess their impact on efficacy of the biocide. In the first experiment, 1.0 g/L of each material was added to a week-old biofilm for 1 hour. Biocide was added after the particles were washed out in the bulk fluid for about one hour. Biofilm slides were periodically removed to obtain plate count data. In the second experiment particles were added continuously during biofilm development. 50 mg/L each of $CaCO_3$ and kaolin were fed into the reactor along with the medium. The disinfection study was conducted on a

week-old biofilm. Biofilm slides were removed periodically to obtain plate count data.

Flow Cell

The apparatus used for the measurement of oxygen concentration profiles in the biofilm during monochloramine treatment is illustrated in Figure 2. The flow cell had dimensions of 2 x 2.5 x 20 cm and was made of oven heated polycarbonate so that it could be autoclaved. The system was thoroughly cleaned and purged with sterilized medium before the start of the experiment. The effluent of the annular reactor was connected to the flow cell influent. The recycle ratio in the flow cell was very high thus enabling the system to be treated as a CSTR. The residence time in the reactor was 3 minutes, which is short enough to neglect the effect of cells in the bulk phase. The microelectrode used for the experiment was calibrated by equilibrating with N_2, air, and pure O_2 prior to use. The electrode did not exhibit any demand for NH_2Cl nor did NH_2Cl interfere with oxygen measurement. A week old biofilm slide from the reactor was immersed into the flow cell. The measurements were taken after a steady state fluid flow and bulk oxygen concentration were attained. The steady state flow conditions could be theoretically achieved if the fluid is passed through the reactor at least 3 residence times.

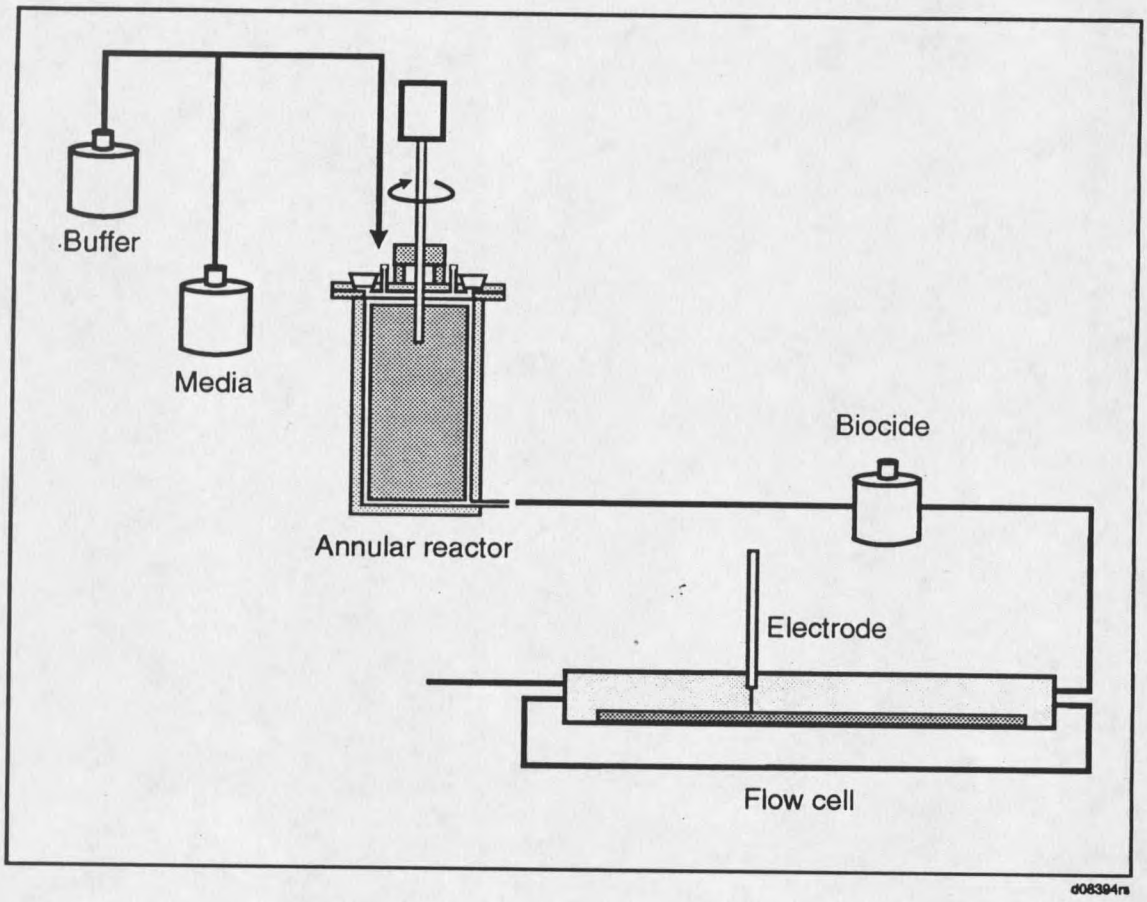

Figure 2 Schematic representation of flow cell arrangement used to measure oxygen profiles in the biofilm during monochloramine treatment.

Analytical Methods

Plate counting

Culturable cells were determined by serial dilution and plating. The tubes used for serial dilution were cleaned and autoclaved for 30 mins. The tubes were filled with 9 ml of sterile buffer solution, which consisted of phosphate buffer and 0.01% of sodium thiosulfate as a neutralizer for monochloramine. The agar media used for plate counting was R2A (Difco) agar. Plates were poured 4 to 5 days prior to usage, then screened for contamination before use.

The homogenized solution was diluted using serial dilution tubes and spread plated on R2A plates in triplicate for each dilution. The plates were incubated at 35°C for 24 hrs before enumerating the colony forming units.

Total cell count

The part of the sample obtained for total cell counts was fixed with 2% formaldehyde. The cells were double stained with acridine orange (AO) and 4'-6-diamidino-2-phenylindol (DAPI) and then examined as follows.

A polycarbonate membrane (Nucleopore) with a pore size of 0.2 μm and a diameter of 25 mm was placed on a cell-free glass filter apparatus (Millipore). 1 mL of the sample was slowly dropped on the filter membrane with the suction off, the solution was stained with 0.5 mL of DAPI solution (5 μg/L) for 10 mins, then counter stained with AO (5 μg/L) for 2-3 minutes. The solution on the membrane was next filtered using a vacuum pump. The

membrane was washed with 2-3 mL of filtered PBS and water to remove excess stains. The polycarbonate membrane was removed and placed on the microscope slide using a drop of FF immersion oil. The membrane was covered with a cover slip. The sample was sealed with ordinary clear nail polish, and the slides could be stored without any loss of fluorescence for up to 6 months. Total cells were enumerated microscopically (Olympus BH2). At least 20 fields were examined to obtain the average areal distribution of cells on the membrane.

TOC

Glass vials used for collecting samples for organic carbon analysis were preheated in a muffle oven at 500°C to eliminate any contaminants and organics. Once collected, samples were acidified to pH 2.0 with 10% phosphoric acid, then stripped with O_2 to remove CO_2. Samples were then analyzed using a Dohrman DC-90 Carbon Analyzer in accordance with operating instructions. Samples were analyzed in triplicate (0.2 mL injection).

SOC

Twenty mL of the sample obtained during bulk fluid disinfection was centrifuged in a Sorvall RC-5C automatic super speed refrigerated centrifuge at 20,000 rpm for 20 mins. The supernatant (5-6 mL) was taken as a sample for TOC analysis, which in turn gave the amount of soluble organic carbon (SOC) present. The sample was refrigerated at 4°C until analyzed.

Glucose

The supernatant (7-8 mL) of the remaining centrifuged solution was used for glucose analysis. Glucose concentration was determined using a commercially available test kit (Sigma Diagnostics). The preparation of the glucose standard solution and the method used to obtain glucose concentrations were in accordance with instructions.

Monochloramine

Monochloramine was the biocide used in all the experiments. The preparation procedure involved maintaining a 3:1 molar ratio of ammonia to free chlorine (Chen et al (1993)). The formulation is described below.

Five mL of 5.25 % HOCl (Clorox) was dissolved in 500 mL of distilled water to obtain 0.01 N of free chlorine. 0.788 gms of ammonium chloride was dissolved in 500 mL of distilled water. This gave a concentration of 0.03 N which is three times higher than the HOCl solution. The pH of the ammonium chloride solution was adjusted to 9.0 and the hypochlorite solution was gently added with continuous stirring, pH was maintained at 9.0. The reaction was allowed to go to completion by mixing the solutions for about 30-45 mins. The final concentration of monochloramine was approximately 260 mg/L. This was verified using a Hach test kit for determination of free and total chlorine in a solution. Monochloramine is the only form of combined chlorine present around pH 9.0 (Water Chlorination (1984)), therefore the total chlorine concentration reflects the amount of

reflects the amount of monochloramine present.

The Hach test kit for determination of free and total chlorine concentrations was used in all the experiments. 5 mL of sample solution was taken in a test tube as blank. Another 5 mL was taken in second test tube, to which the reagent pill was added. The reaction was instantaneous and the color change (gauged by eye) indicated directly the concentration of monochloramine.

Oxygen microelectrode

The dissolved oxygen (DO) microelectrode as shown in Figure 2 was made up of a 0.1 mm high purity (99.99%) platinum wire etched electrochemically (with one end in KCN) to a tip diameter of about 2 μm. The wire was rinsed with concentrated HCl and ethanol and covered with soda-lime glass. The tip of the platinum wire was exposed by grinding on a rotating diamond wheel. The exposed platinum tip was subsequently etched in KCN to yield a recess of about 10 μm. Half of this recess was filled with gold by electrochemical plating. The operation was performed under a microscope with a mounted TV camera and observed on a video screen. The tip of the electrode was covered with a thin layer of polymer (TePeX) to serve as the oxygen permeable membrane. The measuring setup consisted of a picoammeter and a polarizing voltage source. The microelectrode was cathodically polarized to 800 mV, against a silver/silver chloride reference electrode. The current in the circuit, in the range of picoamperes, is proportional to the concentration

of dissolved oxygen. The electrode was calibrated in water equilibrated with N_2, air, and pure O_2. The current is typically 10-30 pA for N_2 and 70-400 pA for air. Before the measurement the microelectrode was mounted on a micromanipulator and moved across the biofilm at predetermined increments. After each stop the current in the system was measured and compared with the calibration curve to calculate the dissolved oxygen concentration (Lewandowski et al (1991)).

Confocal imaging

Binary population biofilm developed in the presence of particles was observed using a confocal laser microscope. The binary population biofilm was grown in an annular reactor for a week. The biofilm slide was taken from the reactor and transferred to a sterile water solution. The biofilm was viewed under a MRC BIO-RAD Confocal Scanning Laser Microscope equipped with krypton or argon laser (568 nm) and the images captured by using BIO-RAD cosmos software. Images were taken and stored on this sample using reflected light. The biofilm was then stained with propidium iodide at 1 μg/L for about 30 minutes to obtain images of total cells at the same spot as reflected light images. The images were superimposed and unstained mass was believed to be the particles. Thus the overall distribution of particles and cells were observed in the biofilm system.

THEORETICAL APPROACH

This section presents the theoretical basis applied for analysis of experimental data. The reactor system was treated as a continuous stirred tank reactor (CSTR). Material balance equations were applied to determine various rate coefficients as indicators of disinfection efficacy.

The following assumptions were used to solve the equations.

i) The reactor is well mixed.

ii) The dilution rate is high enough that planktonic growth can be neglected. The biomass monitored in the effluent stream, therefore, reflects only detached biofilm cells.

iii) The consumption of substrate and biocide is wholly due to biofilm.

iv) First order decay and reaction rates are assumed.

v) Cell growth is negligible compared to decay during biocide treatment.

Decay rate coefficients

Three types of decay rates were estimated to evaluate the efficacy of the biocide against biofilms. These are the overall decay rate coefficient (D_{de}), the detachment rate coefficient (D_{det}), and the disinfection rate coefficient (D_{di}). First order decay is assumed in evaluating the decay parameters.

Overall decay rate coefficient (D_{de})

This parameter was evaluated using the plate count data obtained during the study of biofilm disinfection and removal. The equation used to estimate the rate coefficient was

$$\frac{dX_{bV}}{dt} = -D_{de}\, X_{bV} \qquad (1)$$

where X_{bV} (cfu/m^2) is the biofilm viable cell density, and D_{de} (hr^{-1}) is the decay rate coefficient. Integrating we obtain an equation of the form

$$X_{bV} = X_{bVo} \exp(-D_{de} t) \qquad (2)$$

Where X_{bvo} is the cell density at time zero. The natural logarithm of X_v/X_{vo} was plotted against time t. A least squares regression analysis was performed on the resulting curve to estimate D_{de}.

Detachment rate coefficient (D_{det})

This parameter was estimated using the total cell count obtained during biofilm disinfection and removal experiments and applying an approach analogous to that described above. For total cells,

$$X_{bT} = X_{bTo} \exp\,(-D_{det} t) \qquad (3)$$

where X_{bTo} (#/m^2) is the initial total cell number before biocide addition, X_{bT} is the cell density at a particular time, and D_{det} (hr^{-1}) is the detachment rate coefficient.

Disinfection rate coefficient (D_{di})

The decay rate coefficient is the sum of the detachment rate coefficient (D_{det}) and disinfection rate coefficient (D_{di}). The disinfection rate coefficient is calculated from the equation

$$D_{dl} = D_{de} - D_{det} \quad (4)$$

Glucose uptake rate (R_S)

A mass balance of substrate in the system was performed and used to obtain the specific glucose consumption rate. The macroscopic balance on substrate is

$$V\frac{dS}{dt} = Q(S_o - S) - \mu\frac{X_{eV}}{Y_{XS}}V - R_S A \quad (5)$$

where V (m^3) is the volume of the reactor, Q (m^3/hr) is the volumetric flow rate, S_o (g/m^3) is the influent substrate concentration, μ (hr^{-1}) is the specific growth rate, X_{eV} (cfu/m^3) is the bulk fluid viable cell concentration, S (g/m^3) is the effluent substrate concentration, Y_{XS} is the yield coefficient, R_S (g/m^2-hr) is the specific glucose uptake rate, and A (m^2) is the biofilm surface area in the reactor. The dilution rate, $D = Q/V$ (hr^{-1}) in the reactor being very high, the effect of planktonic growth can be neglected. In addition, decay predominates growth during disinfection. Eliminating the planktonic cell term the equation becomes

$$\frac{dS}{dt} = D\,(S_o - S) - R_S\,\frac{A}{V} \qquad (6)$$

A second order quadratic polynomial fit was performed on the S versus t data. The polynomial equation obtained was differentiated to obtain the value of dS/dt, allowing the remaining unknown, R_S, to be calculated.

Detachment rate (K_d)

The mass balance on biomass in the system permits evaluation of K_d, the detachment rate. The effect of planktonic cells again being neglected yields

$$V\,\frac{dX_{eT}}{dt} = r_d - Q\,X_{eT} \qquad (7)$$

where V (m^3) is the volume of the reactor, X_{eT} (#/ml) is the total cell concentration in effluent stream, Q (m^3/hr) is the volumetric flow rate, where r_d (#/hr) is expressed as

$$r_d = K_d\,A \qquad (8)$$

where K_d (#/m^2-hr) is the detachment rate.

$$\frac{dX_{eT}}{dt} = K_d\,\frac{A}{V} - D\,X_{eT} \qquad (9)$$

A second order polynomial fit to the curve of X_{eT} vs t was differentiated to give the value of the accumulation term. K_d could then be obtained since it is the only unknown parameter in the equation.

Monochloramine uptake rate (R_M)

The mass balance on the biocide, monochloramine, yields an estimate of the monochloramine consumption rate. Monochloramine consumption by planktonic cells is neglected since biofilm organisms far outnumber planktonic bacteria.

The differential mass balance on monochloramine is

$$\frac{dM}{dt} = D\,(M_o - M) - R_M \frac{A}{V} \qquad (10)$$

where M_o and M are the influent and effluent monochloramine concentration (g/m^3), A (m^2) is the surface area of the biofilm, D (hr^{-1}) is the dilution rate, and R_M (g/m^2-hr) is the monochloramine consumption rate.

The M versus t data were split into two curves, since there was a steep drop of concentration in the first 5 mins. The first portion between zero and 5 minutes was fit with a line. The portion of the curve between 5 and 60 mins was fit to a second order polynomial. The fit equations were differentiated to obtain dM/dt. Since the only unknown parameter in the equation is R_M, it could be calculated.

Oxygen flux ratio

An oxygen microelectrode was used to obtain profiles of oxygen concentration in the biofilm during biocide treatment in the flow cell (Figure 2). The oxygen flux into the biofilm is calculated by using the equation,

$$J = D_{O_2} \frac{(C_o - C)}{L_f} \qquad (11)$$

Where J (g/m^2-hr) is the flux of oxygen into the biofilm, D_{O2} (m^2/hr) is the diffusion coefficient of O_2 in bulk fluid, C_o is the bulk fluid oxygen concentration in the flow cell and C is the concentration of O_2 at the biofilm surface both expressed as g/m^3, and L_f (m) is the concentration boundary layer or thickness in the system. The fluid dynamics being the same during the experiment, L_f is assumed to be a constant. Since L_f is not known, the ratio of oxygen fluxes was used to assess the effect of monochloramine. The flux ratio was found to be insensitive to assumed biofilm thickness values. The oxygen flux ratio at any time t is obtained by dividing the flux at time t by the flux at time zero. This is expressed as

$$\frac{J(t)}{J(0)} = \frac{(C_o - C(t))}{(C_o - C(0))} \qquad (12)$$

RESULTS

This section reports the results of monochloramine disinfection experiments of binary and monopopulation biofilms. Two types of analysis were performed: on the biofilm and on the reactor effluent. Biofilm analysis consisted of analyzing biofilm slides for plate and total cell counts. These data were used to obtain overall decay and detachment rate coefficients. Reactor effluent was analyzed for total cell counts, glucose concentration and monochloramine concentration. The effluent data were used to obtain detachment and consumption rates, respectively. The results section is divided into three subsections. The first subsection reports results of biofilm analysis pertaining to overall biofilm disinfection and removal. The second subsection focuses on the effect of abiotic particles on disinfection. The third subsection compares mono and binary population biofilm systems using both biofilm and effluent data.

Overall biofilm disinfection and removal

During monochloramine treatment the net decay rate of biomass is obtained from plate count data and the detachment rate of cells from the biofilm is obtained from AODC counts. The net decay is the combined processes of detachment and disinfection.

The net decay of cells during treatment in a binary population biofilm with 4 mg/L monochloramine based on R2A counts is shown in Figure 3. Viable cell counts for biofilm of 10^{11} cfu/m^2 initial cell density decreased by

2.5 log, viable cell counts for biofilms starting at 10^{12} cfu/m^2 decreased by 3.5 log, while the cell counts in a biofilm of 10^{14} cfu/m^2 initial cell density decreased by only 20%.

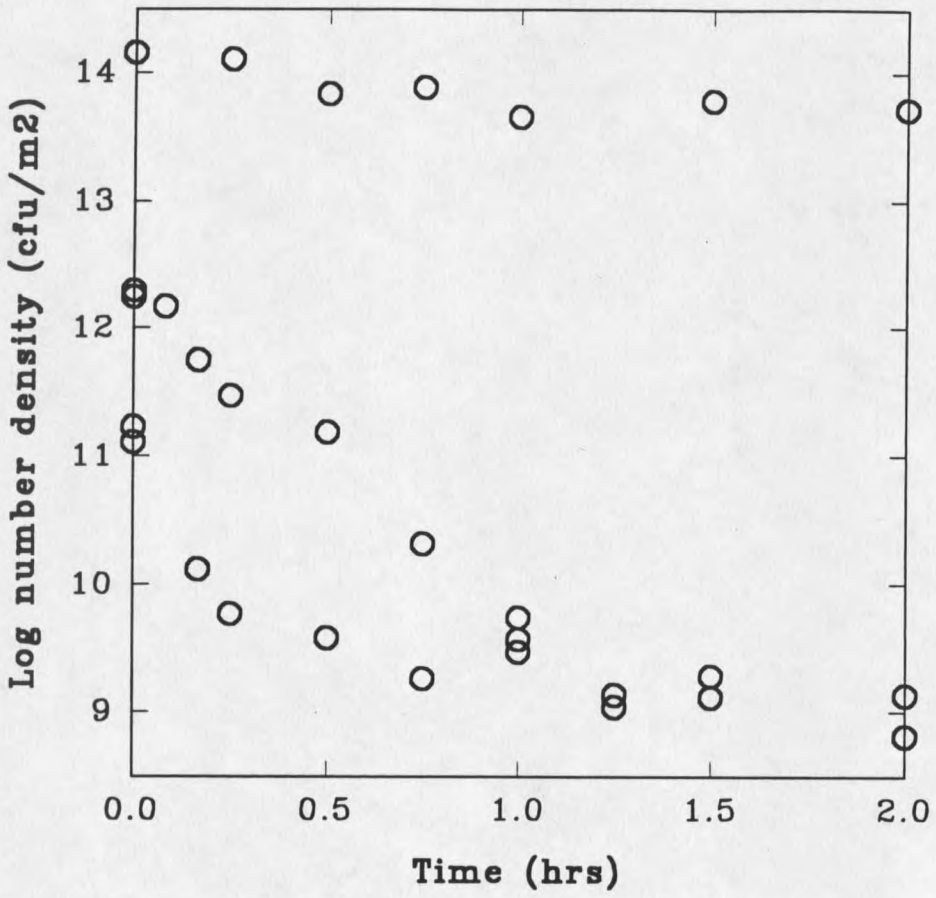

Figure 3 Viable areal cell density of binary population biofilm during disinfection with monochloramine. Three different runs are shown each with a different initial cell density.

The total cell count data (Figure 4) reflect the effect of monochloramine on detachment of cells from the biofilm. The total cell number decreased by approximately 10 to 50% during biocide treatment.

Tables 5 through 9 summarize the calculated overall decay, detachment, and disinfection rate coefficients for all three types of biofilm systems. In these tables, X_{vo} is the initial viable cell density, f_P is the fraction of *P. aeruginosa* in the biofilm, and *SE* is the standard error of the slope.

Table 5 shows the calculated overall decay rate coefficient, which is obtained by performing a linear regression on plate count data. The slope of the line gives the decay rate coefficient. The decay is highest for initial cell densities around 10^{12} cfu/m^2, but decreases at lower or higher initial cell densities.

Table 5 Overall decay rate coefficients (D_{de}). These rates are obtained by performing a linear fit to the summed plate count data for all species.

log X_{vo} (cfu/m^2)	f_P	D_{de} (hr^{-1})	r^2	SE
14.16	0.23	0.498	0.64	0.167
13.26	0.01	0.38	0.38	0.198
12.57	1.0	5.96	0.752	1.2
12.56	0.834	5.88	0.92	0.55
12.29	0.812	4.56	0.93	0.41
12.04	0	5.28	0.87	1.78
11.23	0.212	2.08	0.624	0.48
11.15	0	1.34	0.41	0.51
10.98	0	1.28	0.57	0.414

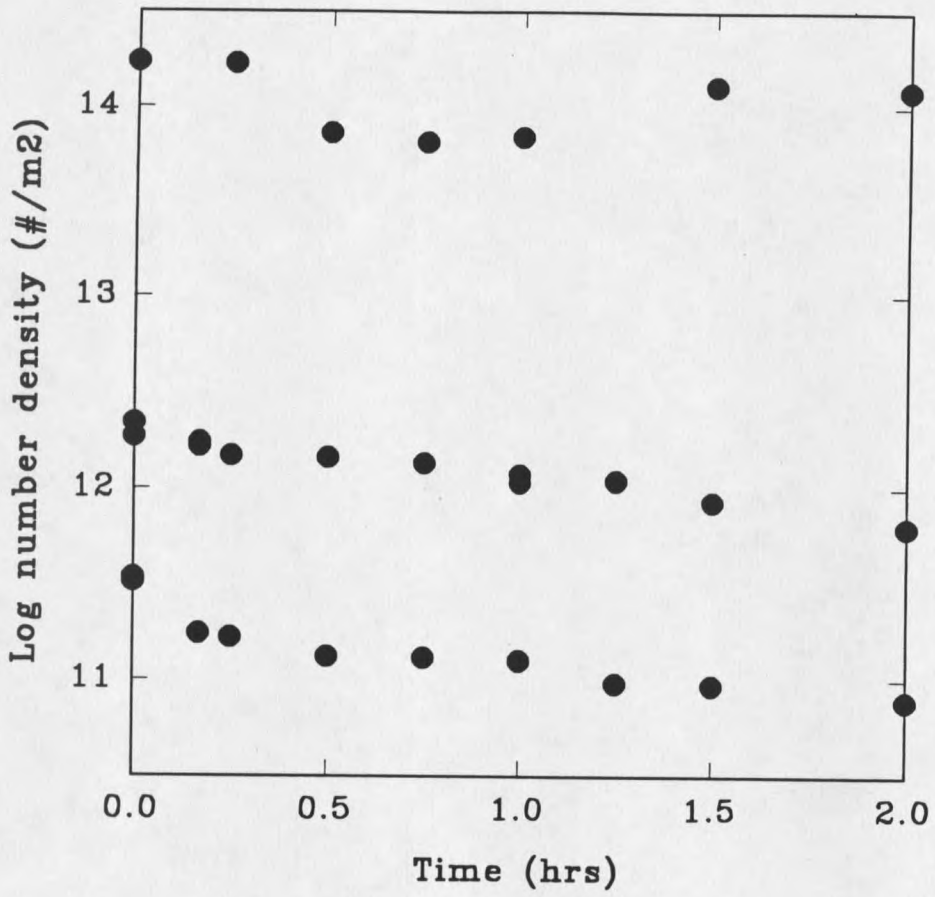

Figure 4 Total areal cell density of binary population biofilm during disinfection with monochloramine. Three runs are shown.

Table 6 reports the detachment rate coefficients obtained by performing linear regression on total cell count data.

The disinfection rate coefficient is just the difference between the decay and detachment rate coefficients. As shown in Table 7, disinfection rate coefficients were generally larger than detachment rate coefficients.

Abiotic particle study

The effect of the presence of abiotic particles (kaolin and calcium carbonate) in the biofilm on biocide efficacy against binary population biofilms is shown in Figures 5 and 6. Two methods of developing the biofilms were used. In the first study, the particles were added to a mature biofilm for a period of one hour, and were washed from the bulk liquid for an hour before the addition of biocide. Monochloramine was added for one hour and biofilm plate count data were obtained during this period. As shown in Figure 5, a biofilm without the particles experienced a decrease in viable cell number of about 2.5 log. The decrease in viable cell number for a biofilm of similar initial areal cell density with the particles was only about 1.5 log.

In the second study, biofilm was developed in the continuous presence of particles. As shown in Figure 6, the decrease in viable cell number for biofilms without particles was about 3 log. Viable cell number decreased for biofilms with the particles by about 2 log. The solution containing the particles had a demand of 0.2 mg/L for monochloramine. Statistical analysis of these data are presented in the discussion section. In

summary, the efficacy of the disinfectant was reduced by these particles.

Table 6 Overall detachment rate coefficient (D_{det}). These rates are obtained by performing a linear fit to the total cell count data for all species

log X_{vo} (cfu/m^2)	f_P	D_{det} (hr^{-1})	r^2	SE
14.16	0.23	0.097	0.026	0.266
13.26	0.01	0.354	0.73	0.09
12.57	1.0	0.091	0.42	0.09
12.56	0.834	0.52	0.95	0.037
12.29	0.812	0.34	0.85	0.049
12.04	0	1.79	0.87	0.26
11.23	0.212	0.65	0.82	0.107
11.15	0	0.34	0.29	0.168
10.98	0	0.65	0.57	0.414

Table 7 Overall disinfection rate coefficient (D_{dis}). These rate coefficients are obtained as the difference between overall decay and detachment rate coefficients.

log X_{vo} (cfu/m^2)	D_{dis} (hr^{-1})
14.16	0.4
13.26	0.026
12.57	5.87
12.56	5.36
12.29	4.22
12.04	3.49
11.23	1.43
11.15	1.0
10.98	0.63

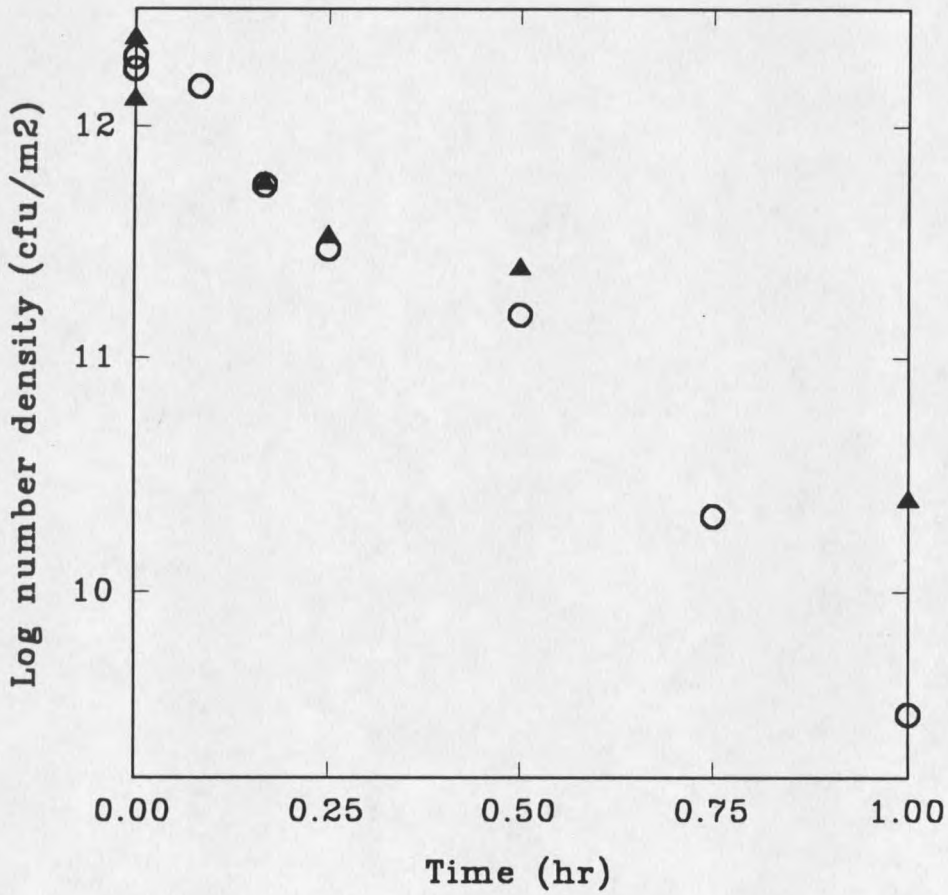

Figure 5 Comparison of viable cell number during disinfection with monochloramine of binary population biofilms with (▲) and without particles (○). The abiotic particles were added to a mature biofilm.

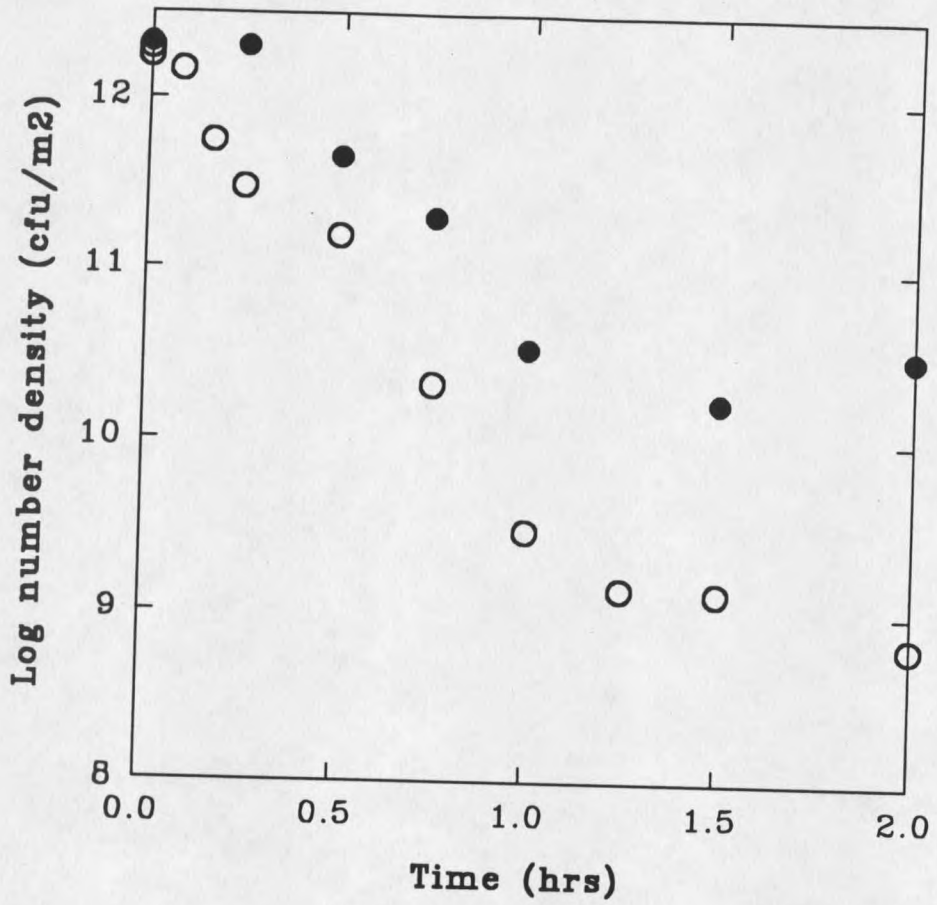

Figure 6 Comparison of viable cell number of binary population biofilms during monochloramine treatment with (●) and without particles (○). The biofilm was developed in the continuous presence of particles.

Comparison between mono and binary population biofilms

In this study comparison was made between the three types of biofilm systems with respect to both biofilm and bulk fluid dynamics.

Biofilm decay

Figure 7 shows the efficacy of monochloramine against *K. pneumoniae* in mono and binary population biofilms of similar initial cell densities. The drop in viable cell number of *K. pneumoniae* in the mono population biofilm is approximately 4.5 log compared with 4.75 log in the binary population biofilm. The binary population biofilm was composed of 78% *P. aeruginosa*. Table 8 gives the overall decay rate coefficient of *K. pneumoniae* in the mono and binary population biofilms. The decay rate coefficient was highest at cell densities near 10^{12} cfu/m^2 and lower at either extreme.

Figure 8 shows the efficacy of monochloramine against *P. aeruginosa* in mono and binary population biofilms of similar cell densities. Both mono and binary population biofilms experience a 4 log decrease in viable counts. Table 9 gives decay rate coefficients of *P. aeruginosa* in mono and binary population biofilms.

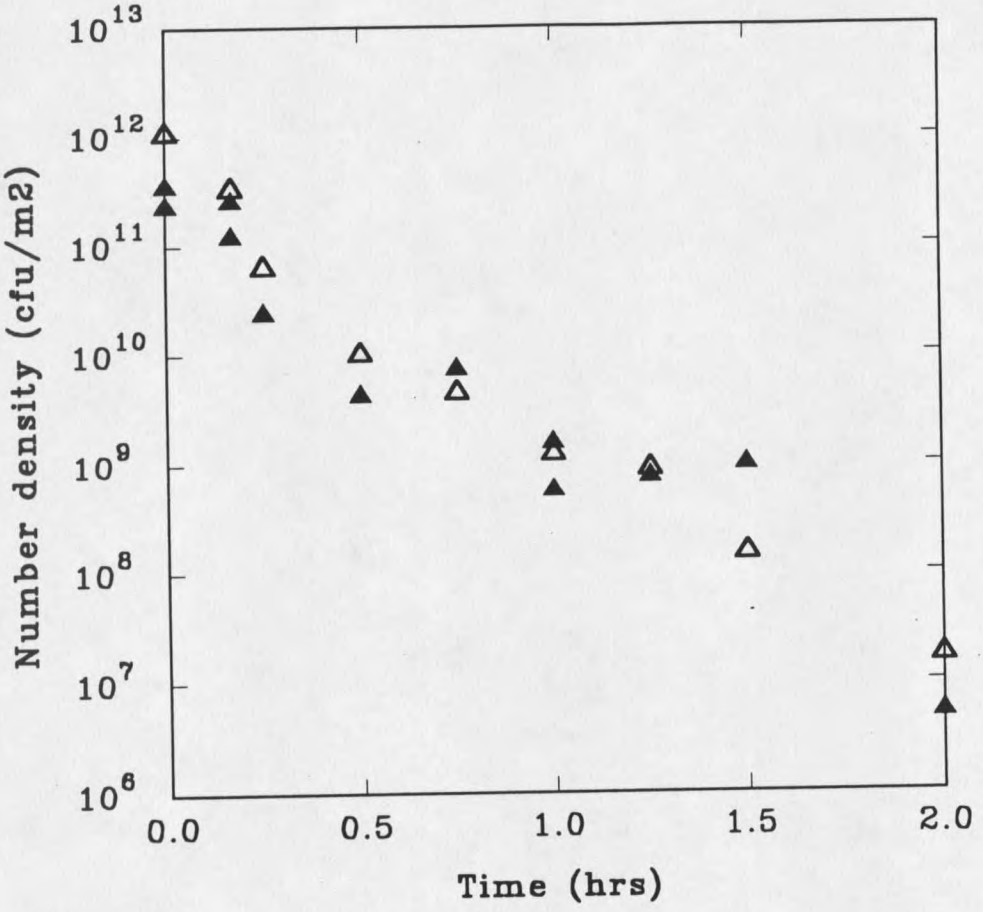

Figure 7 Comparison of viable cell areal density of *K. pneumoniae* in mono (△) and binary population biofilms (▲). The biofilms were approximately of the same initial cell density.

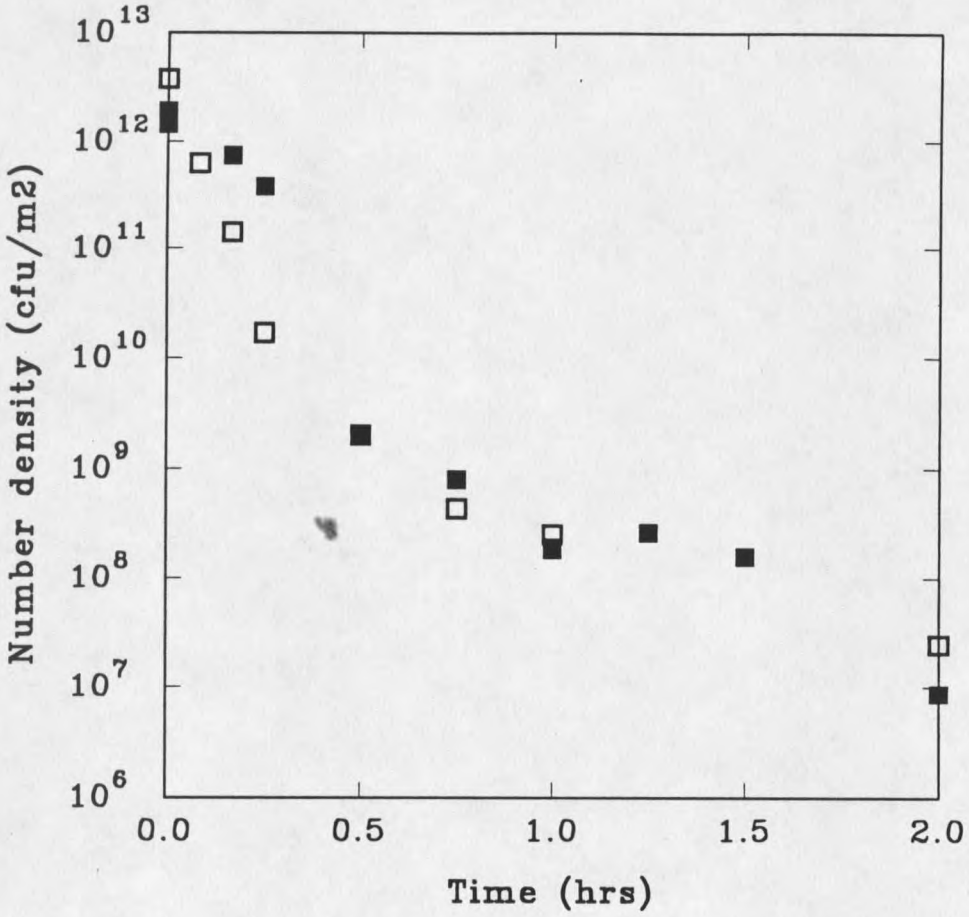

Figure 8 Comparison of viable cell areal density of *P. aeruginosa* in mono (□) and binary population biofilms (■). The biofilms were approximately of the same initial cell density.

Table 8 Decay rate coefficient (D_{de}) of *K. pneumoniae* in mono and binary population biofilms

log X_{vo} (cfu/m^2)	f_P	D_{de} (hr^{-1})	r^2	SE
14.16	0.23	0.39	0.6	0.12
13.26	0.01	0.38	0.38	0.198
12.56	0.812	2.22	0.92	0.204
12.29	0.834	3.39	0.94	0.29
12.04	0.0	5.28	0.87	1.79
11.23	0.212	2.02	0.62	0.52
11.15	0.0	1.34	0.41	0.51
10.98	0.0	1.28	0.57	0.41

Table 9 Decay rate coefficient (D_{de}) of *P. aeruginosa* in mono and binary population biofilms.

log X_{vo} (cfu/m^2)	f_P	D_{de} (hr^{-1})	r^2	S.E
14.16	0.23	1.74	0.8	0.39
13.26	0.01	0.33	0.26	0.22
12.57	1.0	5.96	0.75	1.2
12.56	0.812	6.51	0.88	0.756
12.29	0.834	10.43	0.96	0.78
11.23	0.64	2.76	0.212	0.68

Glucose consumption

The effluent glucose concentration during 1 hour of monochloramine treatment is shown in Figure 9 for three different runs with binary population biofilms. The glucose concentration is represented in terms of carbon. During biocide treatment the rise in the concentration of glucose as monitored in the effluent of the reactor is small. An increase of only 1.5 to 2 mg/L was observed compared to the influent glucose concentration of 8 mg/L. The overall glucose consumption rate was calculated from these data using Equation 6 and is shown in Figure 10. The rate is plotted as a fraction of the initial rate. The drop in the ratio indicates that glucose consumption was reduced, but only by about 25% . This is much less than the 99% decrease observed in viable plate counts.

Figure 11 shows the effluent glucose concentration during monochloramine treatment in reactors with *K. pneumoniae* biofilms. Two different runs are represented on the figure. The glucose level rose to around 40-50% of its influent value after one hour of treatment. Calculated normalized glucose consumption rates are shown in Figure 12. The glucose consumption rate decreased to around 20 to 40% of its initial value. Both runs follow the same trend.

Figure 13 shows the effect of monochloramine on glucose concentration in the effluent of reactors with *P. aeruginosa* biofilm. The glucose concentration rose to its influent level during one hour of treatment.

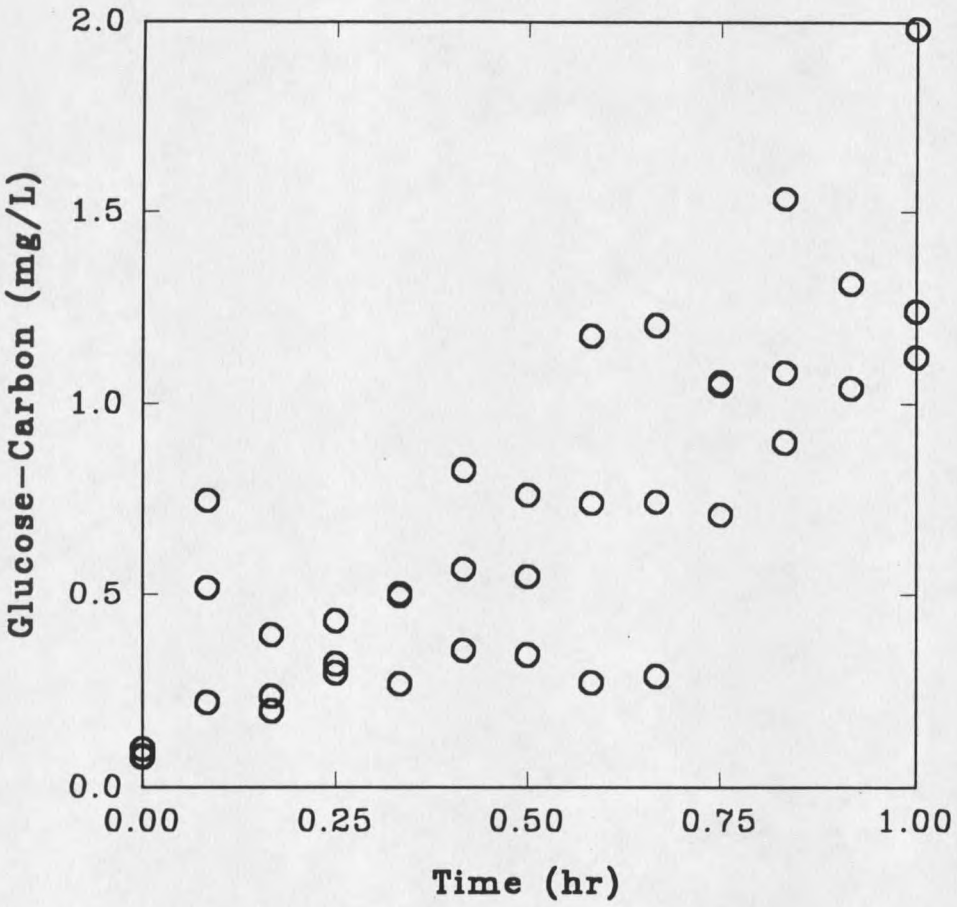

Figure 9 Effluent glucose concentration in binary population biofilm reactors during monochloramine treatment for 1 hr. Three runs are represented on the figure.

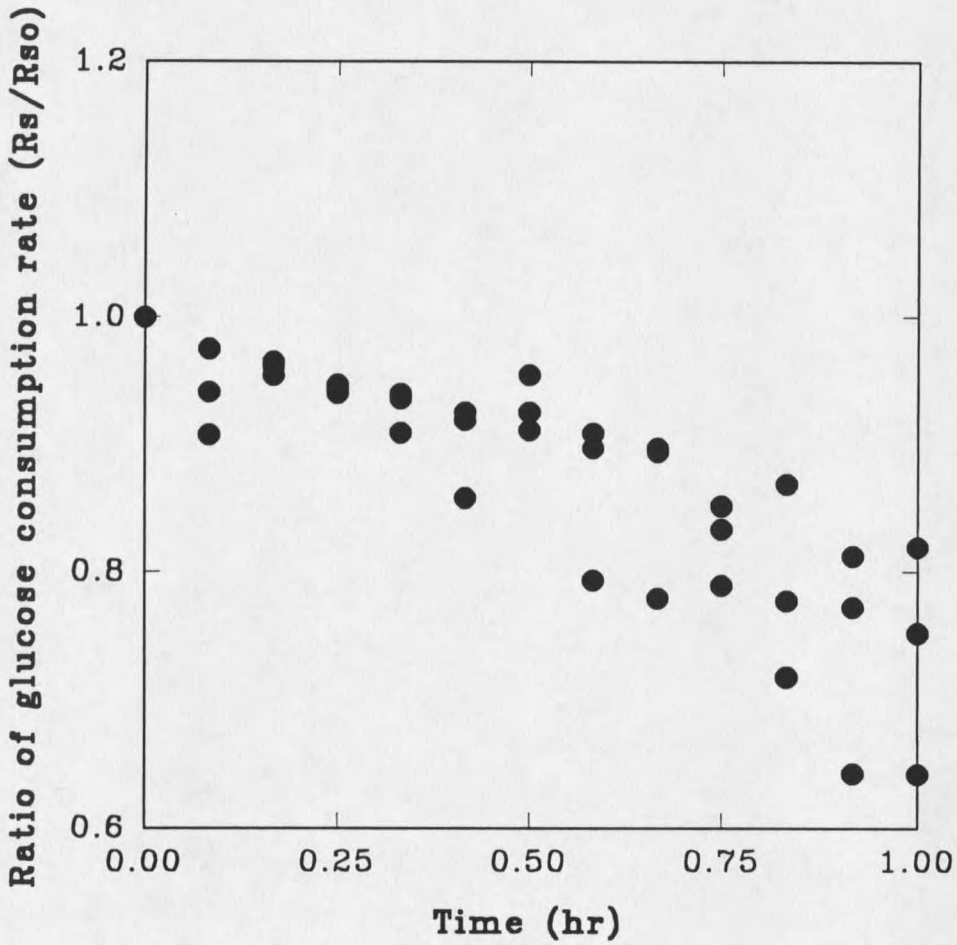

Figure 10 Calculated ratio of glucose consumption rate in binary population biofilms during monochloramine treatment for 1 hr. Data for three experiments are shown.

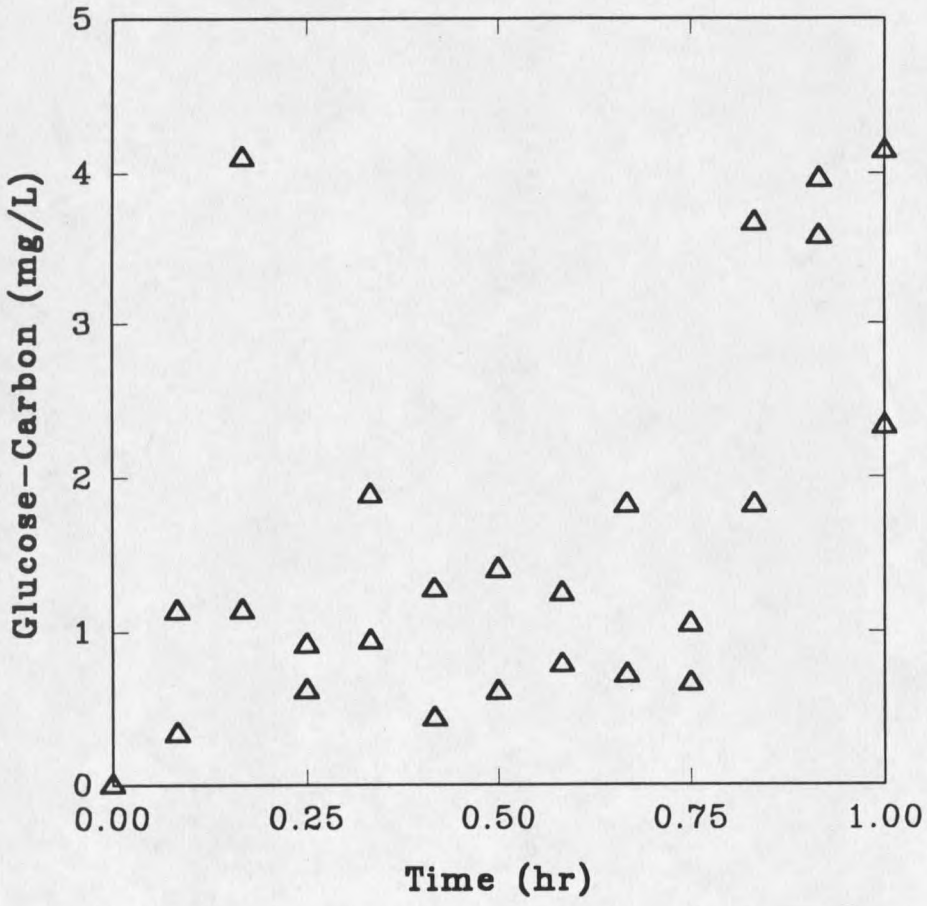

Figure 11 Effluent glucose concentration in *K. pneumoniae* biofilm reactors during monochloramine treatment for 1 hr. Two runs are represented on the figure.

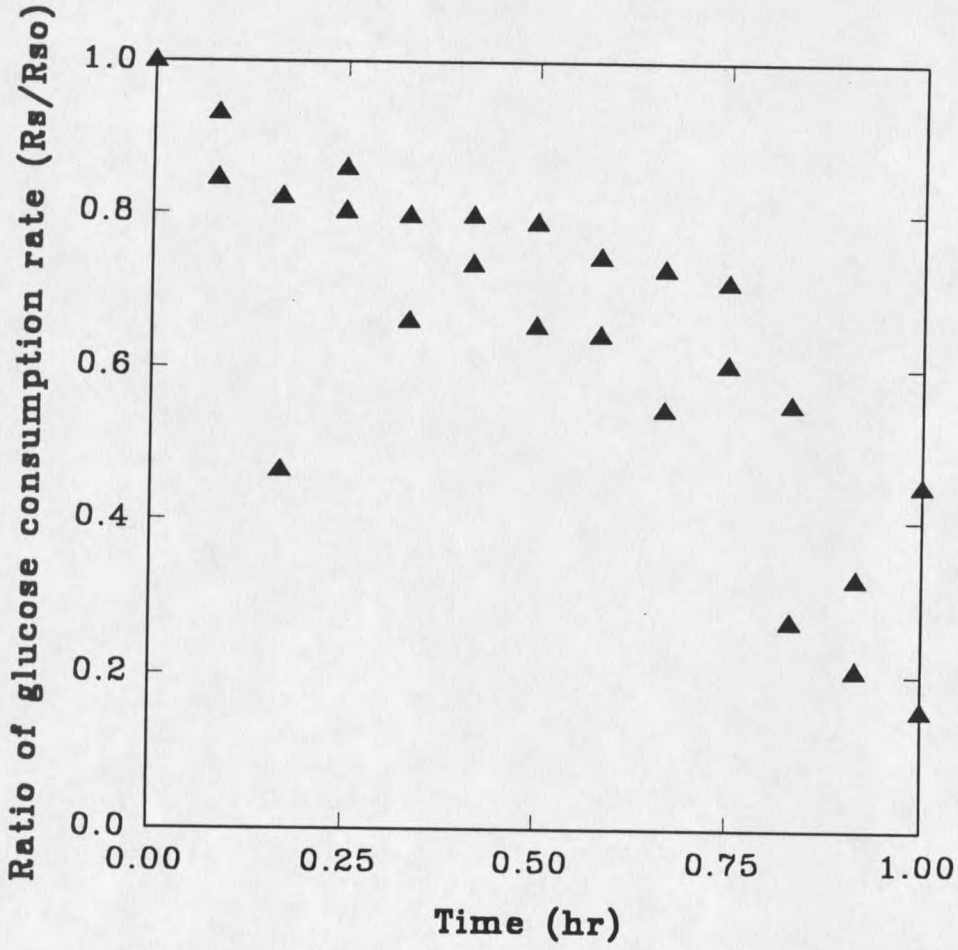

Figure 12 Calculated ratio of glucose consumption rate of *K. pneumoniae* biofilm during monochloramine treatment for 1 hr. Two runs are represented on the figure.

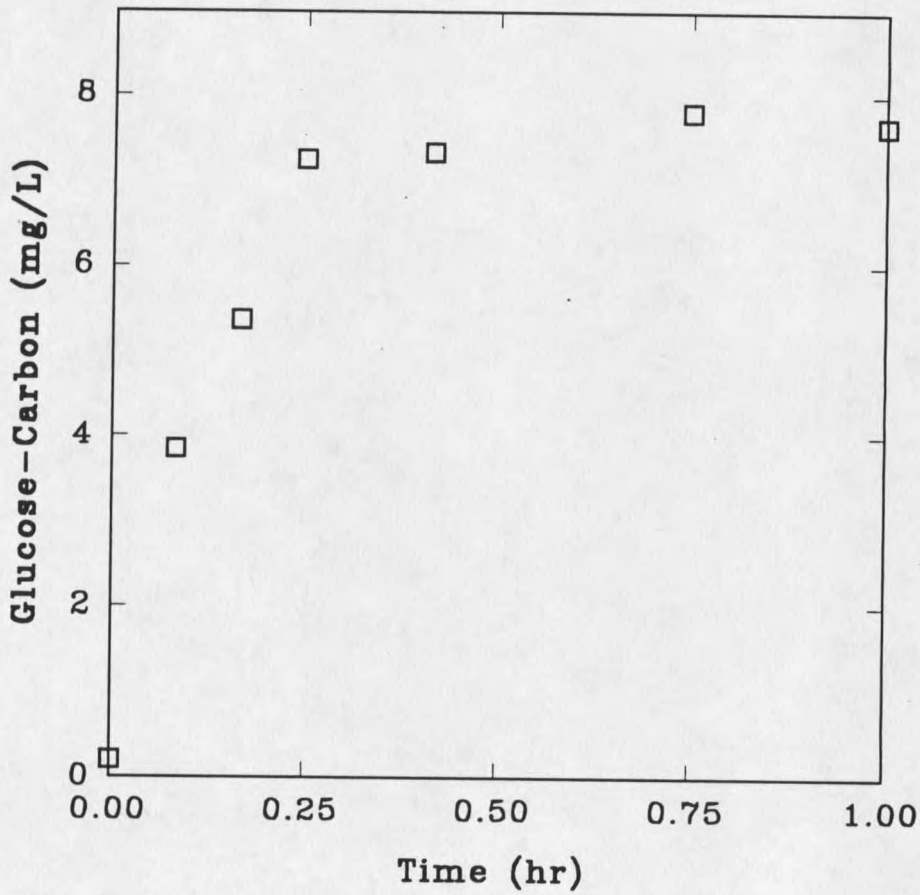

Figure 13 Effluent glucose concentration in *P. aeruginosa* biofilm reactors during monochloramine treatment for 1 hr.

Monochloramine consumption

Effluent monochloramine concentration measured during treatment of binary population biofilms is shown in Figure 14. After the first 5 minutes effluent monochloramine concentrations were relatively constant at 0.1 to 0.9 mg/L. The overall consumption rate of monochloramine for these three runs is shown in Figure 15. The rate is calculated from Equation 10. The consumption rate drops from 0.15 to 0.03 mg/m^2-hr in the first 10 minutes and stays constant thereafter. The trend between the two figures seem to be the same.

Effluent monochloramine concentration in *K. pneumoniae* biofilm reactors is shown in Figure 16. The effluent concentration drops from 4 to approximately 1.6 mg/L in the first ten minutes, and then rises to almost the influent concentration. As shown on Figure 17 the consumption rate is an order of magnitude less than for the binary population biofilm system.

Effluent monochloramine concentration in *P. aeruginosa* biofilm reactors is shown in Figure 18. The effluent concentration drops from 4 to 0.5 mg/L in the first five minutes then stays constant. As shown on Figure 19, the consumption rate drops from 0.1 to 0.03 mg/m^2-hr in the first ten minutes and remains steady thereafter. This trend mirrors that seen for binary population biofilm data.

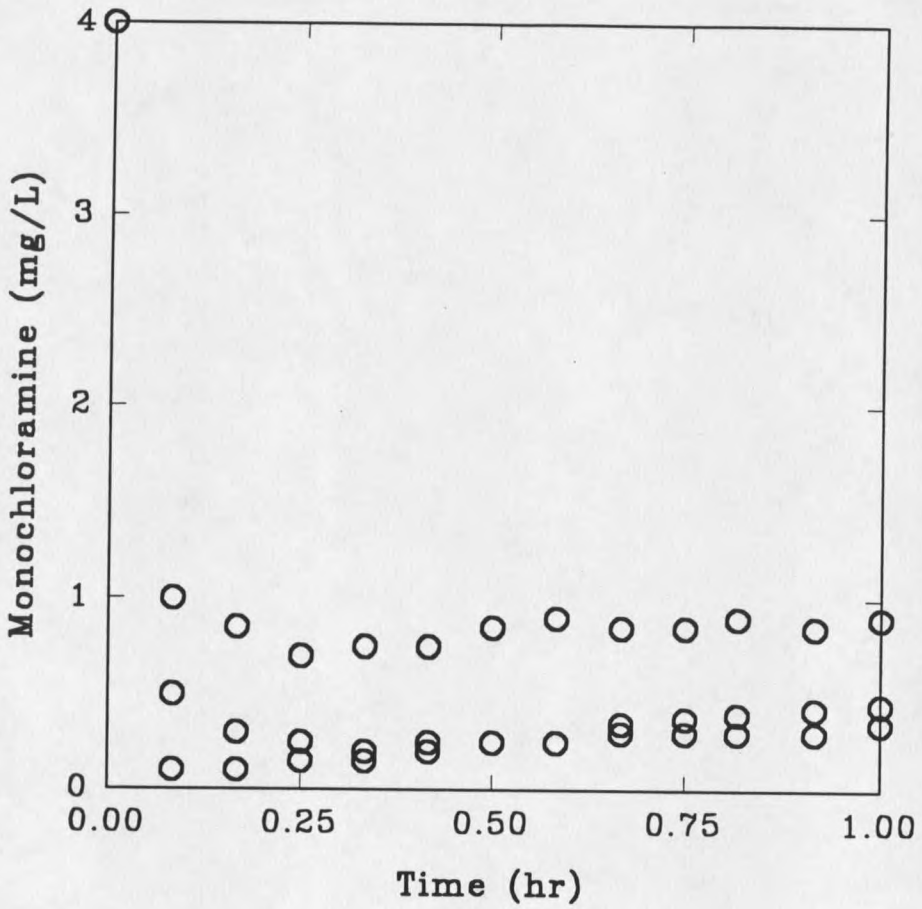

Figure 14 Effluent monochloramine concentration in binary population biofilm reactors during monochloramine treatment for 1 hr. Three separate runs are represented on the figure.

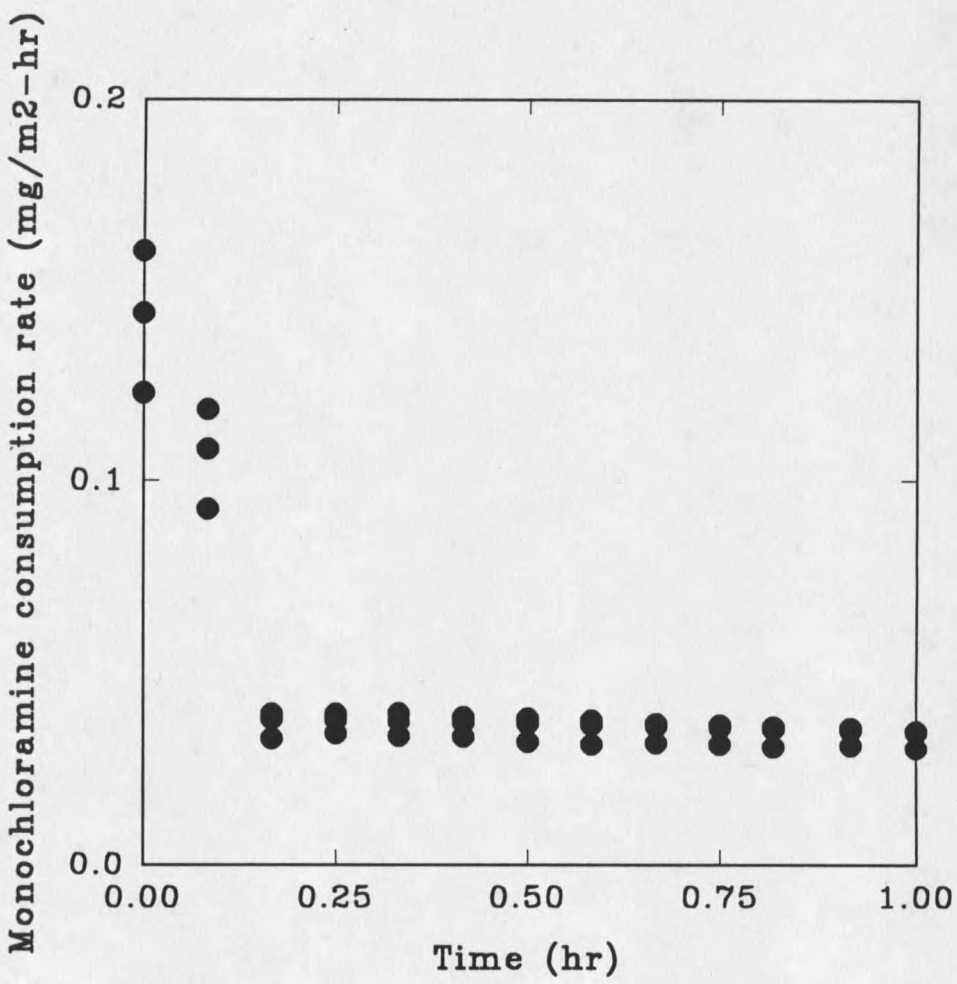

Figure 15 Calculated monochloramine consumption rate in binary population biofilms during monochloramine treatment for 1 hr. Three runs are represented on the figure.

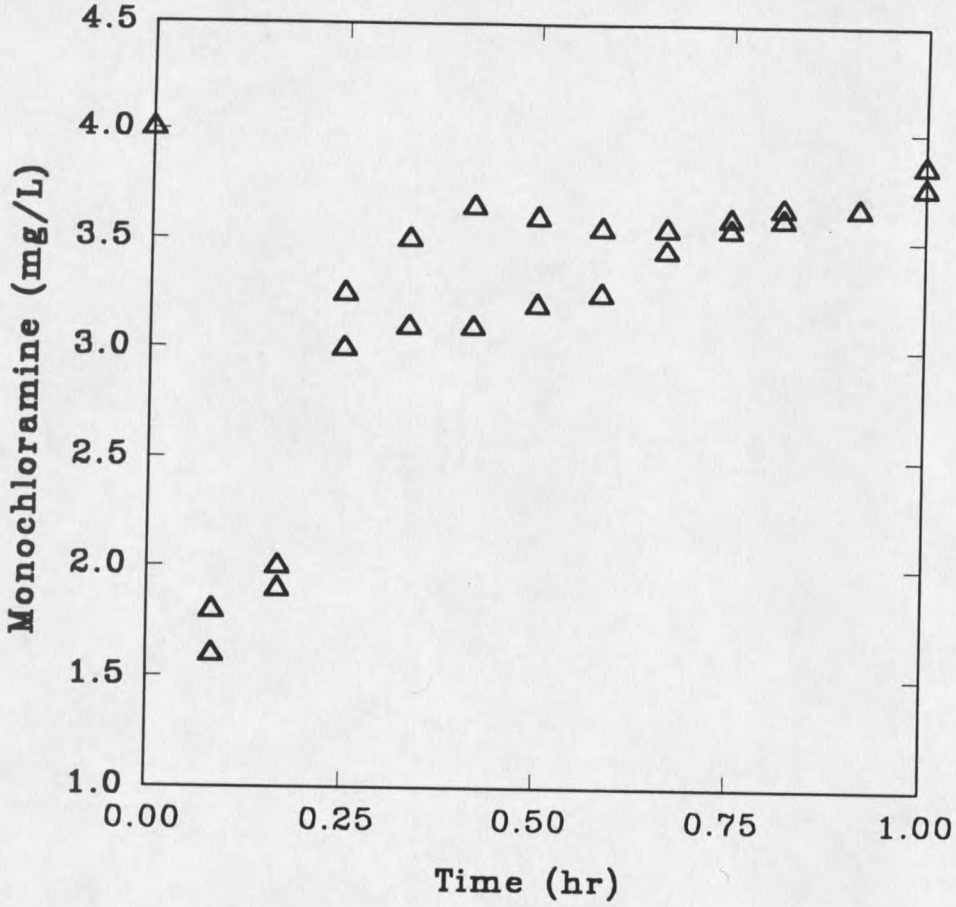

Figure 16 Effluent monochloramine concentration in *K. pneumoniae* biofilm reactors during monochloramine treatment for 1 hr. Two runs are represented on the figure.

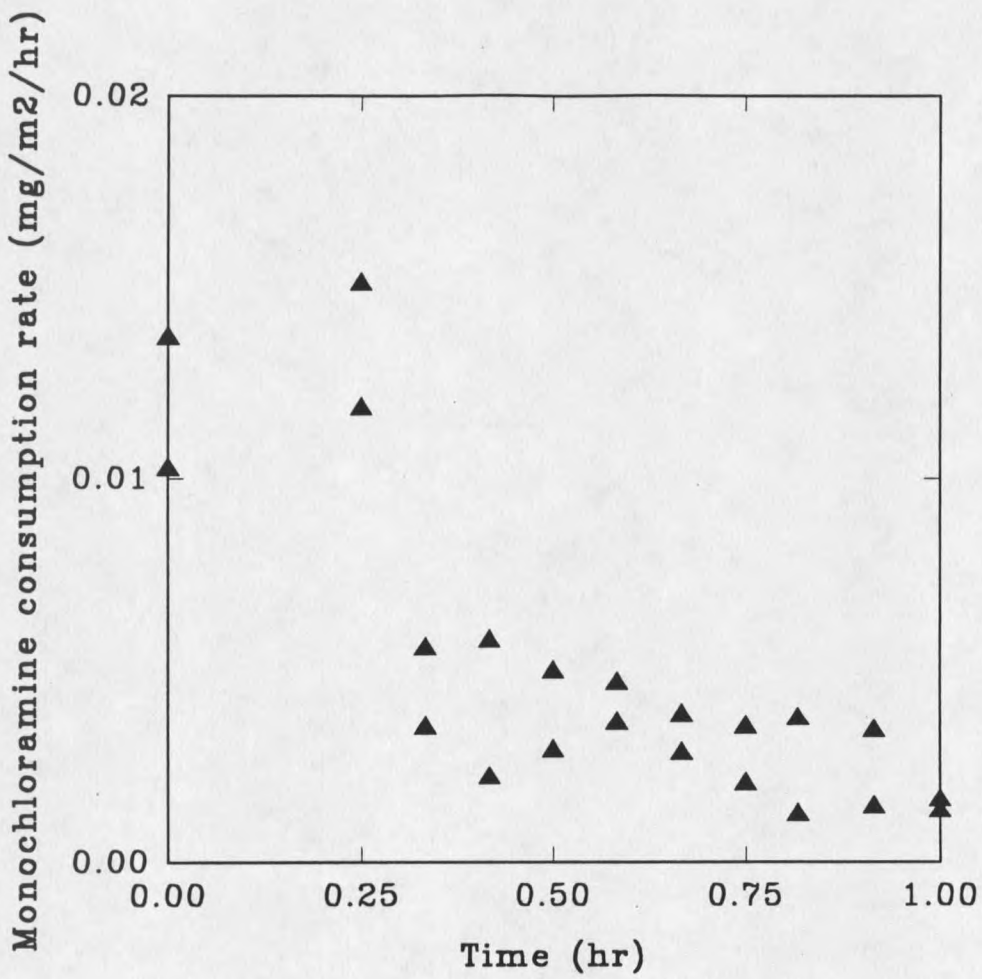

Figure 17 Calculated monochloramine consumption rate of *K. pneumoniae* biofilms during monochloramine treatment for 1 hr. Two runs are represented on the figure.

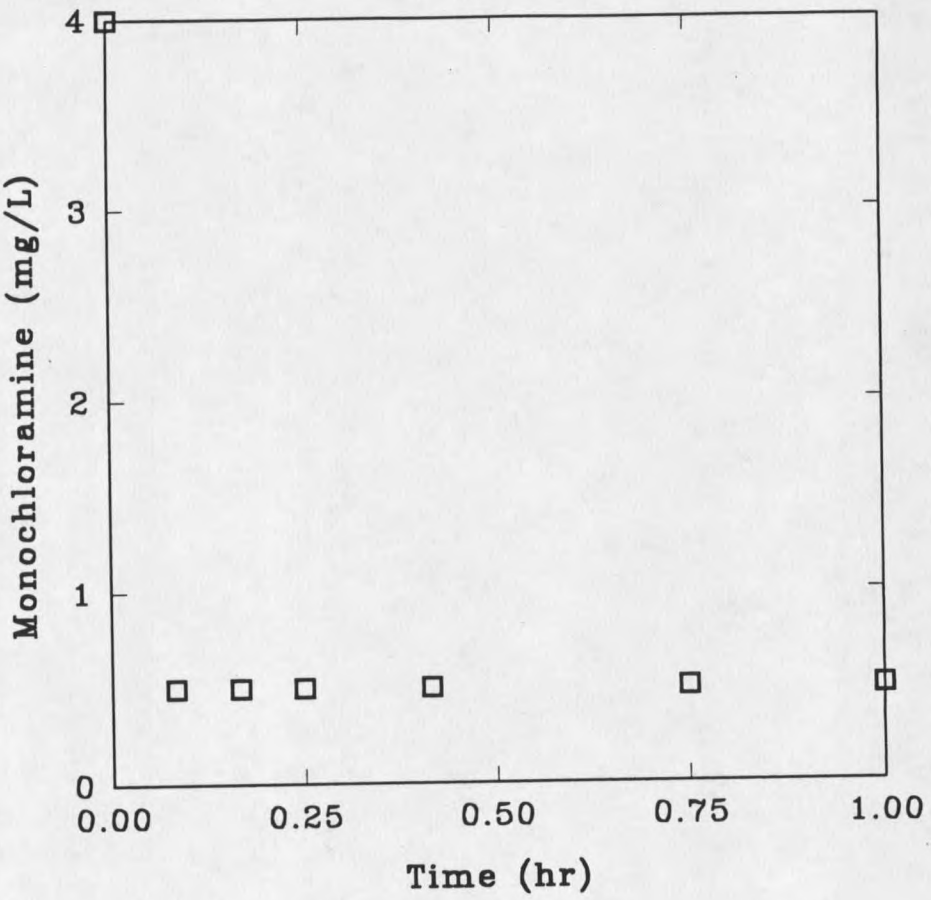

Figure 18 Effluent monochloramine concentration in *P. aeruginosa* biofilm reactors during monochloramine treatment for 1 hr.

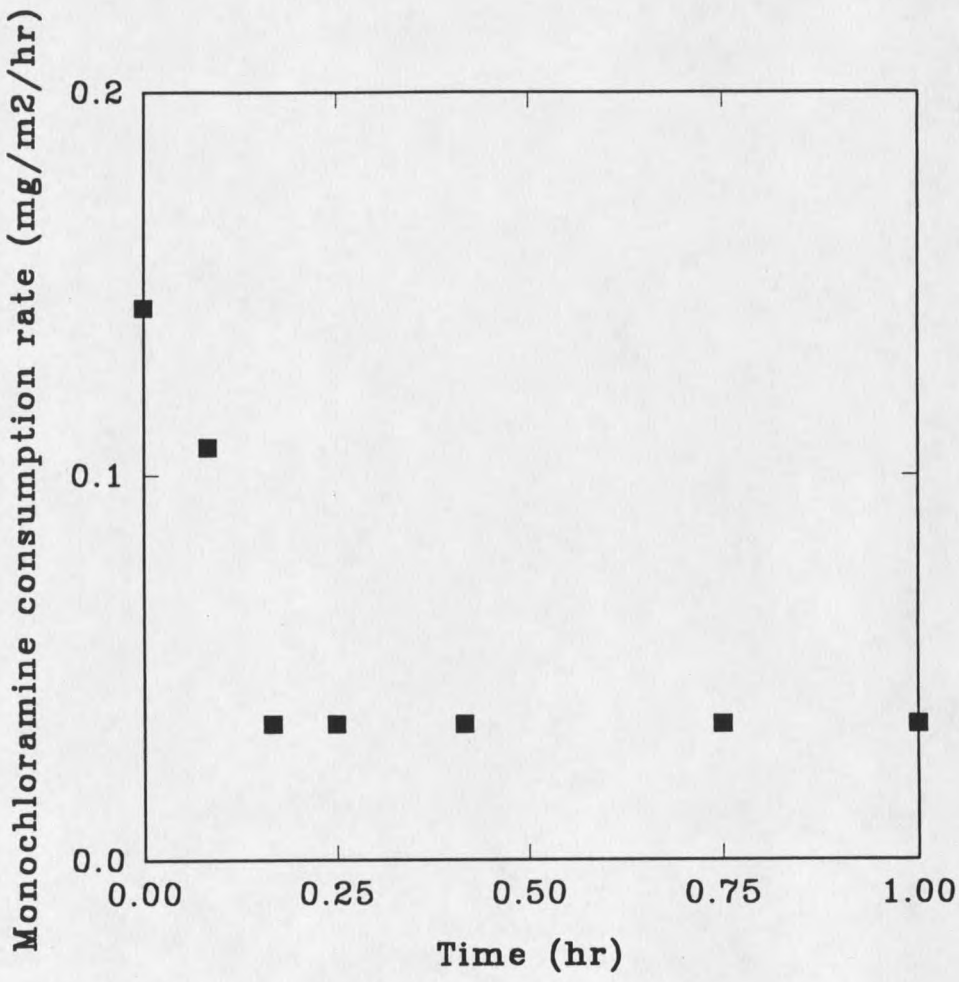

Figure 19 Calculated monochloramine consumption rate of *P. aeruginosa* biofilms during monochloramine treatment.

Detachment rate

Figure 20 reflects the detachment of cells from binary population biofilms during disinfection. The detachment rate shown in Figure 21 is obtained from Equation 9. The detachment rate remains essentially constant within each run. Similar behavior of effluent cell number and detachment rates are seen for *K. pneumoniae* (Figures 22 and 23) and *P. aeruginosa* (Figures 24 and 25) biofilms.

Growth and recovery

The growth and recovery after biocide treatment of binary population biofilms are shown on Figure 26. At time zero the reactor was fed continuously with the medium and the reactor effluent was monitored for contamination and detached cells. Assuming that as the biofilm grows the detachment of cells also increases, the increase seen in detached viable cells is taken as an indicator of biofilm growth. The biocide was added for a period of one hour. The later part of the graph depicts the recovery. The growth and recovery of monopopulation biofilms of *K. pneumoniae* and *P. aeruginosa* are shown on Figure 27 and 28 respectively. In all cases, the viable cell number in the effluent is near its pretreatment value within 24 to 48 hours of biocide treatment.

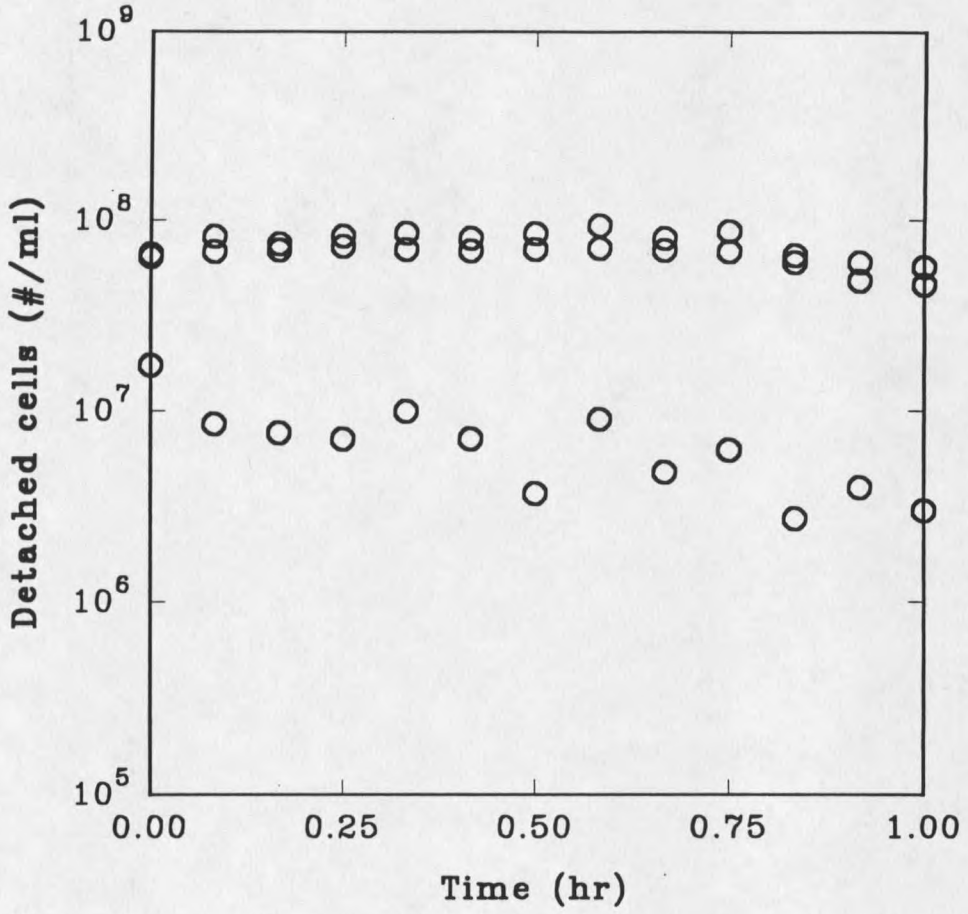

Figure 20 Effluent total cell number in binary population biofilm reactors during monochloramine treatment for 1 hr. Three runs are represented.

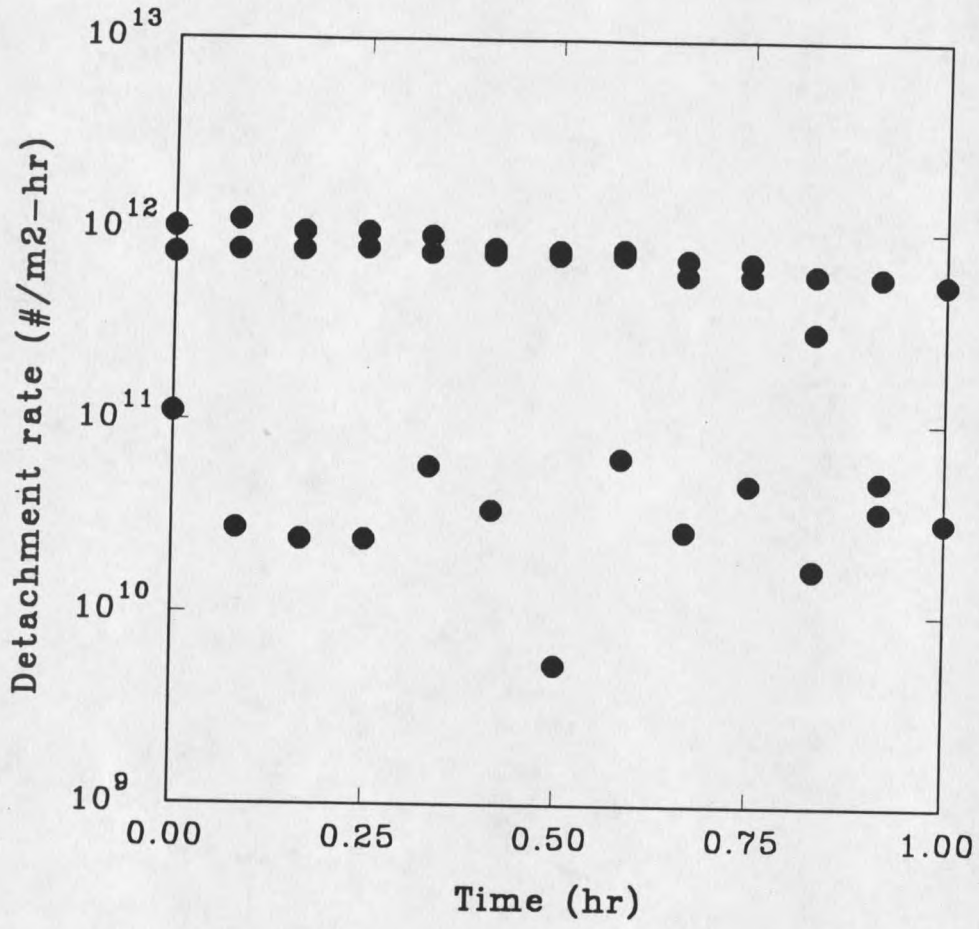

Figure 21 Calculated detachment rate of cells from binary population biofilms during monochloramine treatment. Three runs are represented.

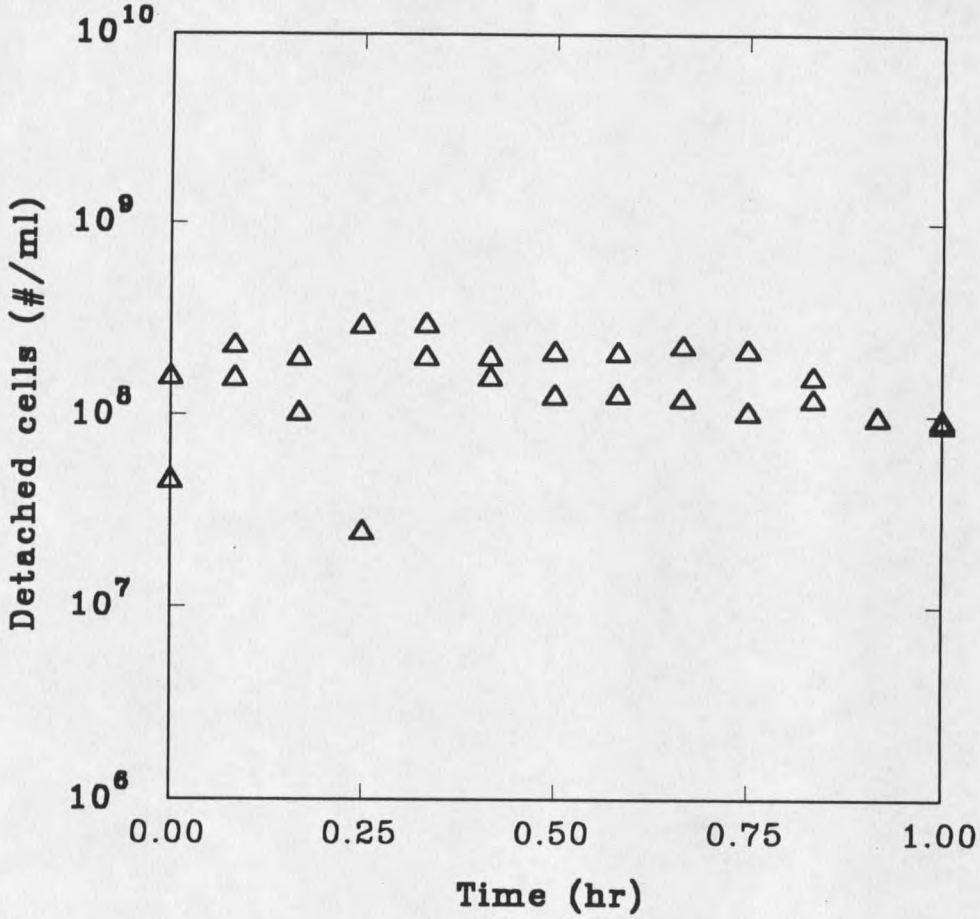

Figure 22 Effluent total cell number in *K. pneumoniae* biofilm reactors during monochloramine treatment for 1 hr. Two runs are represented.

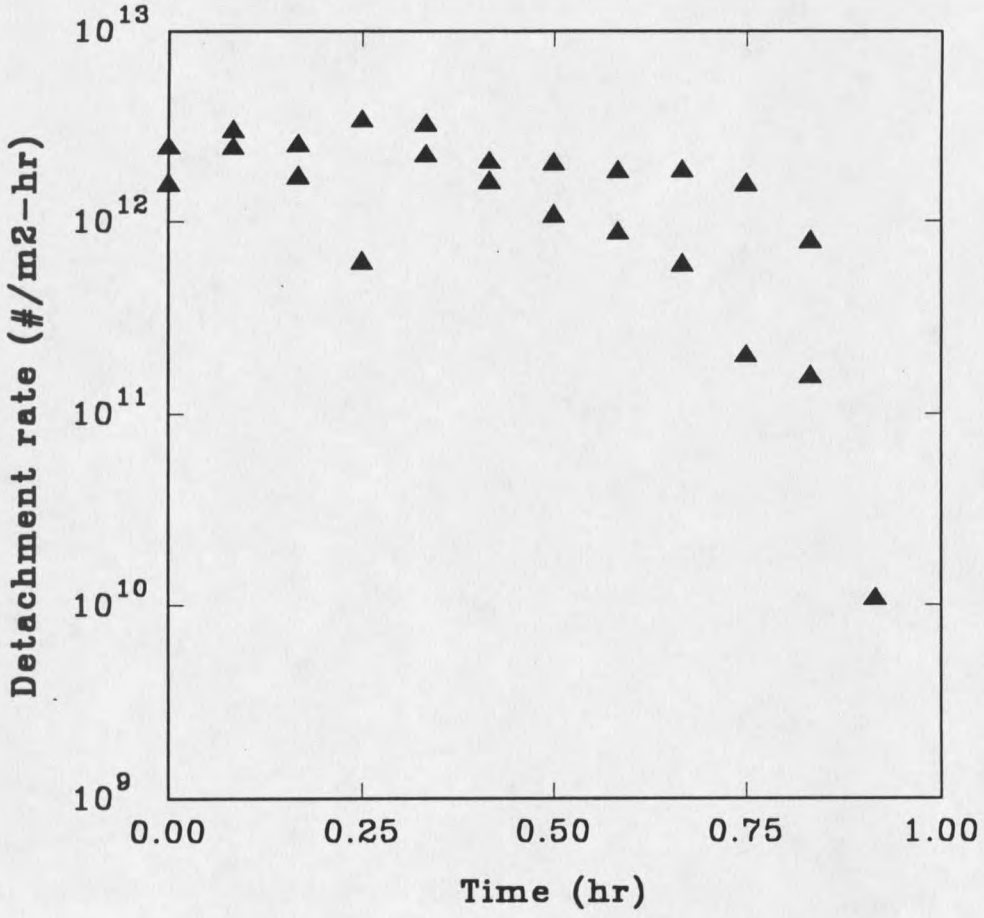

Figure 23 Calculated detachment rate of cells from *K. pneumoniae* biofilms obtained during monochloramine treatment for 1 hr. Two runs are represented.

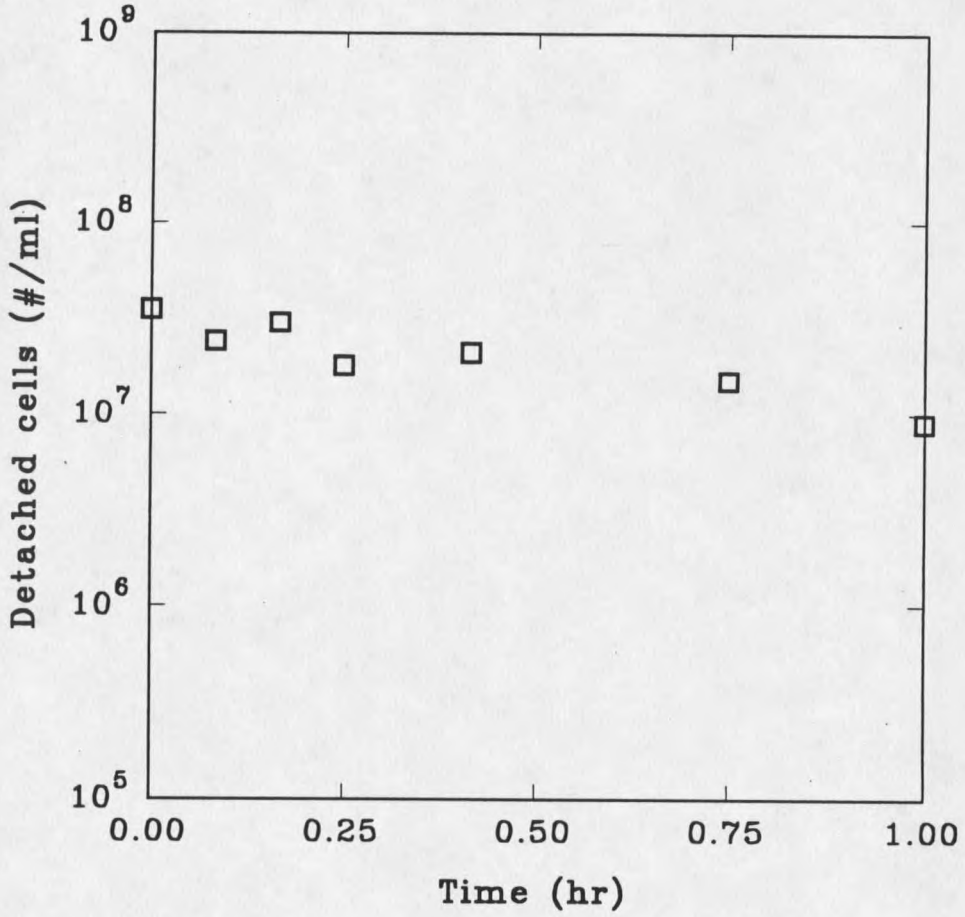

Figure 24 Effluent total cell number in *P. aeruginosa* biofilm reactors during monochloramine treatment for 1 hr.

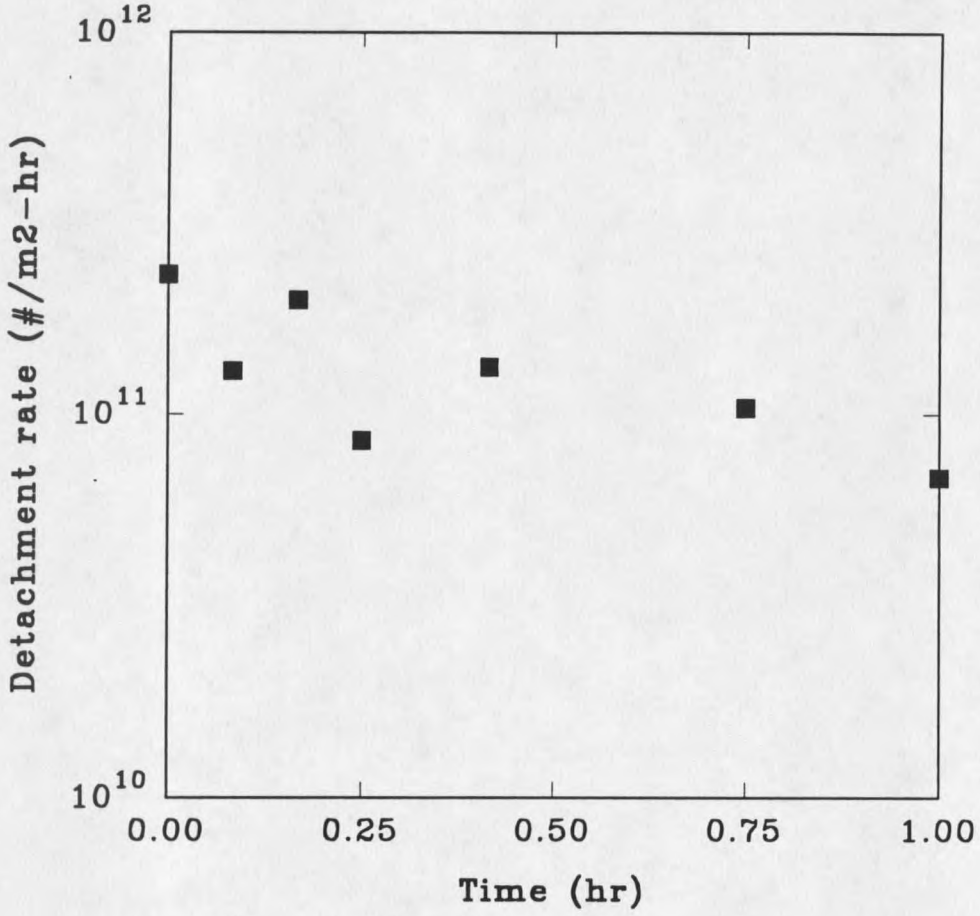

Figure 25 Calculated detachment rate of cells from *P. aeruginosa* biofilm during monochloramine treatment.

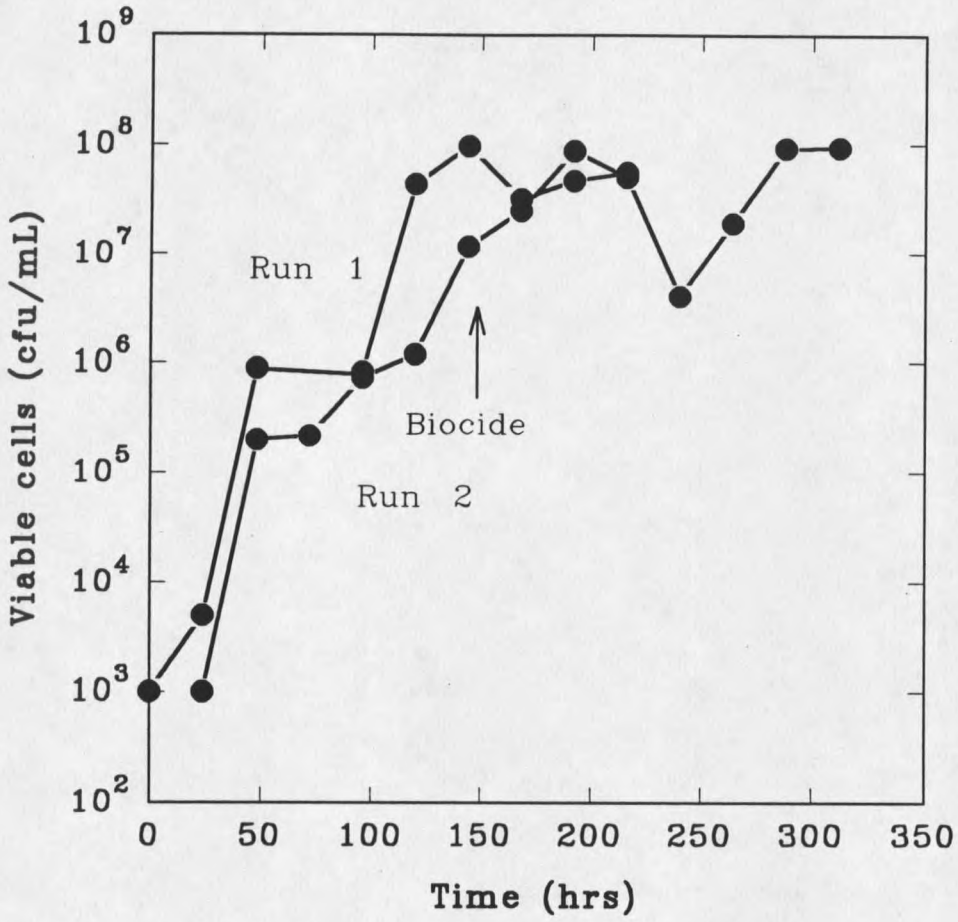

Figure 26 Growth and regrowth data of binary population biofilms. Two different runs are represented. Biocide was added in both runs at 144 hrs for a period of one hour.

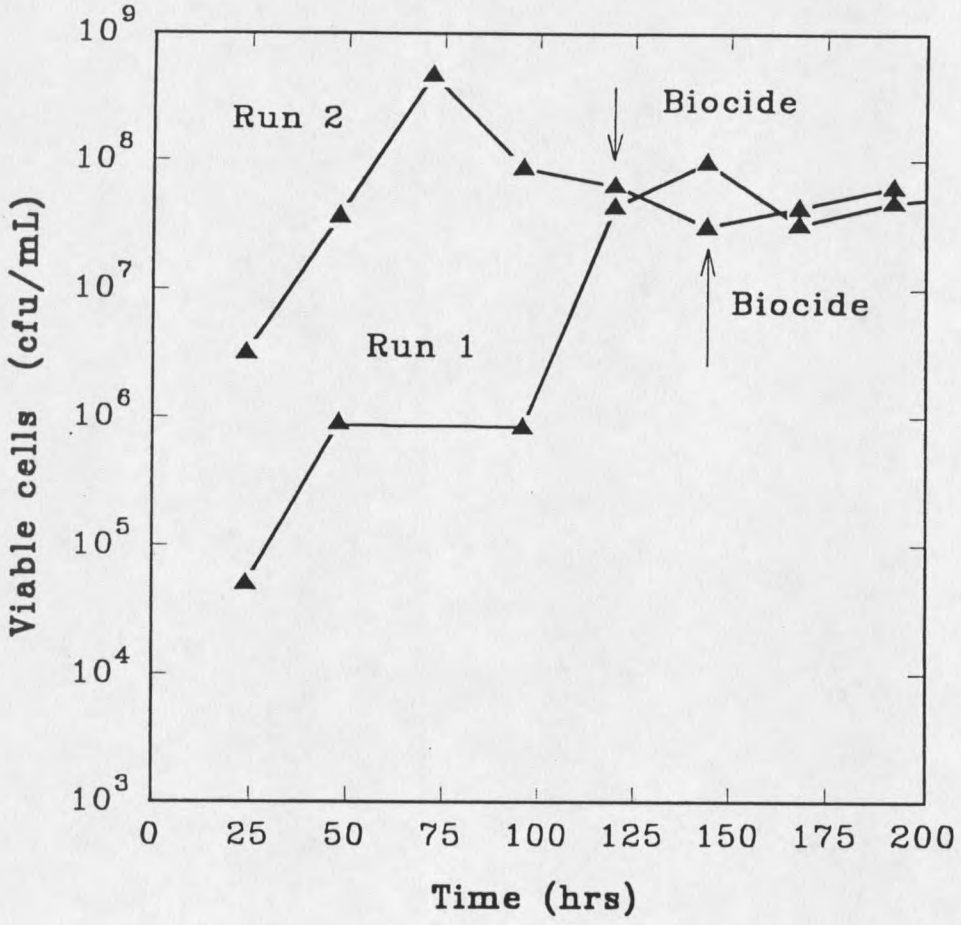

Figure 27 Growth and regrowth data of *K. pneumoniae* biofilms. Two different runs are represented. The biocide for run 1 was added at 144 hrs and for run 2 it was added at 120 hrs. Biocide was added for a period of one hour.

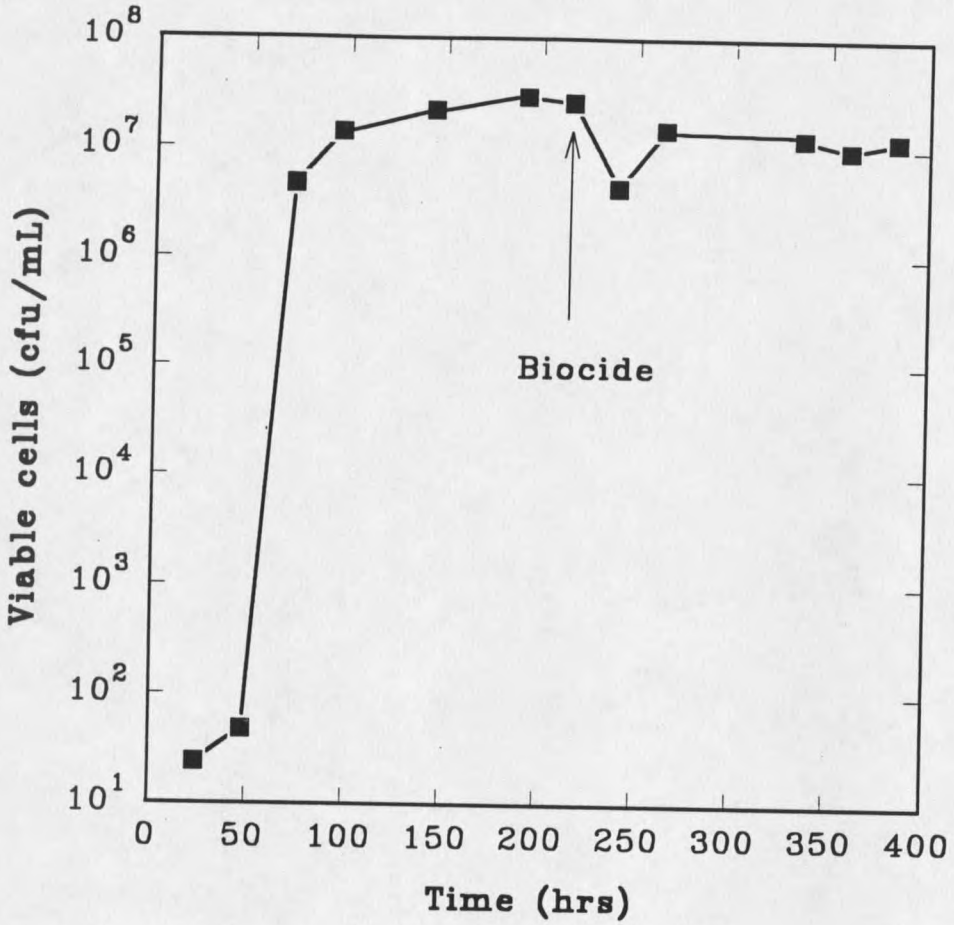

Figure 28 Growth and regrowth data of *P. aeruginosa* biofilm. The biocide was added at 192 hrs for a period of one hour.

Comparison of respiratory activity and culturability

Biocide efficacy as measured by various techniques on binary popualtion biofilm systems is shown in Figures 10, 29, 30 and 31. Figure 29 shows the difference in biocide efficacy as determined by plate counts and CTC reducing cell numbers. The plate count data (R2A) indicated a 4 log drop in viable cell count whereas the CTC data (Stewart et al (1994)) indicated a 2 log drop. The number density for both the measures at time zero was the same. The biofilm sample was also plated on MT7, which is a coliform selective media. The data obtained from both R2A and MT7 agar plates were similar, indicating that R2A plate count provided a good estimation for both species.

Oxygen consumption

Typical oxygen profiles obtained using a microelectrode are shown in Figure 30. The distance on the x axis indicates the travel of the electrode from the bulk fluid towards the substratum. The data shown is for the control slide that was treated with 2% formaldehyde. The oxygen profile before the addition of HCHO has a steep gradient indicating consumption of oxygen right near the substratum. After the addition of HCHO, the profile is very flat, indicating that oxygen is not consumed by the biofilm.

The normalized oxygen flux obtained using Equation 12 at different time intervals during monochloramine treatment is shown in Figure 31. The bulk fluid concentration was around 0.24 mol/m^3 and the concentration of

oxygen at a distance of 60 μm away from the substratum (the estimated distance of the biofilm - bulk fluid interface) was obtained from the profile. The concentration difference between these two points was proportional to the flux into the biofilm. The oxygen flux decreased by only 10% during biocide treatment.

Glucose consumption (Figure 10) and oxygen utilization (Figure 31) show similar decreases, while plate count data (Figure 29) indicated a much higher efficacy of monochloramine on biofilms.

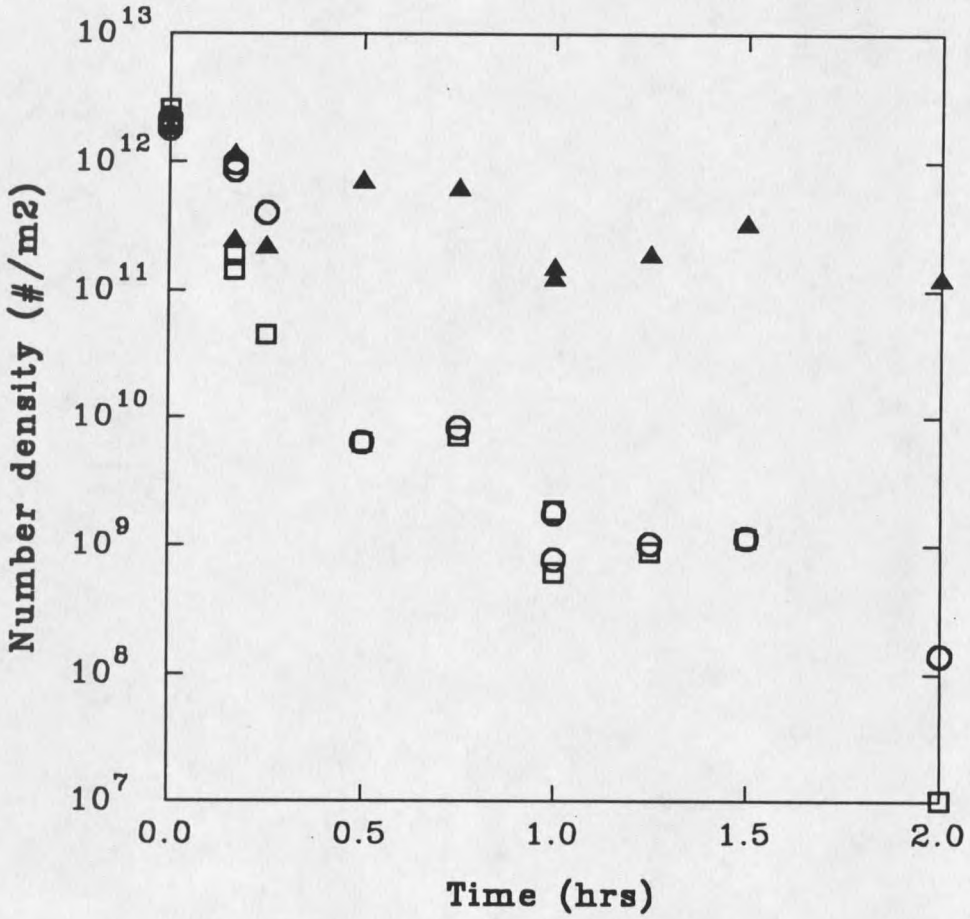

Figure 29 Comparison of plate count data on R2A (○), MT7 (□) with CTC (▲) reducing cells in binary population biofilms during monochloramine treatment for 2 hrs.

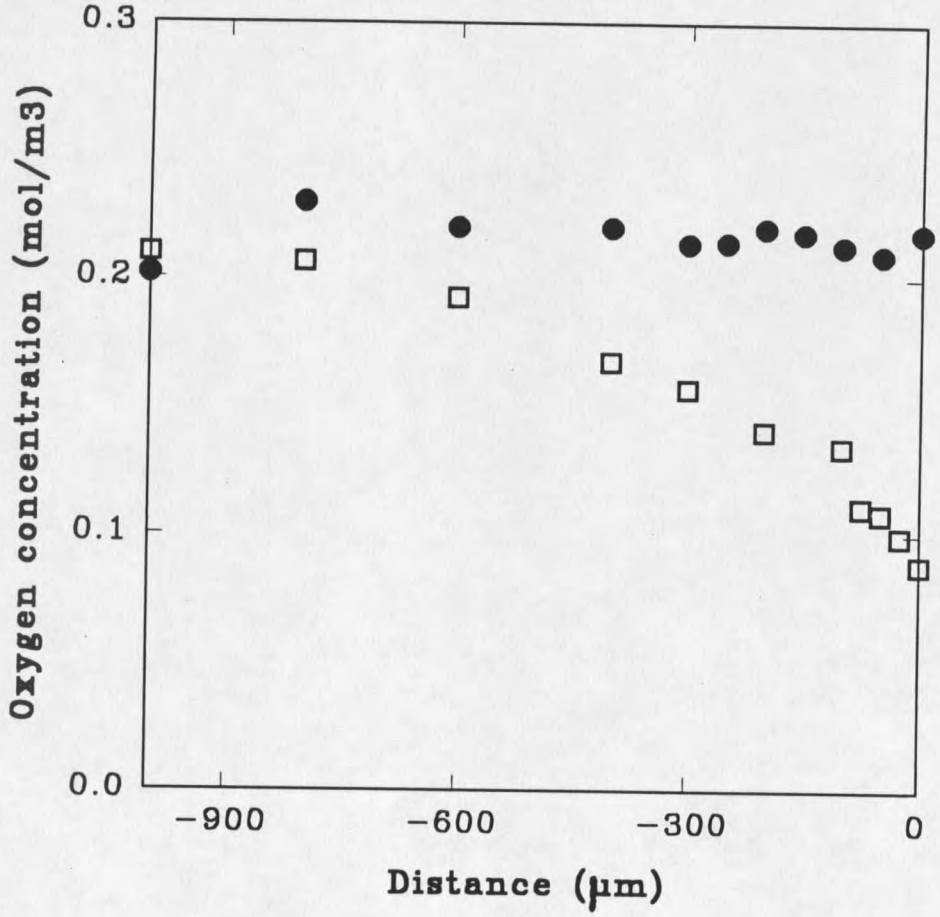

Figure 30 Typical concentration profiles of oxygen in binary population biofilm as measured in the flow cell. The profiles shown are for a control slide to which 2% formaldehyde was added. The profiles were taken before (□) and after 15 minutes of formaldehyde addition (●). Zero on the x axis corresponds to the substratum.

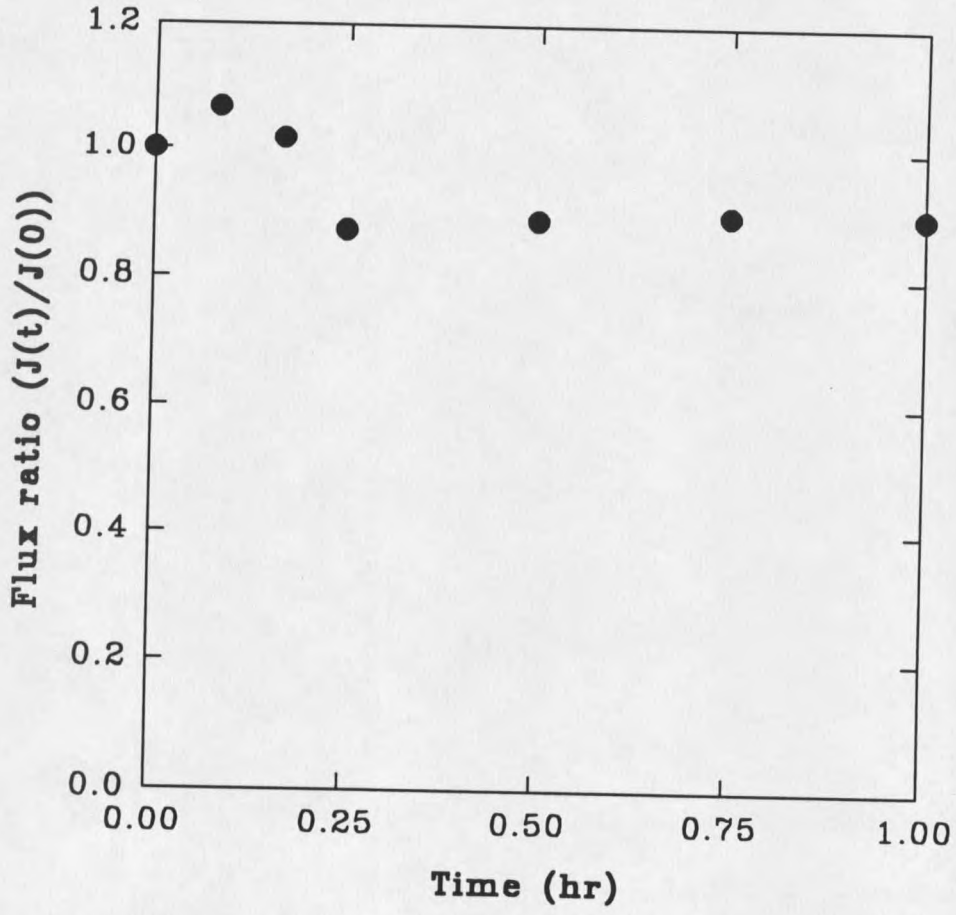

Figure 31 Calculated oxygen flux ratio of binary population biofilms obtained during monochloramine treatment.

DISCUSSION

The discussion is divided into three topics: biofilm parameters impacting biocide efficacy, measures of biocide efficacy, and comparison of rates between mono and binary population biofilms.

Biofilm parameters affecting biocide efficacy

Many phenomena are known to affect biocide efficacy. In this study three parameters were identified that impacted biocide efficacy. These parameters are initial cell density, species composition, and the presence of abiotic particles.

Effect of initial cell density

The overall decay rate coefficient displayed an unexpected dependence on initial areal cell density (Figure 32). As the cell density increases from 10^{12} cfu/m^2 to 10^{14} cfu/m^2 the decay rate coefficient decreased from 5 to 0.5 hr^{-1}. As the cell density approached 10^{11} cfu/m^2 the decay rate coefficient decreased to about 1.2 hr^{-1}. The peculiar parabolic dependence of decay rate coefficient on initial cell density observed in this study could be explained by various hypotheses.

The first hypothesis relates to the thickness of the biofilm (Figure 33). As the biofilm areal cell density increases the overall thickness of the biofilm also increases. Biocide efficacy could be limited by the rate of biocide transport into a thick biofilm. The biocide cannot penetrate (Figure 33) fully into the biofilm because it is reacted quickly at the surface of the biofilm and

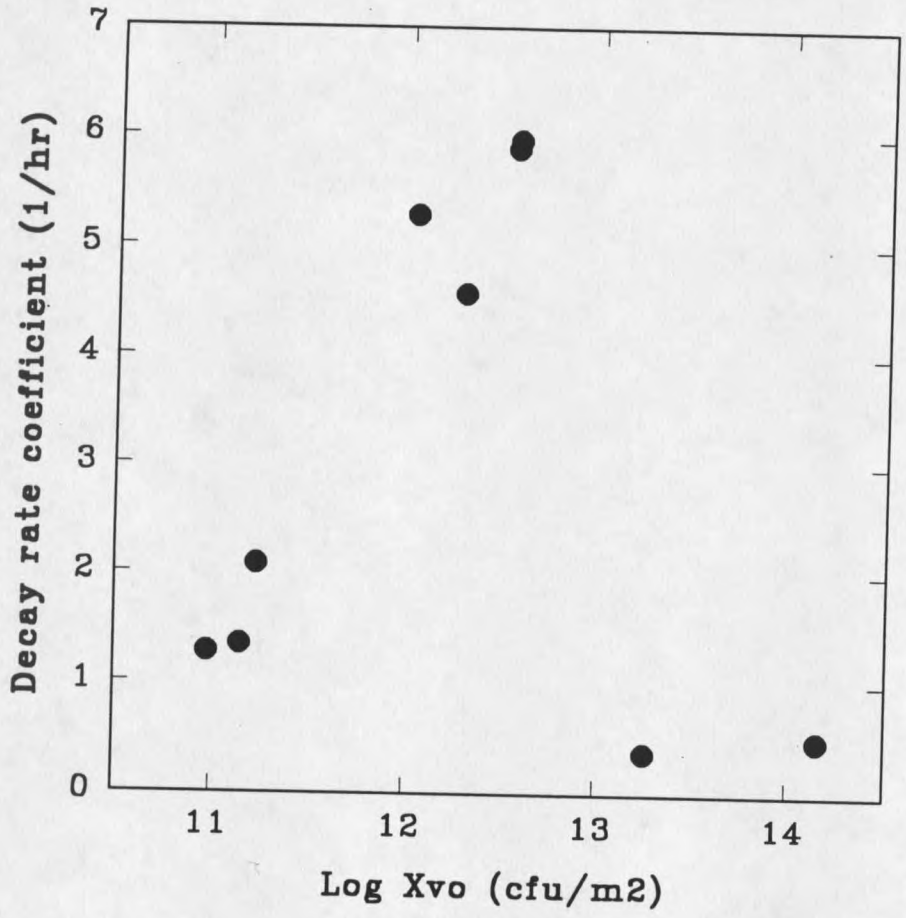

Figure 32 Calculated decay rate coefficients of all types of biofilm systems with varying initial cell densities.

its concentration decreases as it progresses towards the substratum. Diffusion and reaction together play a role in reducing the efficacy of the disinfectant according to this hypothesis.

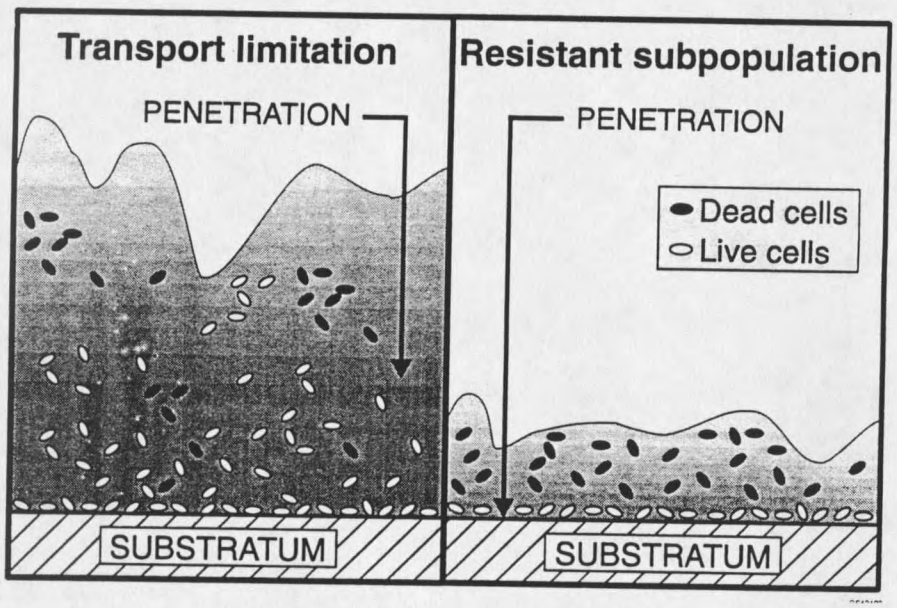

Figure 33 The schematic diagram of two hypotheses

The second hypothesis suggests the presence of a constant subpopulation within the biofilm that is physiologically different from the rest of the biomass and less susceptible to disinfection. Possible evidence for such a subpopulation is seen in Figure 3, where biphasic decay was observed for a thin biofilm. There was rapid initial decay in the first fifteen minutes followed by a slower loss of cells for the remainder of the period. This suggests the presence of a constant number of cells that are protected from biocide action. Similar behavior was observed with initial cell densities around 10^{12}

cfu/m^2. There was a continuous drop in viable cells until the number reached 10^8-10^9 cfu/m^2, after which there was little additional kill. These two hypotheses could be tested using physiological probes to observe spatial patterns of activity inside the biofilm (Yu et al).

The dependence of biocide efficacy on initial cell density as described in these hypotheses was used to develop a mathematical model.

Model

A model was developed that integrates two possible resistance mechanisms. i) transport limitation and ii) presence of a resistant subpopulation. The decay rate coefficient is a complex function of initial cell density and species composition: these two factors are considered in the model. The effect of transport is incorporated as a multiplicative factor of the decay rate coefficient that is analagous to an effectiveness factor as applied in heterogeneous catalysis. Independent first order deacy rate coefficients are assumed for the two species. The decay of the two species is additive giving the basic model equation

$$X_v = (1-f_P)\, X_{vo} \exp(-b_k \eta\, t) + X_{vo}\, f_P \exp(-b_P \eta\, t) + X_R \quad (13)$$

where,

f_P is the fraction of *P. aeruginosa* in the biofilm, b_K and b_P are the decay rate coefficients of *K. pneumoniae* and *P. aeruginosa* in the biofilm respectively. X_{Vo} is the initial biofilm areal cell density, X_R is a constant subpopulation in the biofilm, η is the efficiency factor, and X_V is the total viable areal cell density at any time t. If X_K and X_P are the areal cell density of *K. pneumoniae* and *P. aeruginosa*, respectively, in the biofilm, then

$$X_V = X_K + X_P \qquad (14)$$

The efficiency factor η, is defined as

$$\eta = \frac{X_D}{X_{Vo}} \qquad for\ X_D < X_{Vo} \qquad (15)$$

$$\eta = 1 \qquad for\ X_D > X_{Vo} \qquad (16)$$

The parameters η and X_D capture the effect of transport limitation in thick biofilms on biocide efficacy. As the cell density increases, η

decreases, leading to less effective disinfection. In thin biofilms, when X_{vo} is less than X_D, no transport limitation is encountered since η is equal to 1. X_D is assumed to be a constant. X_R is a constant subpopulation in the biofilm which offers resistance to biocide. This population is important in decreasing the efficacy of the biocide in thinner biofilms.

The model captured the qualitative behavior of the experimental data (Figure 34). A biofilm of higher initial cell density is hardly disinfected. Biphasic disinfection is predicted for biofilms of lower initial cell density. This behavior is very similar to that exhibited by the experimental data as shown in Figure 3. Additional experimental data would be needed to test the model.

A third hypothesis to explain the resistance of biofilms to biocide action involves the now accepted structural heterogeneity of biofilms. Even in an apparently thin biofilm, there could be occasional thick microcolonies that are protected by transport limitation of biocide. These colonies could constitute a resistant subpopulation.

The fourth hypothesis involves the effect of biomass growth rate inside the biofilm on the efficacy of the biocide. As the biofilm thickness increases, the layer of cells at the bottom-most part will grow more slowly and may thereby be more difficult to disinfect. The upper portion of biomass, where cells are growing rapidly, can be killed readily by comparison. Biofilms harbor cells that are protected by virtue of their slow growth according to this hypothesis. This hypothesis could be tested using

physiological probes in conjunction with the method of cryosectioning (Yu et al (1994)) to visualize physiological gradients inside a biofilm.

Corrosion products in the biofilm could also affect the efficacy of the biocide (Chen et al (1993)).

Biphasic decay

The decay for biofilms of lower initial cell density is biphasic. The decay is rapid in the first 15-30 minutes, but slows drastically after one hour of treatment (Figure 3). The reason for this peculiar behavior is not understood. It could probably be explained by the presence of resistant subpopulation in the biofilm.

Since the analysis applied in this thesis assumed linear rather than biphasic decay, some of the information contained in the raw data was lost. In terms of analyzing underlying mechanisms, it might be most appropriate to examine initial rates of decay. A preliminary analysis of initial rates was disappointing because there were relatively few data points in the initial period and so initial rate coefficient estimates were noisy. This approach could be pursued more effectively in future studies by taking more data in the first 15 minutes.

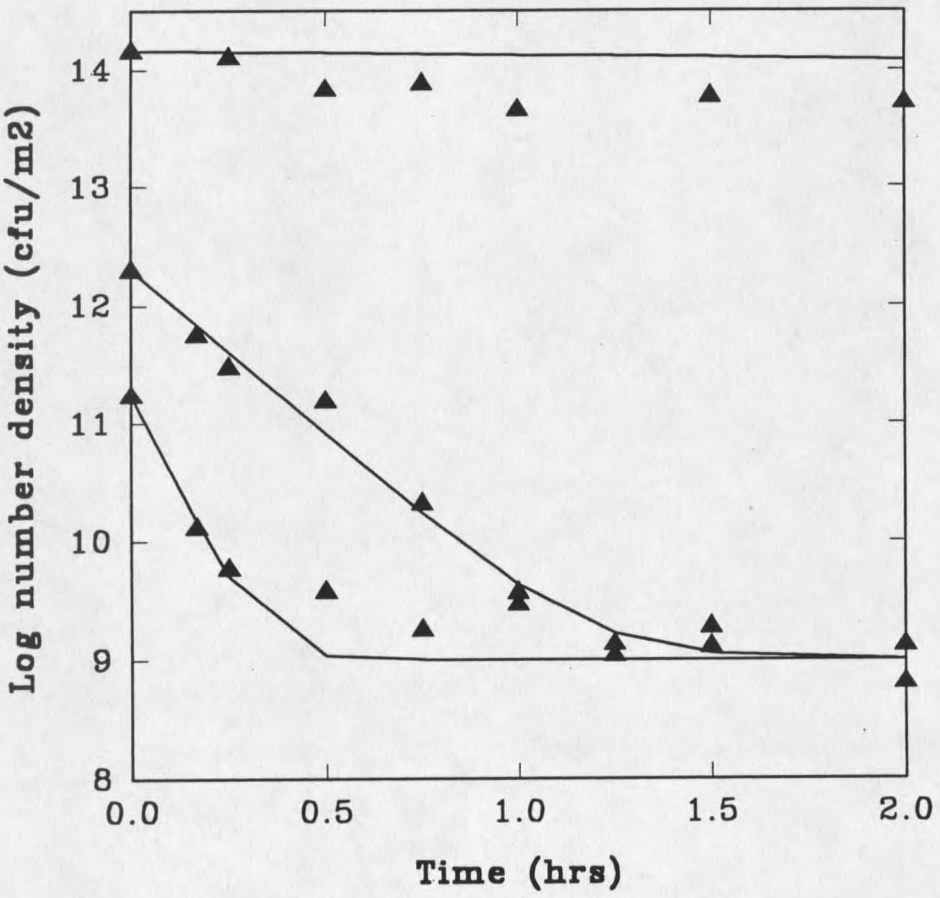

Figure 34 The behaviour of the empirical model (line) in comparison with the experimental data (▲)

Species composition

Siebel et al (1991) found no evidence of species interactions in the biofilm with respect to growth kinetic parameters. In this study species interactions with respect to biocide efficacy were investigated. The effect of the presence of one species on the disinfection of the other was studied by comparing results of experiments with monopopulation and binary population biofilms.

Figures 35 and 36 compare decay rates of *K. pneumoniae* and *P. aeruginosa* in mono and binary biofilms. The decay rates are comparable, indicating that the cells do not interact. This conclusion was supported by non linear statistical analysis of the data (Figures 40 and 41).

The effect of the fraction of *P. aeruginosa* (Figure 37) on the decay rate coefficient of the overall population indicates an increase in decay rate coefficient with increase in fraction of *P. aeruginosa* present in the biofilm. A linear regression performed on these data using MSU STAT gave a p value of 0.026, and a ratio of intercepts at $f_P = 1$ and $f_P = 0$ of 3.7. This result indicates that there is a significant dependence on the species composition of the biofilm, and that *P. aeruginosa* decays approximately 3.7 times as fast as *K. pneumoniae.* In binary population biofilms of similar initial cell density, *P. aeruginosa* decays more rapidly than *K. pneumoniae* (Figure 38). The ratio of the decay rates of *P. aeruginosa* and *K. pneumoniae* is equal to the slope of the line fit to the data in Figure 38. This value was 2.7,

indicating that the decay rate for *P. aeruginosa* is a factor of 2 to 3 higher than for *K. pneumoniae*.

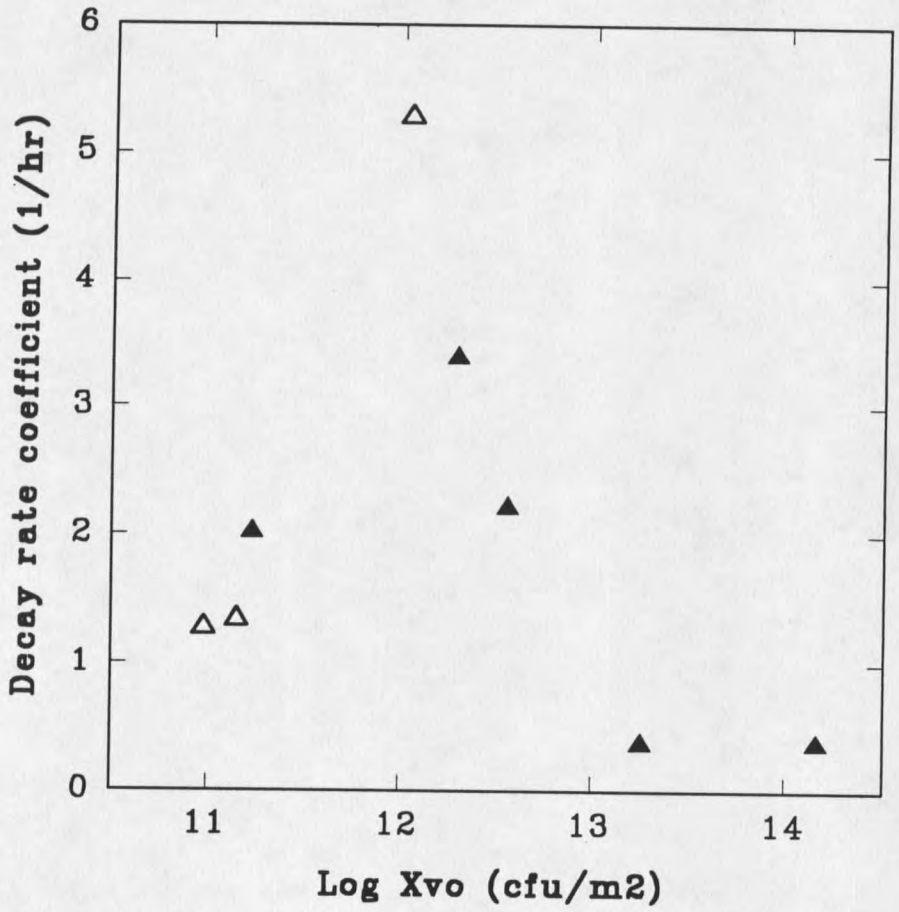

Figure 35 Comparison of calculated decay rate coefficients of *K. pneumoniae* in mono (△) and binary (▲) population biofilms of varying initial cell densities.

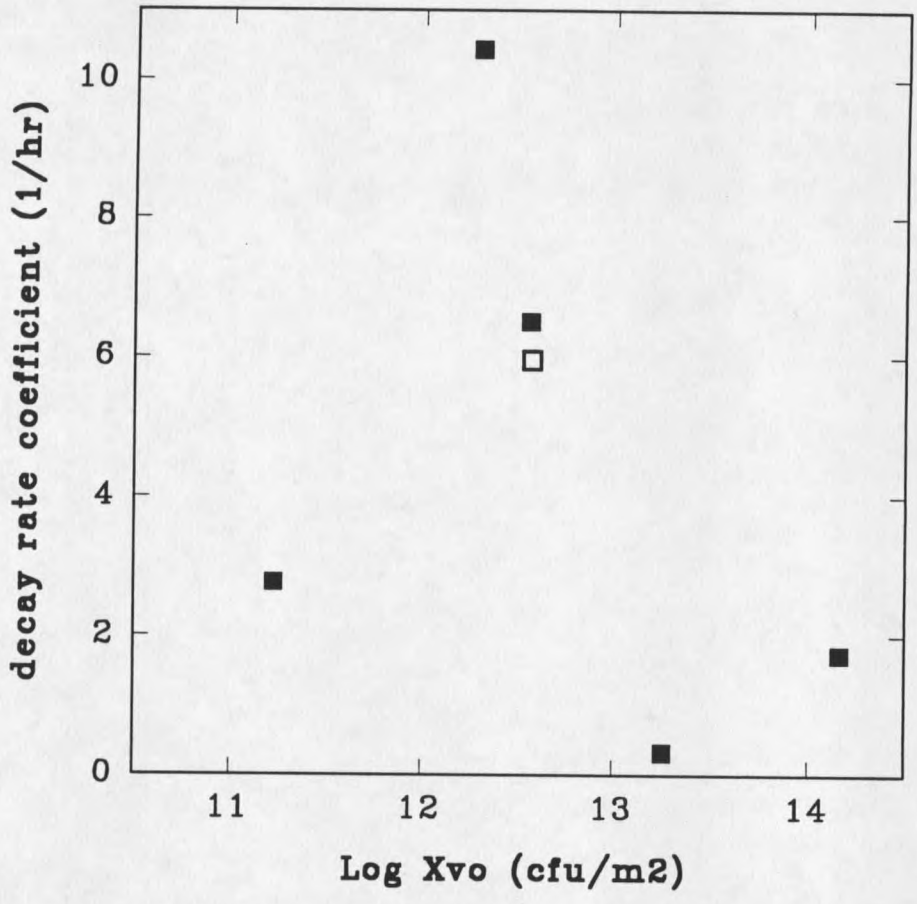

Figure 36 Comparison of calculated decay rate coefficients of *P. aeruginosa* in mono (□) and binary (■) population biofilms of varying initial cell densities.

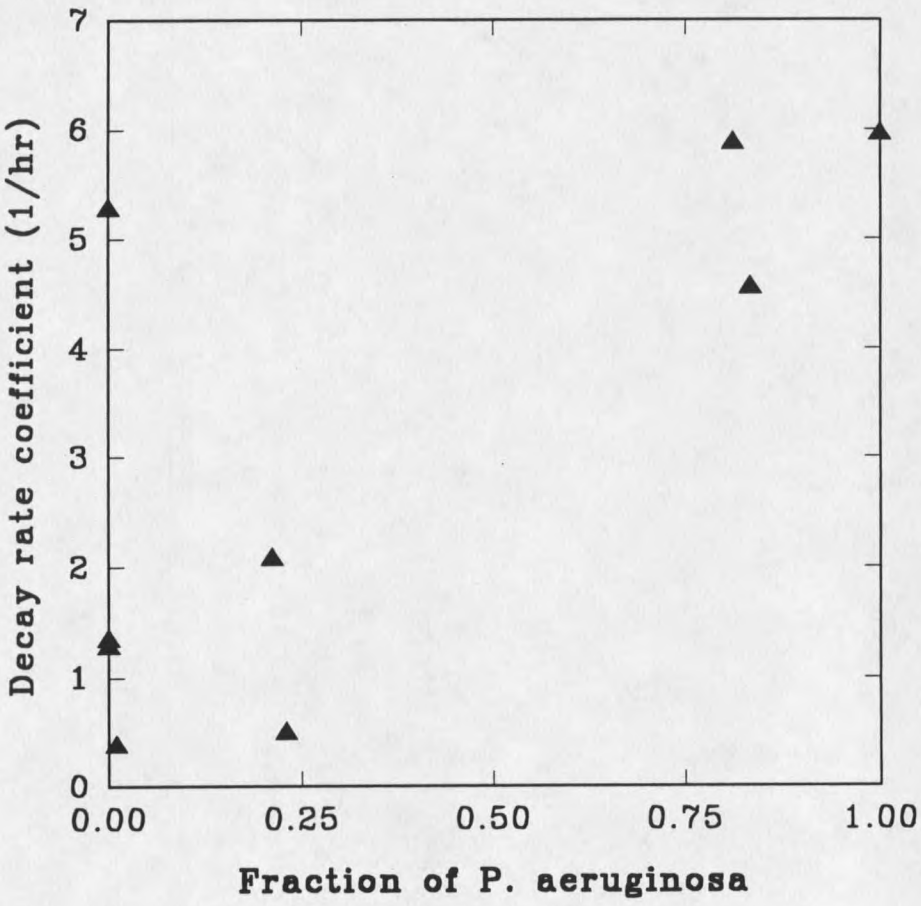

Figure 37 Comparison of calculated decay rate coefficients of all types of biofilm systems of varying composition of *P. aeruginosa*.

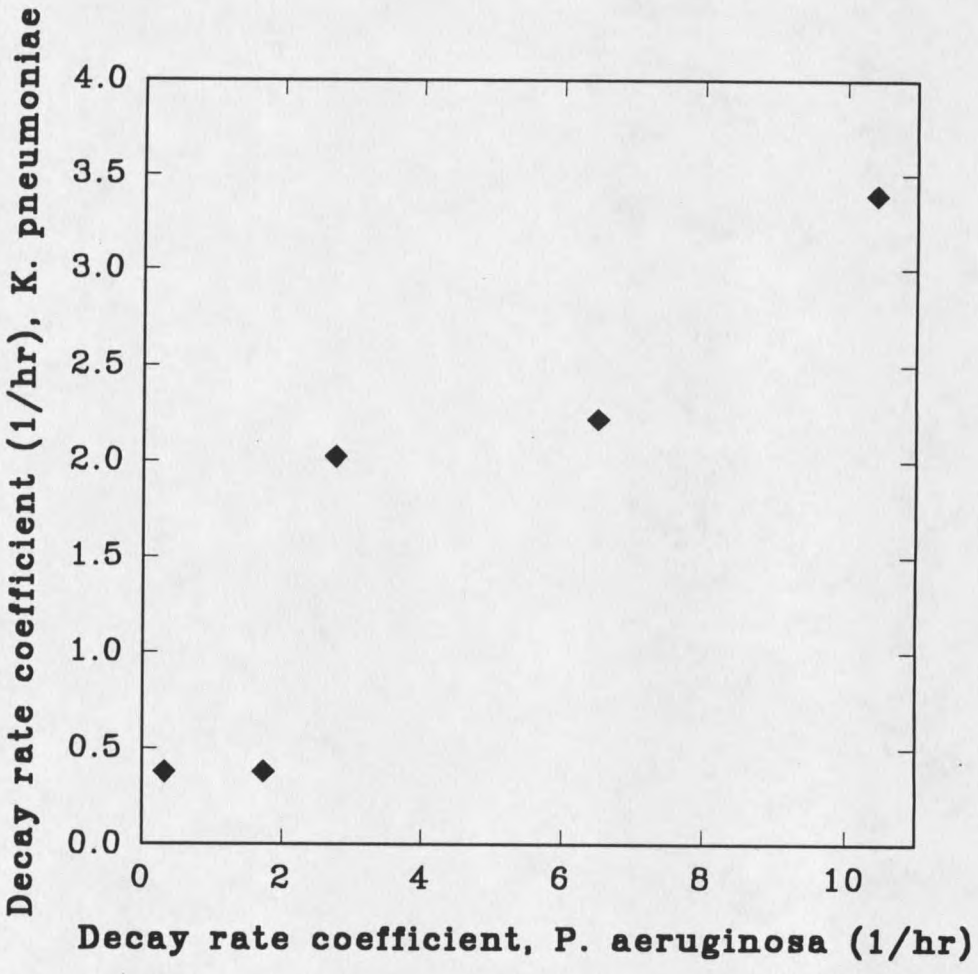

Figure 38 Comparison of decay rate coefficients of *P. aeruginosa* and *K. pneumoniae* in binary population biofilms.

Statistical analysis

A quadratic non-linear model was used to explain the parabolic trend observed in the data (Figure 32). The model assumes independent and additive decay of the two species. A quadratic dependence on initial cell density is fit. The model is expressed as follows

$$b = [(1-f_P) + \rho f_P] \; [\theta \; (\log X_{vo})^2 + \gamma \; (\log X_{vo}) + \delta] + e \qquad (17)$$

Where,

θ, γ, δ and e are fitted parameters, and

$$b = b_K + b_P \; ; \qquad \rho = \frac{b_P}{b_K} \qquad (18)$$

b_P and b_K are the decay rate coefficients of *P. aeruginosa* and *K. pneumoniae* respectively, f_P is the fraction of *P. aeruginosa* and X_{vo} is the viable initial cell denisty. The estimated values of the parameters using non-linear regression on the overall decay data (Figure 32) are

$$\rho = 1.7171; \quad \theta = -1.0828; \quad \gamma = 26.77; \quad \delta = -162.09. \qquad (19)$$

θ, γ, and δ are fitted parameters and have no direct physical interpretation.

The chance error *e*, which is the error associated in estimating the decay rate coefficient, *b* was found to be zero.

For a *P. aeruginosa* mono culture biofilm, the prediction equation is

$$b_P = 1.717\ [-1.0828\ (\log X_{vo})^2 + 26.77\ (\log X_{vo})\ -162.0984] \qquad (20)$$

For a *K. pneumoniae* mono culture biofilm, the prediction equation is

$$b_K = -1.0828\ (\log X_{vo})^2 + 26.77\ (\log X_{vo})\ -\ 162.0984 \qquad (21)$$

The predicted values show similar trends when compared with the experimentally obtained values (Figure 39). The linear model does not capture the data well ($p = 0.0249$), therefore a quadratic fit is better than a linear model.

The comparison of *K. pneumoniae* decay rates in monopopulation biofilms also agrees with the quadratic model (Figure 40). The experimental data lie close to the prediction on two out of three ocassions. The comparison of *P. aeruginosa* decay rates coefficients (Figure 41) in monopopulation biofilms is similar.

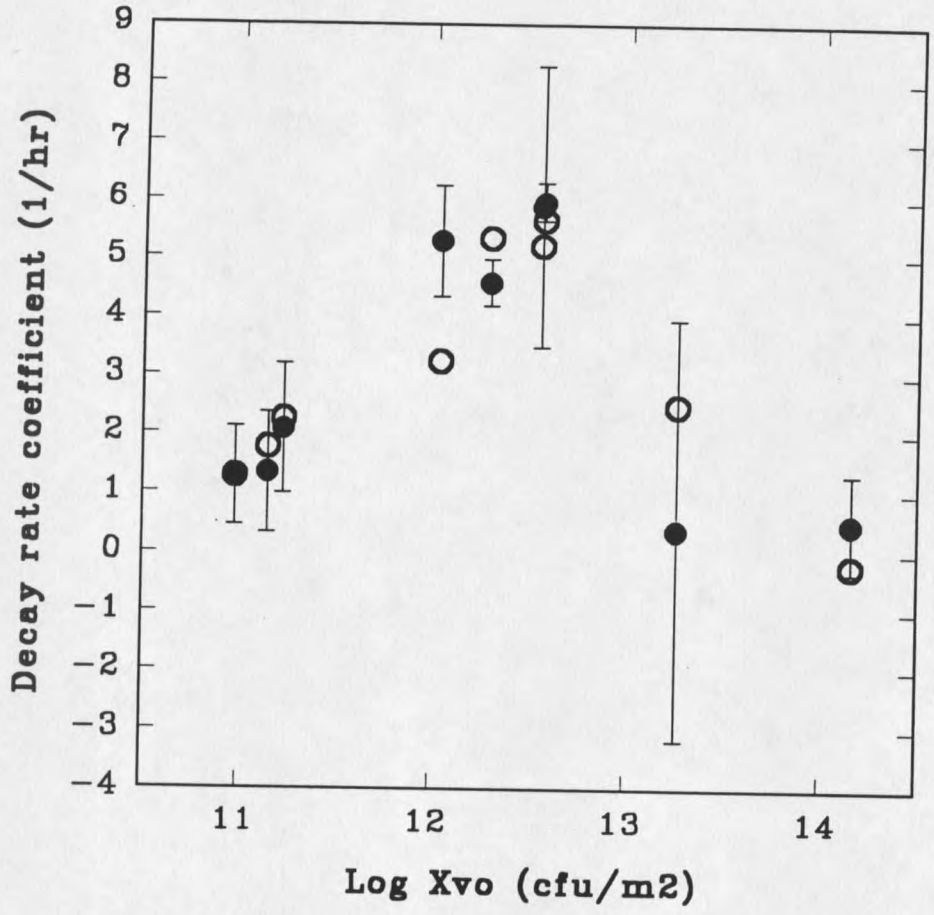

Figure 39 Comparison of the quadratic fit model (○) using non linear regression with that of experimental data (●) for all biofilm species composition. The error bars show ± 2 standard errors.

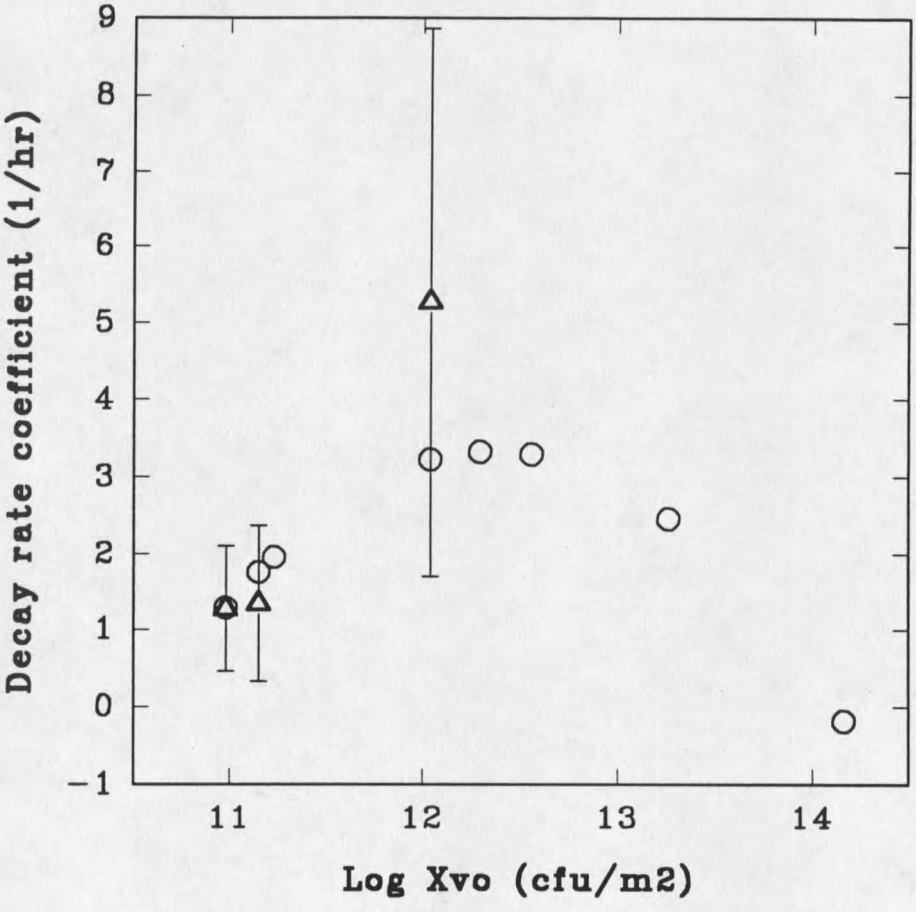

Figure 40 The behavior of the predicted quadratic fit model (○) in comparison with experimental data for *K. pneumoniae* biofilms (△). The error bars show ± 2 standard errors.

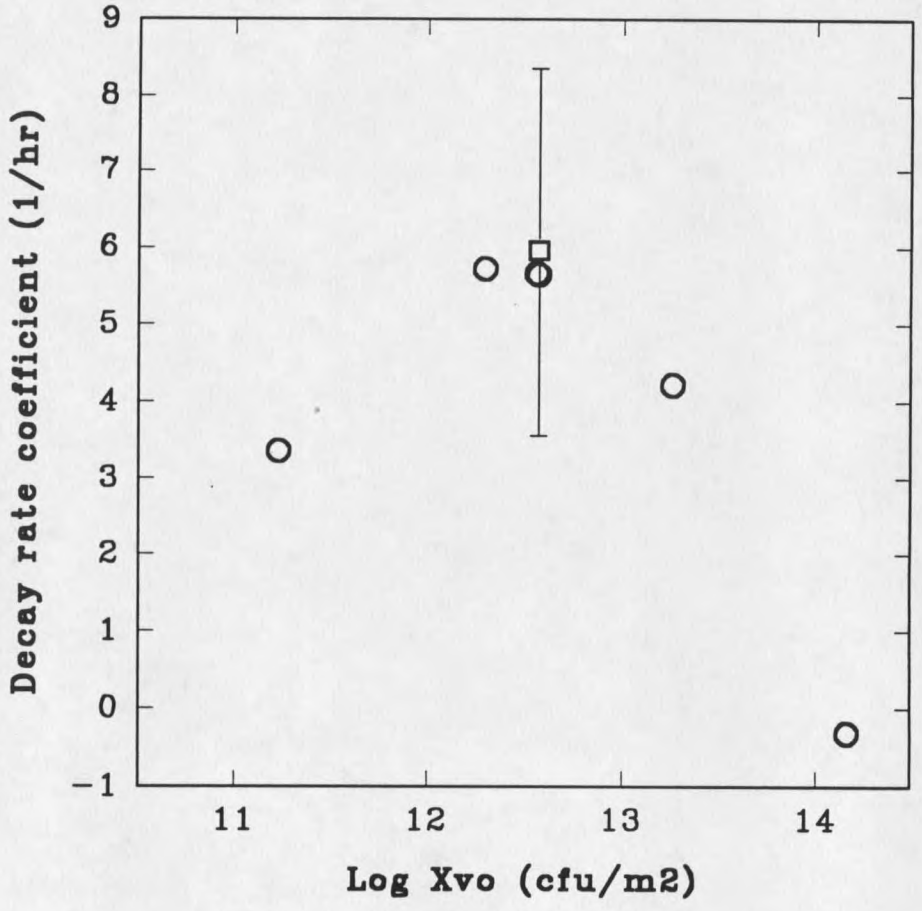

Figure 41 The behavior of the predicted quadratic fit model (○) in comparison with experiemntal data for *P. aeruginosa* biofilms (□). The error bars show ± 2 standard errors.

Abiotic particles

Abiotic particles added to a week-old biofilm reduced the efficacy of the biocide (Figure 9). The decay rate coefficient (Equation 2) for biofilms without particles was 7.7 (± 1.29) hr^{-1} and for biofilms with the particles the decay rate coefficient was 3.15 (± 0.6) hr^{-1}. Performing a t-test on the equality of these two rate coefficients yielded a p-value of 0.0005. This means that the probability that the decay rate coefficients are actually equal is less than 5 in 10,000. Therefore it can be concluded that the particles impacted biocide efficacy. There could be many reasons attributed to the effect observed. The particles could have penetrated into the voids and water channels (Drury (1992)) and thus prevented the biocide entry into the biofilm. Visual examination of the slide after dosing the reactor with the particles suggested that the particles had formed a dense strong layer on the periphery of the biofilm. This layer of particles may have acted as a physical barrier to impede biocide penetration.

Biofilm grown with a continuous supply of abiotic particles were also more resistant than the biofilms without the particles. Figure 10 depicts the difference observed in the efficacy of the biocide against these two biofilm systems. The decay rate coefficient (Equation 2) for biofilms without particles was 4.55 (± 0.42) hr^{-1} and for biofilms with the particles the decay rate coefficient was 2.51 (± 0.54) hr^{-1}. A t-test on the equality of these two values yielded a p-value of 0.0005, this means that the probability the decay

rate coefficients are actually equal is less than 5 in 10,000. Therefore it can be concluded that the particles impacted biocide efficacy. Confocal imaging was done on the biofilm with the particles as shown in Figure 42. The biofilm matrix was mixed homogeneously with the particles. Cryosectioning of the biofilm showed a more heterogenous and thicker biofilm than normal (Murga et al). The biofilm by virtue of being thicker could have affected the biocide penetration and thus decreased the efficacy of the disinfectant.

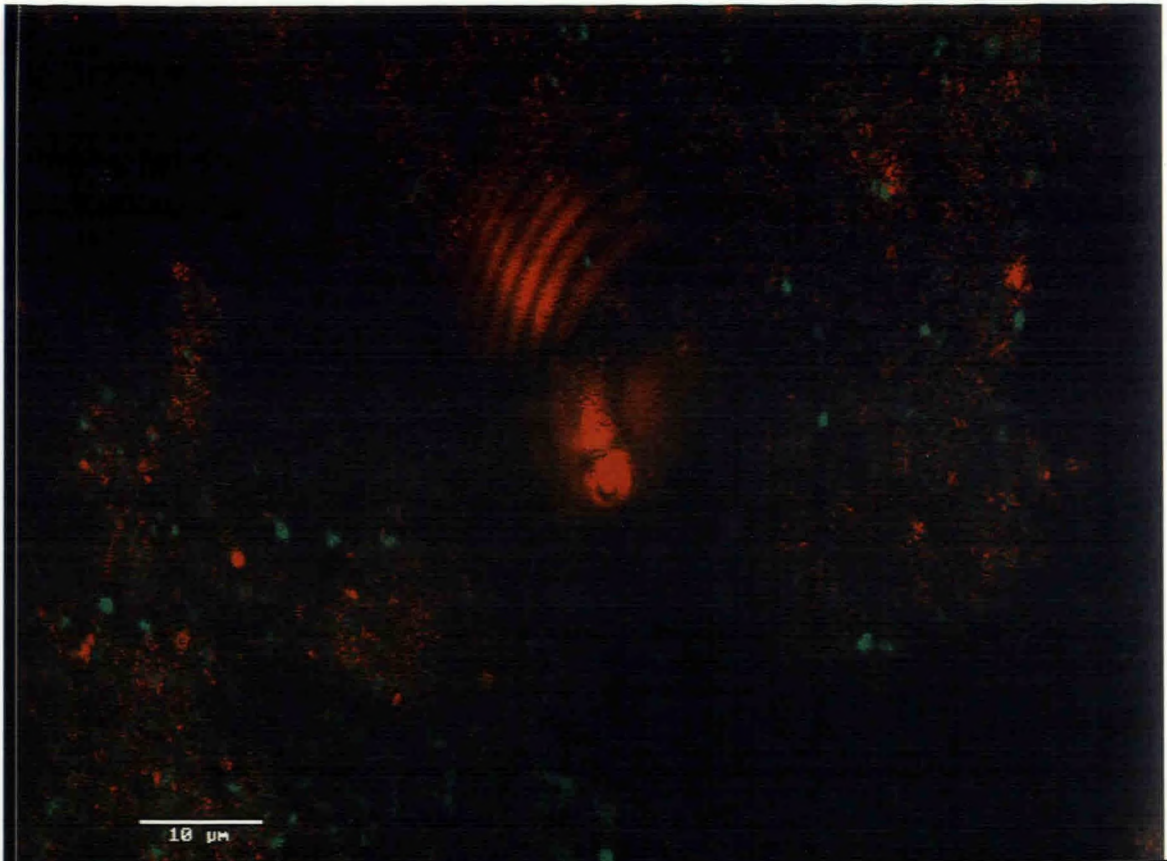
10 µm

Figure 42 The distribution of abiotic particles (red) in the biofilm matrix containing cells stained with propidium iodide (green). The biofilm was grown with continuous supply of particles. The particles are uniformly distributed in the matrix. The red spot seen in the center is an artifact.

Comparison of culturability and respiratory activity

Different measures of biocide efficacy on binary population biofilms were compared. The four different methods used were agar plate counts, glucose consumption rate, oxygen flux into the biofilm and reduction of the redox stain CTC (Stewart et al (1994)). The efficacy of the biocide determined by formation of colonies on R2A media indicated a 3 log drop after 1 hour of exposure to monochloramine (Figure 11). The number of CTC reducing cells dropped by 1 log over the same interval. Glucose consumption fell by only 15% after 1 hour of treatment (Figure 13) and oxygen flux into the biofilm (Figure 15) fell by 10% after 1 hour of treatment. Detachment of cells as determined by total cell count data (Figure 4), showed a reduction of approximately 40%.

Measures of respiratory activity such as glucose consumption rate and oxygen flux into the biofilm indicated much higher levels of residual microbial activity after monochloramine treatment than did R2A plate counts. Both energy source (glucose) and electron acceptor (oxygen) continued to be consumed in the biofilm at rates similar to their respective rates of utilization before disinfection. The reduction in glucose consumption and oxygen utilization were similar. Table 10 summarizes the different measures of biocide efficacy.

Comparing the different measures of respiratory activity, the decrease in CTC reduction was much greater than the decrease in glucose

consumption rate or oxygen utilization. The reasons for this are not clear.

Table 10. Summary comparison of methods for measuring the reduction in microbial activity after monochloramine treatment.

The results are expressed in terms of the log reduction of the fraction of pretreatment activity, *f*. The error estimate is the sample standard deviation (n = 2)

Measured Activity	$\log_{10}$ (f) @ 1 hr	$\log_{10}$ (f) @ 2 hr
R2A agar plate colonies	-3.1 ± 0.3	-3.8 ± 0.4
CTC reducing cells	-1.2 ± 0.3	-1.2 ± 0.3
Glucose consumption rate	-0.15 ± 0.05	ND
Oxygen flux	-0.05	ND
Total cells (AODC)	-0.21 ± 0.07	-0.37 ± 0.14

It is not evident whether the phenomenon of higher respiratory activity observed indicates that the cells are non-viable with residual respiratory activity or merely injured and not detected by culture media. If the cells are injured, then the plate count data overestimates biocide efficacy. If the cells are non-viable, then the respiratory indicators do not reflect the potential for recovery. Observations of rapid recovery (Figure 32, Chen et al, Wende) support the former interpretation.

Alternative approaches for the evaluation of biocide efficacy include DVC (Yu et al (1993)), bacterial luminescence (Walker et al (1992)), and impedimetric techniques (Dhaliwal et al (1992)). Introduction of newer techniques such as cryosectioning (Yu et al (1994)) and scanning confocal

laser microscopy when coupled with respiratory indicators should lead to new assays of biocide efficacy.

Different measures of biofilm activity during biocide treatment gave rise to different biocide efficacies. Plate count data may overestimate the biocide efficacy whereas the respiratory activities may underestimate it. In general, the technique chosen to measure biocide action should be selected based on the ability to predict overall system performance in a specific application.

Comparison of rates

Detachment and disinfection

Measured detachment rate coefficients were almost always lower than disinfection rate coefficients (Figure 43). Since there was only one out of nine experiemnts in which detachmnet exceeded disinfection, the probability that the detachment rate coefficient is actually equal to the disinfection rate coefficient is 2% by statistical analysis (sign test). This corroborates the finding (Chen et al (1993)) that monochloramine as a biocide does not generate much detachment even though it is a good disinfecting agent. Thus the disinfection action of monochloramine predominates the detachment effect.

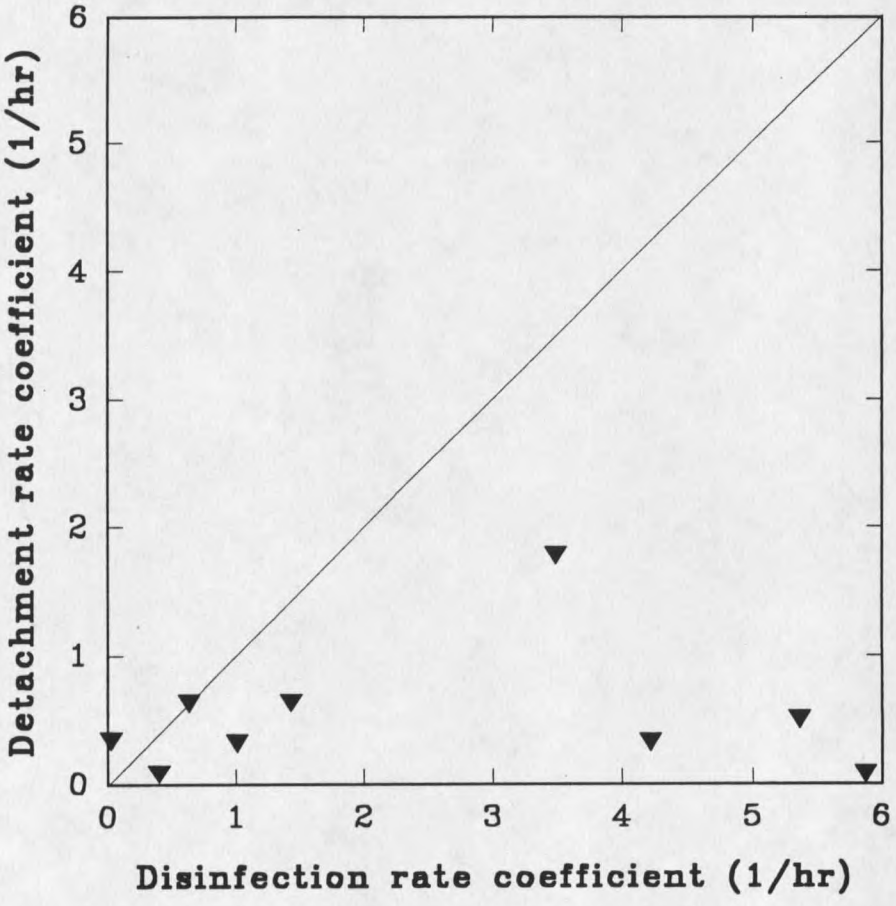

Figure 43 Comparison of detachment and disinfection rate coefficients of all types of biofilm systems.

Glucose consumption rate

Glucose consumption rate can be interpreted as a measure of biofilm activity during disinfection. Three types of biofilm systems, monopulation biofilms of either *P. aeruginosa* or *K. pneumoniae*, and the binary population biofilm combination, were compared with respect to glucose consumption rates.

During one hour of treatment with monochloramine the glucose concentration in the effluent of an annular reactor containing *P. aeruginosa* biofilm (Figure 13), shot up to its influent level. This indicates that the biofilm ceases to be active with respect to glucose consumption. The glucose concentration in the effluent of the reactor (Figure 11) for biofilm systems of *K. pneumoniae* did not rise drastically. Glucose was still consumed indicating that some respiratory activity remained in the biofilm. The calculated ratio of glucose consumption rate indicated a 50% drop (Figure 12) compared to the rate prior to the addition of biocide. The effluent glucose concentration in the binary population biofilm (Figure 9) did not rise by more than 20%. The ratio of glucose consumption rates (Figure 10) calculated also indicated around 15 to 20% drop compared to the initial value. The three biofilm systems differ with respect to glucose consumption even though the decay rates are similar. The reason why the binary population biofilm consumes glucose at the same pace during treatment process is not known. The binary population biofilms are observed to be thicker (Murga (1994)) and could therefore offer more resistance to biocide

action and hence continue to consume glucose. *K. pneumoniae* biofilms are highly heterogenous and their thickness profile varies randomly (Murga (1994)). Perhaps the heterogenous structure of the biofilm affords protection to cell clusters that continue to consume glucose and survive within the biofilm.

Monochloramine consumption rate

The consumption of monochloramine in the biofilm system reflects the reaction of monochloramine with biomass. The effluent concentration of monochloramine in *P. aeruginosa* biofilms reached a constant value of 0.5 mg/L within the first five minutes (Figure 18). The calculated monochloramine consumption rate is observed to be constant (Figure 19) after five minutes. This indicates that monochloramine is consumed quickly and reaches a steady level in the reactor. The effluent concentration of monochloramine in the binary population biofilm (Figure 14) system was similar to that observed in the *P. aeruginosa* biofilm systems. The concentration reached a steady level in the first 5 minutes. The monochloramine consumption rate (Figure 15) also remained constant after the first five minutes. This indicates that the biocide is consumed rapidly in the system. The lower bulk fluid concentration observed could also be a factor in the decrease in efficacy of the biocide. The concentration of monochloramine in the effluent stream for biofilm systems of *K. pneumoniae* differed from the other biofilm systems (Figure 16). The concentration dips

down and raises up. The monochloramine consumption rate is very low compared to the other biofilm systems (Figure 17). This peculiar trend could be due to the fact that the method used to determine the amount of monochloramine in the solution is not specific. Experiments should be conducted using alternative analytical methods to test whether the effect is real. Thus the monochloramine consumption rates differed for all three types of biofilms.

Detachment rate

The concentration of cells in the reactor effluent reflects the amount of cells detached from the biofilm. The detachment rate coefficient indicates the number of cells detached per unit area per hour. Figure 24 depicts the amount of cells seen in the effluent of the reactor for the biofilm system of *P. aeruginosa*. The decrease in cell number during disinfection is around 50%. The calculated detachment rate decreases accordingly (Figure 25). The same effect is observed in the binary population biofilm system (Figure 21). The *K. pneumoniae* biofilm system also behaved similarly (Figure 23). These results show that monochloramine does not promote detachment in these systems.

CONCLUSIONS

The following conclusions are made based on the results obtained in experimental studies of monochloramine treatment of biofilms of *K. pneumoniae* and *P. aeruginosa*.

1) Decay rate is a complex function of initial viable cell density.

2) Disinfection predominates over detachment.

3) There is no evidence of species interactions during disinfection.

4) Abiotic particles reduced biocide efficacy.

5) There is a significant difference between measures of respiratory activity and colony forming units during disinfection.

RECOMMENDATIONS

The recommendations that follow are offered as improvements on the experimental design used in this research or as new approaches that could yield valuable information concerning the mechanisms of biofilm resistance to antimicrobial agents.

Physiological probes Biofilms are thought to be more resistant to biocides by virtue of physiological differences from their planktonic counterparts. To investigate this possibility, physiological probes such as respiratory activity indicators (CTC), growth rate indicators (RNA probes), and gene probes could be used in conjunction with embedding and sectioning (Yu et al (1994)) to visualize physiological gradients within the biofilm.

Microelectrodes Microelectrodes should be developed to study the penetration of biocides into biofilms. Concentration profiles thus obtained would allow an immediate assessment of the ability of a biocide to penetrate the biofilm. These results could also be used to verify mathematical models of biocide action on biofilms. Together with the application of physiological probes, microelectrode measurements would help to identify and understand mechanisms of biofilm resistance to biocides.

Sampling In this thesis separate reactors were analyzed for biofilm and bulk fluid dynamics. This approach grew out of a monopopulation system that gave reproducible biofilms. With the binary population biofilms, this approach was not efficient. The data collected on bulk fluid dynamics are

difficult to interpret since nothing is known about the highly variable biofilm. In the future, bulk fluid and biofilm sampling should be performed on the same reactor.

Time scale In this thesis research, data were collected over a one or two hour disinfection period. It would be valuable to extend the analysis over a longer period, perhaps on the order of a day, so as to capture the phenomenon of recovery.

REFERENCES

REFERENCES

Allison, D. G.(1992). "Polysaccharide interactions in bacterial biofilms". In Biofilms- Science and Technology, L. F. Melo et al (eds). Kluwer Academic Publishers. Netherlands.

Anwar, H., J. L. Strap, K. Chen, and J. W. Costerton (1992). "Dynamic Interactions of Biofilms of Mucoid Pseudomonas aeruginosa with Tobramycin and Piperacillin". Antimicrobial Agents and Chemotherapy. Vol. 36, pp. 1208-1214.

Bailley, J. E, and Ollis, D. F (1986) (eds). "Biochemical Engineering Fundamental". McGraw-Hill.

Blenkinsopp, S. A., A. E. Khoury, and J. W. Costerton (1992). "Electrical enhancement of biocide efficacy against Pseudomonas aeruginosa biofilms". Applied and Environmental Microbiology. Vol. 58, pp. 3770-3773.

Cameroon, G. N., J. M. Symons, D. Bushek, and R. Kulkarni (Oct. 1989). "Effect of temperature and pH on the toxicity of monochloramine to the asiatic clam". Research and Technology, American Water Works.

Characklis W G, Marshall K C (1990) "Biofilms: a basis for an interdisciplinary approach". In: Characklis W G, Marshall K C (eds) Biofilms, John Wiley & Sons Incorporated, New York.

Chen, C.-I., T. Griebe, and W.G. Characklis (1993). "Biocide action of monochloramine on biofilm systems of *Pseudomonas aeruginosa*". Biofouling. Vol. 7, pp. 1-17.

Chen, C.-I., T. Griebe, R. Srinivasan, and P.S Stewart (1993). "Effects of various metal substrata on accumulation of *Pseudomonas aeruginosa* biofilms and the efficacy of monochloramine as a biocide". Biofouling. Vol. 7, pp. 214-251.

Costerton, J. W., G. G. Geesey, P. A. Jones (1987). "Bacterial biofilms in relation to internal corrosion monitoring strategies". National Association of Corrosion Engineers, Corrosion/87, Paper no. 54.

Dhaliwal, D. S., J. L. Cordier, and L. J. Cox. 1992. "Impedimetric evaluation of the efficiency of disinfectants against biofilms". Let. Applied and Environmental Microbiology. Vol. 15, pp 217-221.

Drury, William Joseph. "Interactions of 1⊠m latex microbeads with biofilms".

Ph.D. diss. Montana State University.

Flemming, H. C. "Biofouling in water treatment". Biofouling and Biocorrosion in Industrial Water Systems. Proceedings of the international workshop on industrial biofouling and biocorrosion, Stuttgart, Sept. 13-14, 1990. H. C. Flemming and G. G. Geesey (Eds).

Griebe, T., C.-I Chen, R. Srinivasan, and P.S Stewart (1993). "Analysis of biofilm disinfection by monochloramine and free chlorine". In:Biofouling and biocorrosion in Industrial Water Systems. (ed. by G. Geesey & Z. Lewandowski), Lewis Publishers, Florida.

Jacangelo, J. G., V. P. Oliveri (1984). "Aspects of the mode of action of monochloramine".In Water Chlorination, Vol. 5

Kaperlyants, A. S. and D. B. Kell. 1993. "Dormancy in stationary phase cultures of Micrococcus luteus: flow cytometric analysis of starvation and resuscitation". Applied and Environmental Microbiology. Vol. 59, pp. 3187-3196.

LeChavellier, M.W., S. C. cameron and G. A. Mcfeters. 1982. "New medium for the improved recovery of coliform bacteria from drinking water". Applied and Environmental Microbiology. Vol. 45, pp. 484-492.

LeChavellier, M. W., C. D. Cawthon, R. G. Lee (1988). "Inactivation of biofilm bacteria". Applied and Environmental Microbiology. Vol. 54, pp.2492-2499.

LeChavellier, M. W., C. D. Lowry, and R. G. Lee (July 1990). "Disinfecting biofilms in a model distribution system". Reserach and Technology, American Water works Association.

LeChavellier, M. W., T. S. Hassenauer, A. K. Camper, and G. A. McFeters (1994). "Disinfection of bacteria attached to granular activated carbon". Applied and Environmental Microbiology. Vol. 48, pp. 918-923.

Lewandowski, Z., G. Walser, and W. G. Characklis (1991). "Reaction kinetics in biofilms". Biotechnology and Bioengineering, Vol. 38, No. 8.

McCoy, W. F. "Strategies for the treatment of biological fouling". In. Biological fouling of industrial water systems: A problem solving approach. M. W. Mittleman and G. G. Geesey (eds).

McFeters, G. A. (1990). "Enumeration, occurrence and significance of

injured indicator bacteria in drinking water". In G. A. Mcfeters (ed) Drinking Water Microbiology: Progress and Recent Developments. Springer-Verlag, New York.

Nichols, W. W., S. M. Dorrington, M. P. E. Slack, and H. L. Walmsley (1988). "Inhibition of trobamycin diffusion by binding to alginate" Antimicrobial Agents and Chemotherapy. Vol. 32, pp. 518-523.

Roszak, D. B. and R. R. Colwell (1987). "Survival strategies of bacteria in the natural environment". Microbiological reviews. Vol. 51, pp. 365-379.

Siebel, M. A., and W. G. Characklis (1991). "Observations of binary population biofilms". Biotechnology and Bioengineering. Vol. 37, pp 778-789.

Stewart, P. S., T. Griebe, R. Srinivasan, C.-I. Chen, F. P. Yu, D. deBeer, G. A. Mcfeters. "Comparison of respiratory activity and culturability during monochloramine disinfection of binary population biofilms". Applied and Environmental Microbiology, in press.

Sandholm, T. M., and G. Wirtanen (1992). "Biofilm formation in the industry: A review". Food Reviews International. Vol. 8(4), pp. 573-603.

Tashiro, H.,T. Numakura, S. Nishikawa, and Y. Miyaji (1991). "Penetration of biocides into biofilms". Water Science Technology. Vol. 23, pp. 1395-1403.

Van der Wende, E. "Biocide action of chlorine on *P. aeruginosa* biofilm". Ph.D. diss., Montana State University (1991).

Walker, A. J., S. A. A. Jassim, J. T. Holah, S. P. Denyer and G. S. A. B. Stewart (1992). "Bioluminescent Lysteria monocytogenes provide a rapid assay for measuring biocide efficacy". Fems Microbiological Letters. Vol. 91, pp. 251-256.

Whitman, T. S., and P. D. Gilbert (1993). "Evaluation of a model biofilm for the ranking of biocide performance against sulphate-reducing bacteria". Journal of Applied Bacteriology. Vol. 75, pp. 529-535.

Wolfe, R. L, N. R. Ward, and B. H. Olson. "Inactivation of Heterotrophic Bacterial Populations in Finished Drinking Water by Chlorine and Chloramines". Water Research. Vol. 19, pp. 1393-1403.

Yasuda, H., Y. Ajiki, T. Koga, H. Kawada, T. Yokota (1993). "Interaction between biofilms formed by Pseudomonas aeruginosa and Clarithromycin". Antimicrobial agents and Chemotherapy. Vol. 37, pp. 1749-1755.

Yu, F. P., and G. A. McFeters (1993). "Rapid in situ physiological assessment of bacteria in biofilms using fluorescent probes", abstr. Q-74, p.359. Abstr. 93rd Annual meeting of American Society of Microbiologists. 1993.

Yu, F. P., B. H. Pyle and G. A. Mcfeters (1993). "A direct viable count method for the enumeration of attached bacteria and assessment of biofilm disinfection". Journal of Microbiological Methods. Vol. 17, pp. 167-180.

Yu, F. P., G. M. Callis, P. S. Stewart, T. Griebe, G. A. McFeters. "Cryosectioning of biofilms for microscopic examination". Biofouling in press.

APPENDICES

APPENDICES

The appendix section of the thesis contains all the raw data obtained during the experiments. The data can be broadly classified as;

Growth and regrowth data : The data obtained from the effluent of the reactor before and after biocide addition, the first regrowth data obtained after 24 hrs of withdrawal of biocide.

Disinfection data : The data obtained during the addition of monochloramine into the reactor. The data collection was of two types. For *in situ* biofilm disinfection, plate count data, total cell count data and TOC were measured. For bulk fluid disinfection, plate count data, total cell count data, TOC, SOC, glucose and monochloramine concentrations were obtained.

Oxygen flux into the biofilm : The concentration profile of oxygen in a binary population biofilm was obtained during the disinfection process in a flow cell.

Effect of abiotic particles : disinfection data observing the effects of addition of abiotic particles into the reactor system of a binary population biofilm.

Calculated values of glucose consumption rate, monochloramine consumption rate, and detachment rate coefficient.

APPENDIX A

This section contains data for biofilm system of *P.aeruginosa*

Table 11 Growth and recovery

The biocide was added at 216 hrs for a period of one hr.

Time (hrs)	X_{ev} (cfu/ml)
0	0
24	1.1E06
48	2.9E06
72	4.7E06
96	1.4E07
144	2.2E07
168	2.94E07
192	2.94E07
216	2.63E07
240	4.4E06
264	1.5E07
336	1.26E07
360	9.9E06
384	1.2E07

X_{ev}, is the amount of cells present in the bulk fluid.

Table 12 Biofilm analysis, run 1

Time (hrs)	X_{bv} (cfu/m^2)	X_{bT} (#/m^2)	TOC (mg/m^2)
0.000	3.77E12	4.07E12	370
0.083	6.2E11	3.89E12	360
0.167	1.42E11	3.98E12	428
0.25	1.7E10	3.81E12	460
0.50	2.0E09	4.01E12	377
0.75	4.33E08	4.47E12	423
1.0	2.53E08	4.17E12	410
2.0	2.45E07	---------	---

Table 13 Biofilm analysis, run 2

Time (hrs)	X_{bv} (cfu/m^2)
0.000	1.83E13
0.50	7.42E10
1.0	3.83E09

Table 14 Biofilm analysis, run 3

Time (hr)	X_{bv} (cfu/m^2)
0.000	8.41E12
1.000	7.76E08

X_{bv} and X_{bT} are the number of viable and total cells in biofilm respectively.

Table 15 Bulk fluid analysis

Time hrs	X_{ev} (cfu/mL)	X_{eT} (#/mL)	TOC (mg/L)	SOC (mg/L)	Glu (mg/L)	Mon (mg/L)
0.000	2.5E07	3.5E07	8.5	6.7	0.5	4.0
0.083	1.1E05	2.4E07	24.8	13.1	9.6	0.5
0.167	-------	3.0E07	29.7	15.5	13.4	0.5
0.25	-------	1.8E07	35.1	13.1	18.1	0.5
0.417	-------	2.1E07	36.1	21.5	18.3	0.5
0.75	-------	1.5E07	35.5	29.5	19.5	0.5
1.0	---	9.0E07	35.7	30.3	19.1	0.5

X_{ev} and X_{eT} are the number of viable and total cells in the effluent respectively.

APPENDIX B

This section contains data for the biofilm system of *K.pneumoniae*.

Table 16 Growth and recovery, run 1

The biocide was added at 120 hrs for a period of one hr.

Time (hrs)	X_{ev} (cfu/ml)
0	0
24	3.19E06
48	3.67E07
72	4.67E08
96	8.67E07
120	6.33E07
144	3.05E07
168	4.25E07
192	6.17E07

Table 17 Growth and recovery, run 2

The biocide was added at 144 hrs for a period of one hr.

Time (hrs)	X_{ev} (cfu/ml)
0	0
24	5.0E03
48	9.0E05
72	---------
96	8.35E05
120	4.33E07
144	9.6E07
168	3.18E07
192	4.7E07
216	5.5E07

Table 18 Biofilm analysis, run 1

Time (hrs)	X_{bv} (cfu/m^2)	X_{bT} (#/m^2)	TOC (mg/m^2)
0.0000	1.1E12	1.12E12	1012.5
0.167	3.34E11	6.87E11	208.6
0.25	6.47E10	5.13E11	198.3
0.5	1.02E10	1.24E11	2980.8
0.75	4.51E09	9.25E10	129.2
1.0	1.24E09	9.16E10	131.76
1.25	8.89E08	7.21E10	90.54
1.5	1.5E08	3.72E10	149.75
2.0	1.7E07	3.1E10	174.8

Table 19 Biofilm analysis, run 2

Time (hrs)	X_{bv} (cfu/m^2)	X_{bT} (#/m^2)	TOC (mg/m^2)
0.0000	1.42E11	1.09E12	198.75
0.0000	5.59E11	1.89E12	105.39
0.167	2.23E10	1.47E12	279.0
0.167	1.1E10	1.57E12	100.35
0.25	1.43E10	1.31E12	92.38
0.5	3.0E10	1.32E12	1207.34
0.75	2.01E10	3.24E12	1701.02
1.0	2.7E10	1.67E12	174.99
1.0	1.75E10	1.35E12	396.91
1.25	2.57E10	9.4E11	384.69
1.5	2.13E10	9.11E11	239.37
2.0	1.98E09	6.5E11	1370.11

Table 20 Biofilm analysis, run 3

Time (hrs)	X_{bv} (cfu/m^2)	X_{bT} (#/m^2)	TOC (mg/m^2)
0.0000	9.5E10	1.12E12	237.98
0.167	1.63E10	6.87E11	567.76
0.25	9.21E09	5.13E11	1005.76
0.5	3.68E09	1.24E11	167.89
0.75	1.62E10	9.25E10	127.98
1.0	8.16E09	9.16E10	234.65
1.25	7.52E09	7.21E10	342.32
1.5	3.19E09	3.72E10	212.11
2.0	2.1E09	3.1E10	131.09

Table 21 Bulk fluid analysis, run 1

Time hrs	X_{ev} (cfu/mL)	X_{eT} (#/mL)	TOC (mg/L)	SOC (mg/L)	Glu (mg/L)	Mon (mg/L)
0.000	4.34E07	4.58E08	3.7	2.4	0.001	4.0
0.083	3.38E07	1.54E08	35.1	7.9	0.83	1.6
0.167	9.83E07	1.02E08	32.2	9.81	0.24	1.9
0.25	1.31E07	2.89E08	22.6	6.8	2.29	3.0
0.333	7.78E06	2.94E08	16.4	7.8	4.72	3.1
0.416	2.4E06	1.56E08	23.3	6.6	1.08	3.1
0.5	6.7E05	1.25E08	15.1	6.4	3.51	3.2
0.583	3.75E05	1.27E08	12.2	6.2	3.12	3.25
0.666	4.44E05	1.21E08	11.9	5.9	4.55	3.45
0.75	2.63E05	1.03E08	8.4	6.8	2.62	3.55
0.833	1.55E05	1.2E08	9.1	5.9	9.19	3.65
0.916	9.2E04	9.84E07	8.7	5.9	9.91	3.65
1.0	9.8E04	9.4E07	7.4	5.2	10.35	3.65

Table 22 Bulk fluid analysis, run 2

Time hrs	X_{ev} (cfu/mL)	X_{eT} (#/mL)	TOC (mg/L)	SOC (mg/L)	Glu (mg/L)	Mon (mg/L)
0.000	1.29E07	1.56E08	17.22	16.7	0.001	4.0
0.083	2.31E06	2.26E08	15.84	8.37	2.843	1.8
0.167	4.95E05	1.96E08	16.06	5.98	2.86	2.0
0.25	6.33E05	2.47E07	15.08	8.61	1.54	3.25
0.333	1.02E06	1.98E08	15.09	8.03	2.35	3.5
0.416	4.05E05	1.98E08	16.45	9.55	3.19	3.65
0.5	1.29E05	2.11E08	16.86	15.3	1.52	3.6
0.583	3.67E04	2.09E08	15.73	9.30	1.96	3.55
0.666	1.59E05	2.27E08	16.99	10.0	1.79	3.55
0.75	1.23E05	2.16E08	21.43	10.1	1.65	3.6
0.833	1.99E05	1.57E08	14.42	9.77	4.55	3.6
0.916	1.69E05	9.66E07	13.0	12.4	8.97	3.65
1.0	1.8E05	8.99E07	13.89	16.8	5.82	3.85

APPENDIX C

This section contains data for the binary population biofilm consisting of

Table 23 Growth and recovery, run 1

The biocide was added at 144 hrs for a period of one hr.

Time (hrs)	X_{ev} *K.pneumonaie*	X_{ev} *P.aeruginosa*	X_{ev} total
0	0	0	0
24	1.0E05	1.0E05	2.0E05
48	2.29E07	1.67E07	2.457E07
72	2.25E07	1.85E07	4.1E07
96	2.85E07	1.2E07	4.05E07
120	5.97E07	1.55E07	7.52E07
144	4.67E06	3.67E06	8.34E06
168	2.56E06	1.01E06	3.57E06
192	2.15E07	1.72E07	3.87E07
216	1.95E07	1.82E07	3.77E07
240	3.0E07	1.23E07	4.23E07

Table 24 Growth and recovery data, run 2

The biocide was added at 144 hrs for a period of one hr.

Time (hrs)	X_{ev} *K. pneumonaie*	X_{ev} *P. aeruginosa*	X_{ev} total
0	50	50	100
24	3.5E03	1.5E03	5.0E03
48	4.6E05	4.4E05	9.0E05
72			---------
96	4.4E05	3.95E05	8.35E05
120	3.0E07	1.33E07	4.33E07
144	5.8E07	3.8E07	9.6E07
168	1.2E07	1.98E07	3.18E07
192	9.8E06	3.72E07	4.7E07
216	4.9E07	6.0E06	5.5E07

Table 25 Biofilm analysis, run 1

Time (hrs)	X_{bv} *K.pneumoniae* (cfu/m^2)	X_{bv} *P.aeruginosa* (cfu/m^2)	X_{bT}, total (cfu/m^2)	TOC (mg/m^2)
0.0000	3.3E11	1.66E12	8.13E12	3525
0.0000	2.01E11	1.56E12	7.41E12	1125
0.083	3.46E11	1.14E12	8.32E12	2853.8
0.167	9.25E10	4.7E11	6.46E12	1509
0.25	8.63E10	2.12E11	6.92E12	740.3
0.5	3.94E10	1.15E11	5.62E12	1598.7
0.75	1.97E10	1.22E09	4.9E12	623.3
1.0	2.77E09	1.86E08	5.5E12	612.7
1.25	1.37E09	1.55E07	4.57E12	392.6
1.5	1.31E09	<1000	4.17E12	357.5
2.0	6.49E08	<1000	4.27E12	358.2

Table 26 Biofilm analysis, run 2

Time (hrs)	X_{bv} *K.pneumoniae* (cfu/m^2)	X_{bv} *P.aeruginosa* (cfu/m^2)	X_{bT} (#/m^2)	TOC (mg/m^2)
0.0000	3.55E11	1.4E12	1.7E12	442.8
0.0000	2.34E11	1.91E12	2.13E12	409.8
0.167	1.23E11	7.41E11	1.74E12	609
0.167	2.57E11	7.24E11	1.66E12	356.8
0.25	2.42E10	3.8E11	1.48E12	305.5
0.5	4.27E09	2.04E09	1.45E12	344
0.75	7.41E09	7.94E08	1.36E12	673
1.0	1.578E09	1.82E08	1.17E12	323
1.0	5.75E08	1.95E07	1.07E12	259
1.25	7.59E08	2.63E08	1.1E12	393
1.5	9.77E08	1.58E08	8.51E11	342
2.0	5.25E07	8.71E07	6.24E11	286.3

Table 27 Biofilm analysis, run 3

Time (hrs)	X_{bv} *K.pneumoniae* (cfu/m^2)	X_{bv} *P.aeruginosa* (cfu/m^2)	X_{bT} (#/m^2)	TOC (mg/m^2)
0.0000	1.35E11	3.63E10	3.39E11	357
0.0000	1.14E11	1.62E10	3.24E11	271.3
0.167	1.26E10	4.9E08	1.74E11	201.45
0.25	5.5E09	3.63E08	1.66E11	208.9
0.5	3.55E09	2.29E08	1.32E11	149.6
0.75	1.66E09	1.41E08	1.29E11	4381
1.0	3.63E09	7.24E07	1.25E11	260
1.0	5.25E09	1.82E08	1.26E11	419
1.25	1.0E09	1.05E08	9.55E10	3944
1.5	1.86E09	4.47E07	9.33E10	1344.3
2.0	1.29E09	4.37E07	7.91E10	1456

Table 28 Biofilm analysis, run 4

Time (hrs)	X_{bv} *K.pneumoniae* (cfu/m^2)	X_{bv} *P.aeruginosa* (cfu/m^2)	X_{bT} (#/m^2)
0.0000	1.12E14	3.35E13	1.73E14
0.25	1.05E14	2.31E13	1.69E14
0.5	6.44E13	4.06E12	7.28E13
0.75	7.4E13	3.34E12	6.49E13
1.0	4.38E13	2.31E12	6.92E13
1.5	5.89E13	9.55E11	1.29E14
2.0	5.16E13	1.27E12	1.22E14

Table 29 Biofilm analysis, run 5

Time (hrs)	X_{bv} *K.pneumoniae* (cfu/m^2)	X_{bv} *P.aeruginosa* (cfu/m^2)	X_{bT} (#/m^2)
0.0000	1.82E13	1.31E11	2.65E13
0.25	6.9E12	1.39E11	2.48E13
0.5	5.77E12	1.61E11	2.51E13
0.75	7.8E12	1.55E11	2.22E13
1.0	4.94E12	1.16E11	2.31E13
1.25	7.45E12	1.97E11	2.22E13
1.5	6.9E12	1.32E11	1.27E13
2.0	4.99E12	4.64E10	1.4E13

Table 30 bulk fluid analysis, run 1

Time hrs	X_{ev} (cfu/mL)		X_{eT} (#/mL)	TOC (mg/L)	SOC (mg/L)	Glu (mg/L)	Mon (mg/L)	
	K. pneum	*P. aeru*						
0.000	2.09E06	3.89E06		1.73E07	4.162	1.432	0.55	4.0
0.083	6.75E05	4.33E04		2.26E08	3.339	1.648	0.72	0.5
0.167	4.99E03	8.71E03		7.62E06	4.714	3.086	0.55	0.30
0.250	6.6E02	8.71E03		7.09E06	4.411	3.849	0.72	0.25
0.333	1.25E02	2.19E03		9.93E06	1.516	1.343	0.66	0.20
0.416	1.99E02	1.08E03		7.06E06	14.69	2.19	0.77	0.25
0.500	1.6E01	3.16E02		3.65E06	78.27	1.983	0.83	0.25
0.583				8.99E06	15.30	1.555	0.77	0.25
0.666				4.72E06	16.38	1.635	0.72	0.30
0.75				6.22E06	22.83	5.664	4.66	0.30
0.833				2.70E06	2.59	1.504	0.66	0.30
0.918				3.94E06	2.17	1.769	1.4	0.30
1.0				2.98E06	2.05	1.921	0.25	0.35

Table 31 Bulk fluid analysis, run 2

Time hrs	X_{ev} (cfu/mL) K. pneum	P. aeru	X_{eT} (#/mL)	TOC (mg/L)	SOC (mg/L)	Glu (mg/L)	Mon (mg/L)	
0.000	9.13E06	3.36E07	6.59E07	2.79	1.63	0.19	4.0	
0.083	1.01E07	1.50E07	8.15E07	5.66	4.52	1.18	0.1	
0.167	6.65E07	1.93E07	7.47E07	6.18	1.85	0.49	0.1	
0.250	3.02E07	3.04E07	8.20E07	8.49	4.01	0.80	0.15	
0.333	1.68E07	2.25E07	8.49E07	7.77	3.13	1.24	0.15	
0.416	2.20E07	2.40E07	7.90E07	7.70	3.22	2.07	0.2	
0.500	1.32E07	1.80E07	8.44E07	8.27	3.80	1.90	0.25	
0.583	1.77E07	2.15E07	9.31E07	6.94	3.38	2.95	0.25	
0.666	7.83E06	1.08E07	7.98E07	7.23	3.42	3.01	0.35	
0.750	5.83E06	5.70E06	8.71E07	6.07	3.52	2.62	0.38	
0.833	7.00E06	5.46E06	6.51E07	5.56	3.56	3.84	0.4	
0.916	4.90E06	3.50E06	4.77E07	5.48	4.01	5.16	0.43	
1.000	1.10E06	2.70E06	4.57E07	5.18	1.03	4.96	0.45	

Table 32 Bulk fluid analysis, run 3

Time hrs	X_{ev} (cfu/mL) K. pneum	P. aeru	X_{eT} (#/mL)	TOC (mg/L)	SOC (mg/L)	Glu (mg/L)	Mon (mg/L)	
0.000	4.67E06	3.67E06	6.40E07	3.64	2.98	0.19	4.0	
0.083	6.33E06	2.66E06	6.80E07	5.84	4.87	1.29	1.0	
0.167	1.51E06	6.67E05	6.92E07	9.67	7.82	0.99	0.85	
0.250	1.52E06	1.16E06	7.25E07	14.08	8.76	1.08	0.7	
0.333	1.83E06	5.34E06	6.95E07	10.65	8.03	1.26	0.75	
0.416	6.67E05	3.33E05	6.86E07	7.98	6.78	1.42	0.75	
0.500	3.48E06	8.11E05	6.97E07	8.69	5.89	1.37	0.85	
0.583	8.95E06	1.33E06	7.08E07	10.43	9.67	1.86	0.9	
0.666	8.47E06	6.2E05	6.89E07	12.62	6.98	1.87	0.85	
0.750	6.25E06	8.12E05	6.79E07	8.09	6.59	2.64	0.85	
0.833	4.36E06	7.16E05	5.98E07	7.49	6.98	2.25	0.9	
0.916	3.77E06	4.84E05	5.98E07	9.32	6.11	3.28	0.85	
1.000	4.35E06	3.25E05	5.68E07	6.98	3.82	3.1	0.9	

APPENDIX D

Abiotic particles (calcium carbonate and kaolin), were added to a biofilm 7 days old for an hour. The particles were flushed out of the bulk fluid for an hour and 4 mg/L monochloramine was added to the system for an hour.

Table 33 Biofilm analysis

Time (hr)	X_{bv}, *K. pneumoniae* (cfu/m^2)	X_{bv}, *P.aeruginosa* (cfu/m^2)
0.000 (control)	1.44E12	2.38E12
0.000	4.56E11	1.31E12
0.167	4.57E11	5.72E11
0.25	8.12E10	3.4E11
0.5	1.33E11	2.47E11
1.0	7.57E10	2.47E10

Binary population biofilms were grown along with the abiotic particles (50 mg/l). Monochloramine was added after 6 days.

Table 34 Biofilm analysis

Time (hrs)	X_{bv}, *K.pneumoniae* (cfu/m_2)	Xbv, *P.aeruginosa* (cfu/m^2)
0.000	9.2E11	1.2E12
0.25	1.75E12	2.77E11
0.5	4.062E11	4.31E10
0.75	1.877E11	1.231E10
1.0	3.231E10	1.54E09
1.5	1.63E10	6.154E08
2.0	3.046E10	9.23E08

APPENDIX E

Calculated glucose consumption rates (R_s) for all types of populations. R_s is obtained from Equation 5.

Table 35 *K. pneumoniae*, run 1

Time (min)	GLUC (mg/L)	dS/dt	R_s (mg/m^2-hr)
0	0.0004	-0.0301	0.999
5	1.1372	-0.0201	0.917
10	1.1396	-0.0101	0.988
15	0.614	-0.0001	1.181
20	0.94	0.0099	1.151
25	1.276	0.0199	1.126
30	0.608	0.0299	1.295
35	0.784	0.0399	1.015
40	0.716	0.0499	0.745
45	0.66	0.0599	0.632
50	1.82	0.0699	0.561
55	3.588	0.0799	0.382
60	2.328	0.0899	0.722

Table 36 *K. Pneumoniae*, run 2

Time (min)	GLUC mg/L	dS/dt	R_s (mg/m^2-hr)
0	0.0004	-0.0319	1.455
5	0.3312	-0.0189	1.355
10	0.096	-0.0059	0.677
15	0.916	0.0071	1.168
20	1.888	0.0201	0.957
25	0.432	0.0331	1.160
30	1.404	0.0461	0.952
35	1.248	0.0591	0.934
40	1.82	0.0721	0.793
45	1.048	0.0851	0.879
50	3.676	0.0981	0.392
55	3.96	0.1111	0.299
60	4.14	0.1241	0.225

Table 37 *P. aeruginosa*

Time (min)	GLUC (mg/L)	dS/dt	R_s (mg/m^2-hr)
0	0.2	0	1.312
5	3.84	0.5408	-1.14
10	5.36	0.3648	-0.80
15	7.24	0.1888	-0.51
25	7.32	0.0238	0.033
45	7.8	0.0078	0.006
60	7.64	-0.0042	0.074

ds/dt was evaluated using two fits

0-15, S=-.0176T2+.7168T+.3240
15-60, S=-.0004T2+.0438T+6.6185

Table 38 *Binary*, run 1

Time (min)	GLUC (mg/L)	dS/dT	R_s (mg/m^2-hr)
0	0.22	0.0201	1.00
5	0.288	0.0181	1.08
10	0.22	0.0161	1.24
15	0.288	0.0141	1.19
20	0.264	0.0121	1.28
25	0.308	0.0101	1.33
30	0.332	0.0081	1.43
35	0.308	0.0061	1.51
40	0.288	0.0041	1.58
45	1.864	0.0021	1.31
50	0.264	0.0001	1.63
55	0.56	-0.0019	1.56
60	0.1	-0.0039	1.61

Table 39 *Binary*, run 2

Time (min)	GLUC (mg/L)	dS/dt	R_s (mg/m^2-hr)
0	0.1	-0.0074	1.36
5	0.22	-0.0034	1.32
10	0.236	0.0006	1.3
15	0.296	0.0046	1.28
20	0.268	0.0086	1.27
25	0.356	0.0126	1.24
30	0.344	0.0166	1.23
35	0.272	0.0206	1.23
40	0.288	0.0246	1.21
45	0.712	0.0286	1.13
50	1.08	0.0326	1.05
55	1.04	0.0366	1.05
60	1.12	0.0406	1.02

Table 40 *Binary*, run 3

Time (min)	GLUC (mg/L)	dS/dt	R_s (mg/m^2-hr)
0	0.0776	-0.007	1.36
5	0.7488	-0.003	1.23
10	0.1988	0.001	1.31
15	0.3204	0.005	1.28
20	0.497	0.009	1.23
25	0.828	0.013	1.16
30	0.764	0.017	1.16
35	1.176	0.021	1.08
40	1.204	0.025	1.06
45	1.048	0.029	1.07
50	1.536	0.033	0.98
55	2.064	0.037	0.87
60	1.984	0.041	0.87

Table 41 *Binary*, run 4

Time (min)	GLUC (mg/L)	dS/dt	R_s (mg/m^2-hr)
0	0.0816	0.0084	1.30
5	0.5184	0.0094	1.22
10	0.3956	0.0104	1.24
15	0.432	0.0114	1.23
20	0.504	0.0124	1.21
25	0.568	0.0134	1.20
30	0.548	0.0144	1.20
35	0.742	0.0154	1.16
40	0.746	0.0164	1.16
45	1.056	0.0174	1.10
50	0.9	0.0184	1.13
55	1.312	0.0194	1.05
60	1.24	0.0204	1.06

APPENDIX F

Calculated monochloramine consumption rate for all types of population.

Table 42 *K. pneumoniae* ,run 1

Time (hr)	M (mg/L)	dM/dt	R_M (mg/m^2-hr)
0	4	-0.05	0.01
5	1.8	0.00037	
10	2.0	0.000337	
15	3.25	-0.02075	0.011
20	3.5	0.0075	0.003
25	3.65	0.0065	0.002
30	3.6	0.0055	0.002
35	3.55	0.0045	0.003
40	3.55	0.0035	0.003
45	3.6	0.0025	0.003
50	3.6	0.0015	0.003
55	3.65	0.0005	0.003
60	3.85	-0.0005	0.001

Table 43 *K. pneumoniae*, run 2

Time (min)	M (mg/L)	dM/dt	R_M (mg/m^2-hr)
0	4	-0.06667	0.013
5	1.6	0	
10	1.9	0	
15	3	-0.02425	0.015
20	3.1	0.0172	0.005
25	3.1	0.0162	0.005
30	3.2	0.0152	0.004
35	3.25	0.0142	0.004
40	3.45	0.0132	0.002
45	3.55	0.0122	0.002
50	3.65	0.0112	0.001
55	3.65	0.0102	0.001
60	3.65	0.0092	0.001

Table 44 *P. aeruginosa*

Time (min)	M (mg/L)	dM/dt	R_M (mg/m^2-hr)
0	4	-0.7	0.143
5	0.5	-0.35	0.107
10	0.5	0	0.035
15	0.5	0	0.035
25	0.5	0	0.035
45	0.5	0	0.035
60	0.5	0	0.035

Table 45 *Binary*, run 1

Time (min)	M (mg/L)	dM/dt	R_M (mg/m^2-hr)
0	4	-0.7	0.143
5	0.5	-0.35585	0.108
10	0.3	-0.0097	0.039
15	0.25	-0.0077	0.039
20	0.2	-0.0057	0.039
25	0.25	-0.0037	0.038
30	0.25	-0.0017	0.038
35	0.25	0.0003	0.037
40	0.3	0.0023	0.036
45	0.3	0.0043	0.036
50	0.3	0.0063	0.036
55	0.3	0.0083	0.035
60	0.35	0.0103	0.034

Table 46 *Binary*, run 2

Time (min)	M (mg/L)	dm/dt	R_M (mg/m^2-hr)
0	4	-0.78	0.160
5	0.1	-0.38695	0.118
10	0.1	0.0061	0.038
15	0.15	0.0061	0.037
20	0.15	0.0061	0.037
25	0.2	0.0061	0.037
30	0.25	0.0061	0.036
35	0.25	0.0061	0.036
40	0.35	0.0061	0.035
45	0.375	0.0061	0.035
50	0.4	0.0061	0.035
55	0.425	0.0061	0.034
60	0.45	0.0061	0.034

Table 47 Binary, run 3

Time (min)	M (mg/L)	dm/dt	R_M (mg/m^2-hr)
0	4	-0.6	0.123
5	1	-0.30355	0.092
10	0.85	-0.0061	0.033
15	0.7	-0.0051	0.034
20	0.75	-0.0041	0.033
25	0.75	-0.0031	0.033
30	0.85	-0.0021	0.032
35	0.9	-0.0011	0.031
40	0.85	-0.0001	0.033
45	0.85	0.0009	0.031
50	0.9	0.0019	0.030
55	0.85	0.0029	0.031
60	0.9	0.0039	0.030

APPENDIX G

Calculated detachment rate coeffiicent for all types of populations.

Table 48 *K. pneumoniae*, run 1

Time (min)	dX/dt	X_P (#/mL)	K_d (#/m^2-hr)
0	4210000	1.56E+08	2.44E+12
5	3400000	2.27E+08	2.99E+12
10	2590000	1.96E+08	2.51E+12
15	1780000	24700000	6.15E+11
20	970000	1.98E+08	2.20E+12
25	160000	1.98E+08	2.03E+12
30	-650000	2.11E+08	2.00E+12
35	-1460000	2.09E+08	1.80E+12
40	-2270000	2.27E+08	1.83E+12
45	-3080000	2.16E+08	1.55E+12
50	-3890000	1.57E+08	7.87E+11
55	-4700000	96600000	1.08E+10
60	-5510000	89900000	-2.2E+11

Table 49 *K. pneumoniae*, run 2

Time (min)	dX/dt	X_P (#/mL)	K_d (#/m^2-hr)
0	5355000	45800000	1.56E+12
5	4305000	1.54E+08	2.44E+12
10	3255000	1.02E+08	1.70E+12
15	2205000	2.89E+08	3.37E+12
20	1155000	2.94E+08	3.21E+12
25	105000	1.56E+08	1.60E+12
30	-945000	1.25E+08	1.07E+12
35	-1995000	1.27E+08	8.73E+11
40	-3045000	1.21E+08	5.97E+11
45	-4095000	1.03E+08	2.00E+11
50	-5145000	1.20E+08	1.56E+11
55	-6195000	98000000	-2.8E+11
60	-7245000	94000000	-5.4E+11

Table 50 *P. aeruginosa*

TIME (min)	dX/dt	X_P (#/mL)	K_d (#/m^2-hr)
0	-591000	35000000	2.32E+11
5	-551000	24000000	1.29E+11
10	-511000	30000000	1.98E+11
15	-471000	18000000	8.51E+10
25	-391000	21000000	1.32E+11
45	-231000	15000000	1.04E+11
60	-111000	9000000	6.81E+10

Table 51 *Binary*, run 1

TIME (min)	dX/dt	X_P (#/mL)	K_d (#/m^2-hr)
0	-310000	17300000	1.11E+11
5	-283880	8490000	2.75E+10
10	-257760	7620000	2.40E+10
15	-231640	7090000	2.41E+10
20	-205520	9930000	5.81E+10
25	-179400	7060000	3.45E+10
30	-153280	3650000	5.40E+09
35	-127160	8990000	6.47E+10
40	-101040	4720000	2.69E+10
45	-74920	6220000	4.74E+10
50	-48800	2700000	1.73E+10
55	-22680	3940000	3.51E+10
60	3440	2980000	3.08E+10

Table 52 *Binary*, run 2

Time (min)	dX/dt	X_P (#/mL)	K_d (#/m^2-hr)
0	1770000	65900000	1.03E+12
5	1418000	81500000	1.11E+12
10	1066000	74700000	9.73E+11
15	714000	82000000	9.75E+11
20	362000	84900000	9.32E+11
25	10000	79600000	8.06E+11
30	-342000	84400000	7.82E+11
35	-694000	93100000	7.98E+11
40	-1046000	79800000	5.91E+11
45	-1398000	87100000	5.93E+11
50	-1750000	65100000	2.98E+11
55	-2102000	47700000	5.03E+10
60	-2454000	45700000	-4.2E+10

Table 53 *Binary*, run 3

TIME (min)	dX/dt	X_P (#/mL)	K_d (#/m^2-hr)
0	520000	64000000	7.53E+11
5	465000	68000000	7.82E+11
10	410000	69200000	7.83E+11
15	355000	72500000	8.05E+11
20	300000	69500000	7.63E+11
25	245000	68600000	7.43E+11
30	190000	69670000	7.43E+11
35	135000	70800000	7.43E+11
40	80000	68900000	7.12E+11
45	25000	67910000	6.91E+11
50	-30000	59800000	5.98E+11
55	-85000	59800000	5.86E+11
60	-140000	56800000	5.45E+11

APPENDIX H

This appendix contains data of oxygen concentration profiles during monochloramine disinfection.

Table 54 Oxygen profiles in binary culture at t=0

depth (μm)	pA/100	dev/100	avg O_2 concentration (mmol/m^3)
-2515	-0.710	0.0127	0.250
-2415	-0.657	0.0143	0.229
-2315	-0.748	0.0114	0.264
-2215	-0.627	0.0072	0.218
-2115	-0.622	0.0125	0.216
-2015	-0.649	0.0109	0.226
-1915	-0.639	0.0034	0.222
-1815	-0.591	0.0076	0.204
-1715	-0.670	0.0118	0.234
-1615	-0.693	0.0103	0.243
-1515	-0.630	0.0105	0.219
-1415	-0.600	0.0113	0.207
-1315	-0.606	0.0047	0.210
-1215	-0.582	0.0083	0.200
-1115	-0.569	0.0112	0.195
-915	-0.592	0.0120	0.204
-815	-0.568	0.0035	0.195
-715	-0.569	0.0059	0.196
-615	-0.535	0.0119	0.182
-515	-0.488	0.0135	0.164
-415	-0.528	0.0022	0.180
-315	-0.543	0.0104	0.186
-215	-0.447	0.0107	0.149
-190	-0.440	0.0086	0.146
-165	-0.450	0.0056	0.150
-140	-0.436	0.0055	0.144
-115	-0.440	0.0119	0.146
-90	-0.432	0.0118	0.143
-65	-0.416	0.0114	0.136
-40	-0.416	0.0105	0.136
-10	-0.443	0.0044	0.147
-5	-0.432	0.0109	0.143
0	-0.418	0.0065	0.138

Table 55 Oxygen profiles in binary culture at t=5

depth (μm)	pA/100	dev/100	avg O_2 concentration (mmol/m^3)
-1800	-0.826	0.0059	0.255
-1600	-0.812	0.0089	0.250
-1400	-0.818	0.0049	0.252
-1200	-0.793	0.0093	0.244
-1000	-0.699	0.0070	0.207
-800	-0.680	0.0084	0.201
-700	-0.710	0.0135	0.211
-600	-0.683	0.0106	0.202
-500	-0.661	0.0082	0.195
-400	-0.684	0.0039	0.202
-300	-0.680	0.0103	0.201
-275	-0.655	0.0033	0.193
-250	-0.629	0.0093	0.184
-225	-0.622	0.0220	0.182
-200	-0.605	0.0072	0.177
-175	-0.591	0.0090	0.172
-150	-0.598	0.0078	0.174
-125	-0.561	0.0082	0.162
-100	-0.563	0.0076	0.163
-90	-0.549	0.0091	0.159
-80	-0.555	0.0130	0.160
-70	-0.552	0.0084	0.159
-60	-0.539	0.0098	0.155
-50	-0.544	0.0100	0.157
-40	-0.546	0.0116	0.158
-30	-0.542	0.0045	0.156
-20	-0.548	0.0110	0.158
-10	-0.347	0.0058	0.093
0	-0.283	0.0121	0.072

Where

pA (pico amperes) is current read from the measurements

dev is the standard deviation

Table 56 Oxygen profiles in binary culture at t=10

depth (μm)	pA/100	dev/100	avg O_2 concentration (mmol/m^3)
-2000	-0.810	0.0086	0.250
-1800	-0.794	0.0108	0.244
-1600	-0.793	0.0079	0.244
-1400	-0.683	0.0104	0.207
-1200	-0.740	0.0382	0.226
-1000	-0.712	0.0037	0.206
-800	-0.777	0.0244	0.227
-600	-0.655	0.0181	0.188
-400	-0.581	0.0062	0.164
-300	-0.590	0.0054	0.167
-200	-0.607	0.0070	0.173
-100	-0.551	0.0199	0.155
-75	-0.568	0.0106	0.161
-50	-0.548	0.0077	0.154
-25	-0.506	0.0041	0.141

Table 57 Oxygen profiles in binary culture at t=15

depth (μm)	pA/100	dev/100	avg O_2 concentration (mmol/m^3)
-1000	-0.862	0.007935	0.20584
-800	-0.858	0.004446	0.204843
-600	-0.825	0.009777	0.196322
-500	-0.850	0.005755	0.202587
-400	-0.825	0.007765	0.196325
-300	-0.819	0.007091	0.194823
-200	-0.806	0.004873	0.191445
-175	-0.802	0.004794	0.190444
-150	-0.775	0.011405	0.183424
-125	-0.762	0.009182	0.180171
-100	-0.733	0.008374	0.172785
-75	-0.719	0.004315	0.169035
-50	-0.700	0.00591	0.164275
-25	-0.667	0.003894	0.155889
-15	-0.679	0.007301	0.158889
-5	-0.559	0.002692	0.128095
0	-0.483	0.005259	0.10856

Table 58 Oxygen profiles in binary culture at t=30

depth (μm)	pA/100	dev/100	avg O_2 concentration (mmol/m^3)
-1005	-0.880	0.0038	0.207
-805	-0.853	0.0093	0.200
-605	-0.827	0.0051	0.193
-405	-0.802	0.0067	0.187
-305	-0.813	0.0073	0.190
-205	-0.791	0.0116	0.184
-155	-0.795	0.0071	0.185
-105	-0.777	0.0073	0.181
-80	-0.723	0.0060	0.167
-55	-0.721	0.0108	0.166
-30	-0.705	0.0102	0.162
-5	-0.662	0.0055	0.152
0	-0.480	0.0074	0.106

Table 59 Oxygen profiles in binary culture at t=45

depth (μm)	pA/100	dev/100	avg O_2 concentration (mmol/m^3)
-1005	-0.763	0.0039	0.2069
-805	-0.736	0.0063	0.1990
-605	-0.729	0.0044	0.1967
-405	-0.713	0.0033	0.1923
-305	-0.708	0.0111	0.1905
-205	-0.679	0.0091	0.1821
-155	-0.642	0.0078	0.1712
-105	-0.657	0.0080	0.1757
-80	-0.627	0.0047	0.1670
-55	-0.603	0.0073	0.1598
-30	-0.569	0.0059	0.1499
-5	-0.549	0.0077	0.1439
0	-0.514	0.0048	0.1337

Table 60 Oxygen profiles in binary culture at t=60

depth (μm)	pA/100	dev/100	avg O_2 concentration (mmol/m^3)
-1000	-0.858	0.0104	0.210
-800	-0.814	0.0159	0.198
-600	-0.808	0.0103	0.196
-500	-0.719	0.0059	0.173
-400	-0.754	0.0102	0.182
-300	-0.768	0.0050	0.186
-200	-0.745	0.0089	0.180
-100	-0.663	0.0116	0.158
-75	-0.633	0.0081	0.150
-50	-0.605	0.0103	0.143
-25	-0.526	0.0066	0.122
-15	-0.502	0.0056	0.116
-10	-0.506	0.0041	0.117
-5	-0.523	0.0055	0.121
0	-0.473	0.0113	0.108

Table 61 Oxygen profiles in binary culture at t=0, formaldehyde control.

depth (μm)	pA/100	dev/100	avg O_2 concentration (mmol/m^3)
-1000	-0.375	0.0077	0.209
-800	-0.370	0.0276	0.206
-600	-0.347	0.0048	0.192
-400	-0.307	0.0129	0.167
-300	-0.290	0.0123	0.156
-200	-0.264	0.0115	0.140
-100	-0.253	0.0228	0.133
-75	-0.216	0.0181	0.110
-50	-0.212	0.0200	0.108
-25	-0.198	0.0293	0.099
0	-0.181	0.0280	0.088

Table 62 Oxygen profiles in binary culture at t = 15, formaldehyde control.

depth (μm)	pA/100	dev/100	avg O_2 concentration (mmol/m^3)
-1000	-0.269	0.0205	0.221
-800	-0.272	0.0105	0.223
-400	-0.268	0.0229	0.219
-300	-0.262	0.0101	0.213
-250	-0.262	0.0058	0.214
-200	-0.268	0.0189	0.219
-150	-0.266	0.0213	0.217
-100	-0.261	0.0063	0.212
-50	-0.267	0.0090	0.219
0	-0.266	0.0220	0.217

Table 63 Calculated Oxygen flux ratio during disinfection (Equation 12).

Time (min)	J (t)/J (0)
0	1
5	1.07
10	1.02
15	0.87
30	0.89
45	0.898
60	0.898

APPENDIX I

Model

The values obtained during the simulation of the model as explained in the discussion section of the thesis are shown in Table 53.

The values for the parameters were obtained from the original experimental data. The decay rates were assumed arbitrarily.

X_R = 1E+09 (subpopulation)

X_D = 8.5E+11

b_K = 15.0 (decay rate coefficient of *K. pneumoniae*)

b_P = 15.0 (decay rate coefficient of *P. aeruginosa*)

fP fraction of *P. aeruginosa* in biofilm

X_V Total viable cell density

Table 64 The values obtained by plugging in the numbers for the parameters as described above in equation 15.

Time (hrs)	log X_v (cfu/m^2) f_P=0.23	log X_v (cfu/m^2) f_P=0.834	log X_v (cfu/m^2) f_P=0.21
0	14.16137	12.29885	11.233
0.167	14.15499	11.8348	10.17
0.25	14.15182	11.6043	9.698798
0.5	14.14228	10.91292	9.039027
0.75	14.13273	10.23782	9.000959
1.0	14.12318	9.63178	9.000023
1.25	14.11364	9.220559	9.000001
1.5	14.10409	9.05437	9.0
2	14.085	9.002346	9.0